U.PORTO

MESTRADO EM METABOLISMO – BIOPATOLOGIA E EXPERIMENTAÇÃO

Targeting Cellular Senescence and Lipid Metabolism to Restore Adipose Tissue Function

Beatriz Sá Pinto

M

2026

MASTER IN METABOLISM – BIOPATHOLOGY AND EXPERIMENTAL

Targeting Cellular Senescence and Lipid Metabolism to Restore Adipose Tissue Function

MSc Student: Beatriz Sá Pinto

Supervisor and affiliation

Adriana Rodrigues

Unidade de Biologia Experimental, Departamento de Biomedicina, Faculdade de Medicina da Universidade do Porto (FMUP)

Instituto de Investigação e Inovação em Saúde, Universidade do Porto (i3S)

Faculdade de Ciências da Nutrição e Alimentação, Universidade do Porto (FCNAUP)

Co-supervisor and affiliation

Alexandra Gouveia

Unidade de Biologia Experimental, Departamento de Biomedicina, Faculdade de Medicina da Universidade do Porto (FMUP)

Instituto de Investigação e Inovação em Saúde, Universidade do Porto (i3S)



Agradecimentos

Esta dissertação de mestrado representa o culminar de um percurso desafiante e gratificante, que contribuiu profundamente para o meu crescimento académico e pessoal. Gostaria de expressar os meus sinceros agradecimentos a todos aqueles que, de alguma forma, me acompanharam e apoiaram ao longo deste caminho.

Em primeiro lugar, gostaria de expressar o meu mais profundo agradecimento à minha orientadora, Professora Adriana Rodrigues, por ter aceitado acompanhar-me e orientar-me ao longo deste percurso. Obrigada por toda a disponibilidade e acompanhamento, por todo o conhecimento que partilhou comigo e por me ter incentivado a crescer enquanto investigadora. Tudo o que aprendi sob a sua orientação irá, sem dúvida, acompanhar-me ao longo do meu futuro percurso profissional.

Gostaria também de agradecer à minha coorientadora, Professora Alexandra Gouveia, por toda a disponibilidade e apoio prestados ao longo deste projeto. Ao Professor Henrique Almeida, agradeço por me ter recebido no seu grupo de investigação "Aging & Stress" e por toda a simpatia demonstrada desde o primeiro momento.

Agradeço também a todos os membros do laboratório por terem criado um ambiente tão acolhedor e por estarem sempre disponíveis para ajudar. Um agradecimento muito especial à Nisa, que me acompanhou ao longo de todo este percurso. Obrigada pela paciência infinita, pela disponibilidade constante e por estares sempre disposta a ensinar-me, mesmo quando fazia as mesmas perguntas mais do que uma vez. Aprendi imenso contigo. Obrigada por seres a minha companheira de laboratório aos fins de semana, por partilhares comigo tantas horas de trabalho com as nossas "barrigas" e, sobretudo, por nunca me teres deixado sentir sozinha durante esta experiência. À Ana e à Anabela, um agradecimento igualmente especial pela simpatia, generosidade e constante disponibilidade para me ajudarem.

Gostaria também de deixar um agradecimento especial à Professora Raquel Soares, Diretora do Mestrado, por toda a disponibilidade, simpatia e apoio demonstrados ao longo destes dois anos. Obrigada por estar sempre pronta a ajudar e por todo o

conhecimento que partilhou comigo ao longo deste percurso. Agradeço ainda a forma próxima e dedicada com que sempre acompanhou e apoiou os seus alunos.

Nada disto teria sido possível sem a minha família. Aos meus pais, obrigada pelo apoio constante, por acreditarem sempre em mim e por me incentivarem em todas as decisões que tomei. Às minhas irmãs, Inês e Catarina, obrigada por serem não só as melhores irmãs que poderia pedir, mas também as minhas melhores amigas. Obrigada por celebrarem cada conquista comigo e por estarem sempre ao meu lado, tanto nos momentos mais felizes como nos mais difíceis. Quero também recordar as minhas estrelas-guias - o meu avô Fernando, o meu avô Sá, a minha avó Miguta e a minha tia Nani - que sei que continuam a olhar por mim todos os dias.

À Bia e à Sofia, as minhas primeiras amigas da universidade, obrigada por celebrarem cada conquista minha como se fosse vossa. À Bia por todos os momentos que vivemos juntas, e, em especial, pela experiência inesquecível que partilhamos durante o Erasmus. Acompanhaste grande parte do meu crescimento pessoal e académico, e não poderia ter escolhido melhor parceira para viver esta experiência comigo. À Sofia, a amiga que está sempre com um sorriso no rosto, minha companheira não só de estudo, mas também de tapas e um bom copo de vinho. Obrigada por estares sempre à distância de uma chamada, independentemente dos quilómetros que nos separam.

Um agradecimento muito especial às amigas que partilharam comigo estes últimos dois anos de mestrado**:** Bia, Luísa, Joana e Bea**.** Obrigada pela amizade, pelo apoio e pelo companheirismo. Obrigada por cada almoço, cada lanche, cada gargalhada e cada conversa que tornou mais leves os dias mais stressantes de escrita da tese e que nos relembrou que nunca estávamos sozinhas neste percurso. Que a nossa amizade continue pela vida fora e que continuemos a partilhar muitos momentos, com pouco estudo e muitas viagens!

Por fim, agradeço também a mim própria, pela dedicação e resiliência que me permitiram ultrapassar cada desafio encontrado ao longo deste caminho. Este percurso nem sempre foi fácil, mas ensinou-me a confiar nas minhas capacidades, a encarar cada obstáculo como uma oportunidade para crescer e a não desistir. Não sei o que o futuro me reserva, mas sei que continuarei a procurar aquilo que me faz feliz e a seguir aquilo de que gosto, sempre com entusiasmo e um sorriso no rosto.

Summary

Adipose tissue (AT) is a metabolically active organ that plays a central role in maintaining systemic metabolic homeostasis. During aging, AT is characterized by a chronic low-grade inflammation, commonly referred to as inflammaging and undergoes progressive functional deterioration, including impaired lipid mobilization and thermogenic capacity, reduced adipogenesis, which favors adipocyte hypertrophy, and dysregulated extracellular matrix (ECM) remodeling. Similar alterations occur in obesity, contributing to an adipaging-like phenotype associated with accelerated biological aging and earlier onset of age-related metabolic diseases. Cellular senescence represents an important mechanism linking aging and obesity, as the accumulation of senescent cells (SCs) and their senescence-associated secretory phenotype (SASP) contribute to persistent AT dysfunction.

Although weight-loss interventions improve some metabolic parameters, AT retains a molecular and cellular memory of previous obesity even after substantial weight loss, which may contribute to weight regain. Therefore, interventions capable of targeting persistent mechanisms of AT dysfunction may complement conventional weight-loss approaches. Senolytic compounds, including dasatinib and quercetin (D+Q), selectively target SCs and have shown beneficial effects on inflammatory and metabolic parameters, but may not fully restore AT metabolic function. Therefore, this study investigated whether combining D+Q with the lipolytic stimuli α-MSH and isoproterenol could improve the molecular and functional phenotype of previously obese human subcutaneous adipose tissue (SAT).

Human SAT collected during abdominoplasty from individuals with a history of obesity that underwent bariatric surgery and substantial weight loss was used to establish an *ex vivo* model of previously obese AT. Explants were treated for one and two weeks under six experimental conditions: vehicle, α-MSH (M), isoproterenol (I), D+Q, or the combinations D+Q+M and D+Q+I, and analyzed for lipid mobilization, thermogenesis, cellular senescence, cytoprotection, inflammation, and ECM remodeling.

After two weeks, D+Q-containing treatments reduced adipocyte size and enhanced lipid mobilization, as supported by increased glycerol release and expression of the key lipolytic enzymes ATGL and HSL, together with increased thermogenesis-associated markers, including *UCP1* and *PGC1α*. During the first week, the combination of D+Q with lipolytic stimulation produced a broader metabolic response, particularly in thermogenesis-associated pathways, whereas after two weeks, D+Q alone was sufficient to induce several of these responses.

Treatment also induced time-dependent transcriptional changes. After one week, particularly under D+Q and lipolytic stimulation, *p21*, *ZFAND5*, and *TGF-β*, which are associated with senescence but also participate in stress-responsive and tissue remodeling processes, transiently increased, suggesting an early adaptive response. After prolonged exposure, their expression was reduced, indicating a more coordinated attenuation of senescence-associated features. D+Q-containing treatments also induced cytoprotective markers, including *APOJ* and *HO-1*, further supporting an active tissue response. Importantly, the effects of D+Q extended beyond senescence-associated features, with a concomitant reduction in inflammatory -associated markers, including PAI-1, IL-6 and *IL-1β*, and ECM remodeling-associated markers *FN*, *MMP3*, and *TIMP1*.

Collectively, D+Q was associated with an overall improvement in the dysfunctional phenotype of previously obese human SAT previously obese human SAT. Lipolytic stimulation contributed more prominently to the early metabolic and cytoprotective response, while prolonged D+Q treatment promoted improvements in senescence- and inflammation-associated features, with a more limited additional effect of lipolytic stimulation on metabolic recovery. The persistence of molecular features of AT dysfunction after substantial weight loss is consistent with a residual imprint of previous obesity, supporting cellular senescence as a potential complementary therapeutic target to improve AT function following weight loss.

Keywords: Adipose Tissue; Senescence; Senolytics; Lipolytics; Aging; Obesity

Resumo

O tecido adiposo (TA) é um órgão metabolicamente ativo que desempenha um papel central na manutenção da homeostase metabólica sistémica. Durante o envelhecimento, o TA é caracterizado por um estado de inflamação crónica de baixo grau, comummente designado por *inflammaging*, e sofre uma deterioração funcional progressiva, incluindo uma menor capacidade de mobilização lipídica e termogénica, redução da adipogénese, favorecendo a hipertrofia dos adipócitos, e desregulação da remodelação da matriz extracelular. Alterações semelhantes ocorrem na obesidade, contribuindo para um fenótipo semelhante ao *adipaging*, associado à aceleração do envelhecimento biológico e ao aparecimento precoce de doenças metabólicas relacionadas com a idade. A senescência celular representa um importante mecanismo de ligação entre o envelhecimento e a obesidade, uma vez que a acumulação de células senescentes e o seu fenótipo secretor associado à senescência (SASP) contribuem para a persistência da disfunção do TA.

Embora as intervenções para perda de peso melhorem alguns parâmetros metabólicos, o TA mantém uma memória molecular e celular da obesidade prévia, mesmo após uma perda substancial de peso, o que poderá contribuir para a recuperação do peso perdido. Assim, intervenções capazes de atuar sobre mecanismos persistentes de disfunção do TA poderão complementar as abordagens convencionais para perda de peso. Os compostos senolíticos, incluindo dasatinib e quercetina (D+Q), atuam seletivamente sobre as células senescentes e têm demonstrado efeitos benéficos em parâmetros inflamatórios e metabólicos, embora possam não restaurar completamente a função metabólica do TA. Neste contexto, o presente estudo investigou se a combinação de D+Q com os estímulos lipolíticos α-MSH e isoproterenol poderia melhorar o fenótipo molecular e funcional do tecido adiposo subcutâneo (SAT) obtido de pacientes com histórico de obesidade.

O SAT humano, recolhido durante abdominoplastias de indivíduos com história de obesidade submetidos a cirurgia bariátrica e com perda substancial de peso, foi utilizado para estabelecer um modelo *ex vivo* de TA previamente obeso. Os explantes foram submetidos a seis condições experimentais durante uma ou duas semanas:

veículo, α-MSH (M), isoproterenol (I), D+Q ou as combinações D+Q+M e D+Q+I, e analisados quanto à mobilização lipídica, termogénese, senescência celular, citoproteção, inflamação e remodelação da matriz extracelular.

Após duas semanas, os tratamentos contendo D+Q reduziram o tamanho dos adipócitos e aumentaram a mobilização lipídica, evidenciada pelo aumento da libertação de glicerol e da expressão das principais enzimas lipolíticas ATGL e HSL, juntamente com o aumento de marcadores associados à termogénese, incluindo *UCP1* e *PGC1α*. Durante a primeira semana, a combinação de D+Q com estimulação lipolítica induziu uma resposta metabólica mais ampla, particularmente nas vias associadas à termogénese, enquanto, após duas semanas, D+Q isoladamente foi suficiente para induzir várias destas respostas.

O tratamento também induziu alterações transcricionais dependentes do tempo de cultura. Após uma semana, particularmente na presença de D+Q e estimulação lipolítica, *p21*, *ZFAND5* e *TGF-β*, marcadores associados à senescência, mas também envolvidos em processos de resposta ao stress e remodelação tecidular, aumentaram transitoriamente, sugerindo uma resposta adaptativa precoce. Após uma exposição prolongada, a expressão destes marcadores diminuiu, indicando uma atenuação mais coordenada das características associadas à senescência. Os tratamentos contendo D+Q também induziram marcadores citoprotetores, incluindo *APOJ* e *HO-1*, reforçando a existência de uma resposta tecidular ativa. É de salientar que os efeitos de D+Q estenderam-se para além das características associadas à senescência, verificando-se uma redução concomitante de marcadores inflamatórios e associados ao SASP, incluindo PAI-1, IL-6 e *IL-1β*, bem como de marcadores associados à remodelação da matriz extracelular, incluindo *FN*, *MMP3* e *TIMP1*.

Em suma, D+Q está associado a uma melhoria do fenótipo disfuncional do SAT de indivíduos com histórico de obesidade. A estimulação lipolítica contribuiu de forma mais evidente para uma resposta metabólica e citoprotetora precoce, enquanto o tratamento prolongado com D+Q promoveu melhorias nas características associadas à senescência e à inflamação, com um efeito adicional mais limitado da estimulação lipolítica na recuperação metabólica.

A persistência de características moleculares de disfunção do TA após uma perda substancial de peso é consistente com a existência de uma marca residual da obesidade prévia, apoiando a senescência celular como um potencial alvo terapêutico complementar para melhorar a função do TA após a perda de peso.

Palavras-chave: Tecido Adiposo; Senescência; Senolíticos; Lipolíticos; Envelhecimento; Obesidade

Index

Agradecimentos ..... **iii**

Summary ..... **v**

Resumo ..... **vii**

Introduction **1**

1. Adipose Tissue: Organization, Diversity and Metabolic Function 1

1.1. Adipose tissue subtypes 1

1.2. Adipose tissue composition 4

1.3. Adipose Tissue as an Endocrine Organ 7

1.4. Adipose Tissue Plasticity and Metabolic Adaptation 9

2. Aging- Associated Remodeling and Dysfunction of Adipose Tissue 13

2.1. Age-Related Changes in Adipose Tissue Distribution and Architecture 13

2.2. Age-Related Alterations in Adipose Tissue Metabolism 14

2.3. Inflammaging and adipaging 15

3. Obesity as a Driver of Adipose Tissue Aging 17

3.1. Obesity-Induced Adipose Tissue Dysfunction 17

3.2. Obesity as a Model of Accelerated Aging 18

3.3. Therapeutic Approaches to Obesity and Adipose Tissue Dysfunction 19

3.3.1. Lifestyle and Pharmacological Interventions for Obesity 19

3.3.2. Bariatric Surgery 20

3.3.3. Limitations of Current Therapeutic Approaches 21

4. Cellular Senescence: A hallmark of Adipose Tissue Dysfunction 22

4.1. Molecular Features and Mechanisms of Cellular Senescence 23

4.2. Cellular Senescence in Adipose Tissue.....25

4.3. Senotherapeutic Potential and Limitations.....27

4.3.1. Senolytic and Senomorphic Strategies 27
4.3.2. Senolytic Approaches in Adipose Tissue 28
4.3.3. Limitations of Senotherapeutics Targeting Adipose Tissue Dysfunction 29

Aims.....31

Materials and Methods.....32

1. Adipose Tissue Collection and treatment 32
2. Adipose Tissue processing for paraffin embedding.....34
3. Histological evaluation of Adipose Tissue samples 34

3.1. Sirius Red staining 34

3.2. Computer-assisted morphometric analysis of Adipose Tissue 35

4. Glycerol Release Assay 35
5. Gene Expression Analysis 35

5.1. RNA extraction 35

5.2. Synthesis of cDNA.....36

5.3. Real- time polymerase chain reaction (qPCR).....36

6. Protein analysis 37

6.1. Protein extraction and quantification 37

6.2. Western Blotting 37

7. Statistical analysis 39

Results 41

1. Senolytic and lipolytic treatment induce changes in adipocyte morphology 41
2. Combined senolytic and lipolytic treatment enhances AT basal lipolytic activity 44
3. Combined senolytic and lipolytic treatment restores thermogenic competence of AT 47
4. Senescence-associated markers show a time-dependent response to treatment 49
5. The combination of senolytic and lipolytic agents activate cytoprotective responses 54
6. Combined senolytic and lipolytic treatment modulates inflammatory and extracellular matrix remodeling markers 55
7. Integrated transcriptional response of human SAT explants to treatment 62

Discussion 65

Study limitations and future perspectives 77

Conclusions 79

References 81

List of Abbreviations

α-MSH	Alpha-melanocyte-stimulating hormone
ACC	Acetyl-CoA carboxylase
AMPK	AMP-activated protein kinase
APCs	Adipocyte progenitor cells
ASCs	Adipose-derived stem cells
AT	Adipose tissue
ATGL	Adipose triglyceride lipase
ATMs	Adipose tissue macrophages
ATR	Ataxia telangiectasia and Rad3-related protein
BAT	Brown adipose tissue
BCL-2	B-cell lymphoma 2
BDNF	Brain-derived neurotrophic factor
BMPs	Bone morphogenetic proteins
C/EBPα	CCAAT/enhancer-binding protein alpha
C/EBPβ	CCAAT/enhancer-binding protein beta
C/EBPδ	CCAAT/enhancer-binding protein delta
cGAS-STING	Cyclic GMP-AMP synthase–stimulator of interferon genes
CHOP	C/EBP homologous protein
CLS	Crown-like structures
CRP	C-reactive protein
CVD	Cardiovascular disease
DIO2	Iodothyronine deiodinase 2
DNA	Deoxyribonucleic acid
DSBs	Double-strand breaks
ECs	Endothelial cells
ECM	Extracellular matrix

EBF1	Early B-cell factor 1
FAs	Fatty acids
FFAs	Free fatty acids
FGF21	Fibroblast growth factor 21
GATA	GATA-binding factors
GLUT4	Glucose transporter type 4
HIF-1α	Hypoxia-inducible factor 1-alpha
HSL	Hormone-sensitive lipase
ICAM-1	Intercellular adhesion molecule 1
IL-1β	Interleukin 1 beta
IL-6	Interleukin 6
IL-8	Interleukin 8
JNK	c-Jun N-terminal kinase
KLFs	Krüppel-like factors
LPL	Lipoprotein lipase
MAPK	Mitogen-activated protein kinase
MCP-1	Monocyte chemoattractant protein 1
miRNAs	MicroRNAs
mRNAs	Messenger RNAs
MSCs	Mesenchymal stem cells
mTOR	Mechanistic target of rapamycin
NAFLD	Non-alcoholic fatty liver disease
NRG4	Neuregulin 4
NST	Non-shivering thermogenesis
p16	Cyclin-dependent kinase inhibitor 2A
p21	Cyclin-dependent kinase inhibitor 1A
p-ACC	Phosphorylated acetyl-CoA carboxylase
p53	Tumor protein p53

PAI-1	Plasminogen activator inhibitor 1
PGC1α	Peroxisome proliferator-activated receptor gamma coactivator 1-alpha
PI3K	Phosphoinositide 3-kinase
PKA	Protein kinase A
PPARγ	Peroxisome proliferator-activated receptor gamma
PRDM16	PR domain containing 16
Rb	Retinoblastoma protein
ROS	Reactive oxygen species
RPA	Replication protein A
SA-β-gal	Senescence-associated beta-galactosidase
SAHF	Senescence-associated heterochromatin foci
SASP	Senescence-associated secretory phenotype
SAT	Subcutaneous adipose tissue
SCAPs	Senescent cell anti-apoptotic pathways
SC	Senescent cell
SCs	Senescent cells
SREBP1	Sterol regulatory element-binding protein 1
SVF	Stromal vascular fraction
T2DM	Type 2 diabetes mellitus
TGF-β	Transforming growth factor beta
TGs	Triglycerides
TNF-α	Tumor necrosis factor alpha
UCP-1	Uncoupling protein 1
VAT	Visceral adipose tissue
VCAM-1	Vascular cell adhesion molecule 1
VEGF	Vascular endothelial growth factor
VLDL	Very-low-density lipoprotein

WAT	White adipose tissue

List of Figures

Figure 1. Anatomical sites of brown and white adipose tissue depots in humans. While WAT is widely distributed across subcutaneous and visceral regions, BAT remains restricted to specific thermogenic sites, primarily concentrated in the cervical, supraclavicular, axillary, paravertebral, and perirenal areas. Created by BioRender Template. 4

Figure 2. Appearance of adipocytes. (A) White adipocytes act as the body´s energy store, which contain a single lipid droplet, a flattened nucleus situated at the periphery, and low mitochondrial content. **(B)** Brown adipocytes are heat producers, by NST. They are characterized by multilocular lipid droplets, nucleus centrally positioned and a high number of mitochondria. **(C)** Beige adipocytes, generated through de novo adipogenesis or transdifferentiation of WAT, resemble brown adipocytes in both structure and function. Adapted from (5)..... 6

Figure 3. Adipose Tissue plasticity through browning and whitening. Browning of WAT involves the recruitment of thermogenic beige adipocytes through the transdifferentiation of mature white adipocytes or de novo differentiation of APCs. This process can be induced by several physiological and pharmacological stimulus and is associated with increased thermogenesis and energy expenditure. Conversely, whitening involves the loss of the thermogenic phenotype and acquisition of white adipocyte-like characteristics, favoring lipid storage and adipose tissue dysfunction. The balance between browning and whitening illustrates the dynamic phenotypic and metabolic plasticity of AT. Adapted from (45). 7

Figure 4. Adipose tissue remodeling during aging and obesity. Under health conditions, AT expansion is mediated via adipocyte hyperplasia, supported by adequate angiogenesis and balanced ECM remodeling. Resident anti-inflammatory M2 macrophages maintain tissue homeostasis and suppress inflammation. However, either the progressive expansion of AT along obesity or the metabolic stress observed during chronological aging shift this balance toward adipocyte hypertrophy, that is often accompanied by local hypoxia, due to insufficient angiogenesis. Hypoxia stabilizes HIF-1α, which promotes inflammatory genes expression and increases tissue stiffness and diminishes metabolic flexibility. Prolonged AT hypertrophy promotes the recruitment of pro-inflammatory M1 macrophages, which aggregate around dead

or dying adipocytes to form CLS. Consequently, this severely dysfunction of AT contributes to significantly metabolic dysfunction, which leads to metabolic syndrome. Adapted from (46). 19

Figure 5. Inducing mechanisms and phenotypic hallmarks of cellular senescence. Internal and external factors can trigger the senescent state, including DNA damage, telomere shortening, oncogene activation, epigenetic alterations, oxidative stress and mitochondrial dysfunction. These stimuli induce persistent cell cycle arrest, leading to senescence. Senescent cells are characterized by an enlarged and flattened morphology and are associated with an increase of SA-β-gal activity, upregulated p21/p16, mitochondrial dysfunction, nuclear dysfunction characterized by dysregulated Lamin B1 and epigenetic alterations, leading to the formation of SAHF. Adapted from (144). 25

Figure 6. Schematic representation of the experimental treatment timeline of human SAT explants culture for two weeks. Explants were treated ex vivo with the senolytic combination dasatinib plus quercetin (D+Q) for three consecutive days and with the lipolytic agents α-MSH (M) or isoproterenol (I) every other day. At the end of each treatment period, tissue and culture medium were collected for subsequent analysis. Schematic representation generated with the assistance of ChatGPT (OpenAI). 33

Figure 7. Effect of senolytic and lipolytic treatments on SAT morphology after two weeks of treatment. (A) Representative images of Sirius-Red-stained sections of human SAT. Scale bar = 200 μm. **(B)** Quantification of adipocyte cross-sectional area (μm^2) in human SAT treated with vehicle (V), α-MSH (M), isoproterenol (I), dasatinib plus quercetin (D+Q), and the combined treatments D+Q+M and D+Q+I using a modified version of Adiposoft, a plugin for Fiji (Image J). Data are presented as mean ± SEM. Statistical significance was determined using one-way ANOVA followed by Fisher´s uncorrected LSD test. $p < 0.01$ (**), $p < 0.0001$ (****). 43

Figure 8. Structural integrity and adipocyte membrane boundaries in human SAT explants after two weeks of treatment. Representative images displaying adipocyte membrane outlines in Sirius Red–stained sections of human SAT explants treated with vehicle (V) , α-MSH (M) , isoproterenol (I) , dasatinib plus quercetin (D+Q), or the combinations D+Q+M and D+Q+I. Images were generated using the Adiposoft plugin in Fiji (ImageJ). Scale bar **=** 200 μm. 43

Figure 9. Effect of senolytic and lipolytic treatments on basal glycerol release from human SAT explants. Glycerol release into the culture medium was assessed after one **(A)** and two **(B)** weeks of treatment. Experimental groups included vehicle (V), α-MSH (M), isoproterenol (I), dasatinib plus quercetin (D+Q), and the combined treatments D+Q+M and D+Q+I. Glycerol levels are expressed as fold change relative to vehicle. Data are presented as mean ± SEM (n= 2-5). Statistical significance was determined using one-way ANOVA followed by Fisher´s uncorrected LSD test. p < 0,05 (*), p < 0.01 (**), p < 0.001 (***)..... 44

Figure 10. Effect of senolytic and lipolytic treatments on the protein expression of lipolytic enzymes in human SAT Explants. Representative Western blots of ATGL and HSL are presented after one **(A)** and two **(B)** weeks of treatment. Protein expression levels of ATGL **(C, D)** and HSL **(E, F)** were assessed by Western blotting after one and two weeks of treatment. Experimental groups included vehicle (V), α-MSH (M), isoproterenol (I), dasatinib plus quercetin (D+Q), and the combined treatments D+Q+M and D+Q+I. Protein levels were normalized to β-actin and expressed as fold change relative to vehicle. Data are presented as mean ± SEM (n = 3-13). Statistical significance was determined using one-way ANOVA followed by Fisher´s uncorrected LSD test. p < 0,05 (*), p < 0.01 (**), p < 0.001 (***). 46

Figure 11. Effect of senolytic and lipolytic treatments on thermogenic and browning-associated markers in human SAT Explants. mRNA expression levels of UCP-1 **(A, B)** and PGC1α **(C, D)** were assessed by RT-qPCR after one and two weeks of treatment. Experimental groups included vehicle (V), α-MSH (M), isoproterenol (I), dasatinib plus quercetin (D+Q) and the combined treatments D+Q+M and D+Q+I. Gene expression levels were normalized to IPO8 and are expressed as fold change relative to vehicle. Data are presented as mean ± SEM (n = 2-10). Statistical significance was determined using one-way ANOVA followed by Fisher´s uncorrected LSD test. p < 0,05 (*), p < 0.01 (**), p < 0.001 (***). 48

Figure 12. Effect of senolytic and lipolytic treatments on the mRNA expression of senescence-associated markers in human SAT explants. mRNA expression levels of p21 **(A, B),** ZFAND5 **(C, D)**, and TGF-β **(E, F)** were assessed by RT-qPCR after one and two weeks of treatment. Experimental groups included vehicle (V), α-MSH (M), isoproterenol (I), dasatinib plus quercetin (D+Q) and the combined treatments D+Q+M and D+Q+I. Gene expression levels were normalized to IPO8 and are expressed as fold change relative to vehicle. Data are

presented as mean ± SEM (n = 2-10). Statistical significance was determined using one-way ANOVA followed by Fisher´s uncorrected LSD test. p < 0,05 (*), p < 0.01 (**). 51

Figure 13. Effect of senolytic and lipolytic treatments on the protein expression of senescence-associated markers in human SAT Explants. Representative Western blots of PAI-1 and Lamin B1 are presented after one **(A)** and two **(B)** weeks of treatment. Protein expression levels of PAI-1 **(C, D)** and Lamin B1 **(E, F)** were assessed by Western blotting after one and two weeks of treatment. Experimental groups included vehicle (V), α-MSH (M), isoproterenol (I), dasatinib plus quercetin (D+Q) and the combined treatments D+Q+M and D+Q+I. Protein expression levels were normalized to β-actin and are expressed as fold change relative to vehicle. Data are presented as mean ± SEM (n = 2-7). Statistical significance was determined using one-way ANOVA followed by Fisher´s uncorrected LSD test. p < 0,05 (*), p < 0.01 (**). 53

Figure 14. Effect of senolytic and lipolytic treatments on the mRNA expression of the senescence-associated marker APOJ in human SAT explants. mRNA expression levels of APOJ were assessed by RT-qPCR after one **(A)** and two **(B)** weeks of treatment. Experimental groups included vehicle (V), α-MSH (M), isoproterenol (I), dasatinib plus quercetin (D+Q) and the combined treatments D+Q+M and D+Q+I. Gene expression levels were normalized to IPO8 and are expressed as fold change relative to vehicle. Data are presented as mean ± SEM (n = 3-11). Statistical significance was determined using one-way ANOVA followed by Fisher´s uncorrected LSD test. p < 0,05 (*), p < 0.01 (**). 54

Figure 15. Effect of senolytic and lipolytic treatments on the mRNA expression of the cytoprotective marker HO-1 in human SAT Explants. mRNA expression levels of HO-1 were assessed by RT-qPCR after one **(A)** and two **(B)** weeks of treatment. Experimental groups included vehicle (V), α-MSH (M), isoproterenol (I), dasatinib plus quercetin (D+Q) and the combined treatments D+Q+M and D+Q+I. Gene expression levels were normalized to IPO8 and are expressed as fold change relative to vehicle. Data are presented as mean ± SEM (n = 3-11). Statistical significance was determined using one-way ANOVA followed by Fisher´s uncorrected LSD test. p < 0,05 (*). 55

Figure 16. **Effect of senolytic and lipolytic treatments on inflammatory and immune-related markers in human SAT Explants.** mRNA expression levels of IL-6 **(A, B),** IL-1β **(G,**

H) and CD206 **(I, J)**, were assessed by RT-qPCR after one and two weeks of treatment. Protein expression levels of IL-6 **(E, F)**, and Galectin-3 **(M, N)** were assessed by Western blotting after one and two weeks of treatment. Representative Western blots of IL-6 **(C, D)** and Galectin-3 **(K, L)** are shown after one and two weeks of treatment. Gene expression levels were normalized to IPO8, while protein expression levels were normalized to β-actin, and are all expressed as fold change relative to vehicle. Experimental groups included vehicle (V), α-MSH (M), isoproterenol (I), dasatinib plus quercetin (D+Q) and the combined treatments D+Q+M and D+Q+I. Data are presented as mean ± SEM (n = 2-10). Statistical significance was determined using one-way ANOVA followed by Fisher´s uncorrected LSD test. p < 0,05 (*), p < 0.01 (**), p < 0.001 (***), p < 0.0001 (****). 59

Figure 17. Effect of senolytic and lipolytic treatments on ECM remodeling in human SAT Explants. mRNA expression levels of FN **(A, B),** MMP3 **(C, D)**, and TIMP1 **(E, F)**, as well as the MMP3/TIMP1 ratio **(G, H)** were assessed by RT-qPCR after one and two weeks of treatment. Experimental groups included vehicle (V), α-MSH (M), isoproterenol (I), dasatinib plus quercetin (D+Q) and the combined treatments D+Q+M and D+Q+I. Gene expression levels were normalized to IPO8 and are expressed as fold change relative to vehicle. Data are presented as mean ± SEM (n = 3-11). Statistical significance was determined using one-way ANOVA followed by Fisher´s uncorrected LSD test. p < 0,05 (*), p < 0.01 (**). 61

Figure 18. Integrated heatmap analysis of gene expression profiles in human SAT Explants following senolytic and lipolytic treatment. Heatmap showing the relative expression profiles of genes associated with thermogenesis **(**UCP-1 and PGC1α), senescence and stress response (p21, TGF-β and ZFAND5), cytoprotection (HO-1 and APOJ), inflammation and immune response (IL-6, IL-1β and CD206) and ECM remodeling (FN, MMP3, TIMP1) after one **(A)** and two **(B)** weeks of treatment. Experimental groups included vehicle (V), α-MSH (M), isoproterenol (I), dasatinib plus quercetin (D+Q) and the combined treatments D+Q+M and D+Q+I (n = 2-11). The color scale represents relative gene expression, with green indicating higher and red indicating lower expression. 63

Figure 19. Gene expression stability in vehicle-treated in human SAT Explants during the culture period. Relative mRNA expression levels of genes associated with thermogenesis (UCP-1 and PGC1α) **(A),** senescence and stress response (p21, TGF-β and ZFAND5**) (B)**,

cytoprotection (HO-1 and APOJ) **(C)**, inflammation and immune response (IL-6, IL-1β and CD206) **(D)** and extracellular matrix remodeling (FN, MMP3, TIMP1) **(E)**, were compared between vehicle-treated explants after one (1W) and two weeks (2W) of culture. Gene expression levels were assessed by RT-qPCR and normalized to IPO8. Data are presented as mean ± SEM (n = 2-11). No statistically significant differences were observed between the two time points for most of the analyzed genes, with CD206 being the only gene showing a significant difference between 1W and 2W. Statistical significance was determined using Multiple Unpaired t-test. $p < 0,05$ (*). 64

List of Tables

Table 1. List of primer sequences used in the qPCR experiments. 36

Table 2. Primary and secondary antibodies and experimental conditions used for Western blotting analysis. 38

Introduction

1. Adipose Tissue: Organization, Diversity and Metabolic Function

Adipose tissue (AT) is a complex and metabolically active organ that plays a central role in regulating whole-body energy and metabolic homeostasis. Traditionally described as a passive energy reservoir, AT is now recognized as a vital organ that plays a key role not only in energy storage, but also in other vital functions essential for maintaining metabolic health (1,2). Indeed, AT acts as the largest endocrine organ by secreting adipokines and cytokines systemically, which regulate insulin sensitivity, inflammation, immunity, metabolism and appetite (3).

1.1. Adipose tissue subtypes

AT has been traditionally divided into two main types: white adipose tissue (WAT) and brown adipose tissue (BAT), which differ in their cellular composition, morphology and metabolic function (4). While WAT represents the major site of energy storage and plays a central role in systemic metabolic regulation, BAT is primarily specialized in energy dissipation through thermogenesis (5).

WAT can be further classified, based on its anatomical distribution, into two major depots with distinct biological and metabolic properties: visceral adipose tissue (VAT) and subcutaneous adipose tissue (SAT) (6). VAT is located within the abdominal area and surrounds internal organs, including omental, mesenteric, retroperitoneal, gonadal and pericardial fat depots (Figure 1). In contrast, SAT is located beneath the skin and represents the largest AT compartment in humans (Figure 1) (6,7). Despite these anatomical differences, both depots exhibit significant plasticity, allowing them to adapt to the metabolic demands of their local environment.

SAT is characterized by a high adipogenic and angiogenic capacity, which enables the tissue to expand primarily through hyperplasia, thus ensuring efficient lipid storage while maintaining adequate tissue oxygenation and metabolic homeostasis (8–11). Consequently, SAT typically maintains a protective secretory profile, marked by the high secretion of adiponectin, an adipokine known for its potent anti-inflammatory and

insulin-sensitizing effects (2,12,13). However, when the capacity of SAT to safely expand and store excess lipids is exceeded, further lipid accumulation is increasingly redirected towards visceral and ectopic depots, severely impairing their metabolic function (12,14). In contrast to the predominantly hyperplastic expansion of SAT, VAT expands predominantly through adipocyte hypertrophy, a process linked to limited angiogenic plasticity, which is characterized by a reduced capacity to expand and remodel the vascular network in response to tissue expansion, thereby contributing to local hypoxia. However, VAT is more vascularized than SAT and its proximity to the portal circulation allows for rapid mobilization of free fatty acids (FFAs) directly to the liver. Moreover, VAT is associated with a pro-inflammatory environment characterized by the presence of M1-type macrophages and the release of pro-inflammatory cytokines such as tumor necrosis factor-α (TNF-α), interleukins (IL-6, IL-1β, IL-8) and monocyte chemoattractant protein-1 (MCP-1) (3,7,15). This pro-inflammatory profile explains why VAT is strongly linked to insulin resistance, impaired glycemic control, and increased cardiometabolic risk (7,16).

BAT plays a central role in non-shivering thermogenesis (NST), contributing to the regulation of body temperature, energy expenditure and adiposity (17–20). Morphologically, BAT is visually distinct from WAT due to its characteristic brown coloration, which results from the high density of iron-rich mitochondria within brown adipocytes (5). These mitochondria enable BAT to generate heat through uncoupled respiration, a process mediated by uncoupling protein 1 (UCP-1), which is uniquely expressed in the inner mitochondrial membrane of brown adipocytes and represents the defining molecular hallmark of BAT (17,20).

From an evolutionary perspective, BAT is considered an adaptation to cold environments that supports the maintenance of body temperature in homeothermic species (5,18,21). Smaller mammals, such as mice, rats and hamsters, possess proportionally larger BAT depots than larger mammals, including humans (5,21,22). In rodents, BAT is predominantly located in the interscapular region, but is also found in cervical, axillary, paraaortic, cardiac, mediastinal and perirenal depots (22,23). In humans, BAT is mainly detected in the supraclavicular region, with additional depots present in cervical, axillary, paravertebral, thoracic, abdominal and perirenal areas (Figure 1) (5,21–23).

BAT is also characterized by dense sympathetic innervation and a high degree of vascularization, both of which are essential to support its thermogenic function (17,18,24). The extensive vascular network of BAT ensures efficient delivery of oxygen and metabolic substrates, while also facilitating rapid dissipation of heat to the circulation and surrounding tissues (18,25).

Beyond its role in thermogenesis, BAT also contributes to systemic metabolic regulation through the uptake and utilization of glucose and fatty acids (FAs), and the secretion of bioactive molecules, collectively "batokines" (17,21). Consistent with these functions, activation or transplantation of BAT has been shown to increase energy expenditure, improve glucose tolerance, enhance insulin sensitivity, reduce body weight and reverse hyperinsulinemia in both animal models and humans (20,26–28). While BAT is particularly abundant in human neonates, where it can constitute up to 5% of total body mass, its abundance, functional activity and UCP-1 expression are negatively associated with age and body mass index (BMI), accounting for only 1-2% of total AT mass in adults (29). This age-dependent reduction is accompanied by increased inflammatory activity, macrophage infiltration and impaired thermogenic capacity, changes that are further aggravated in obesity and cardiometabolic diseases (20,21). Consequently, strategies to enhance BAT activity through pharmacological, lifestyle or environmental interventions are being actively explored as potential therapeutic approaches for metabolic disorders, mainly in the field of obesity (5,20).

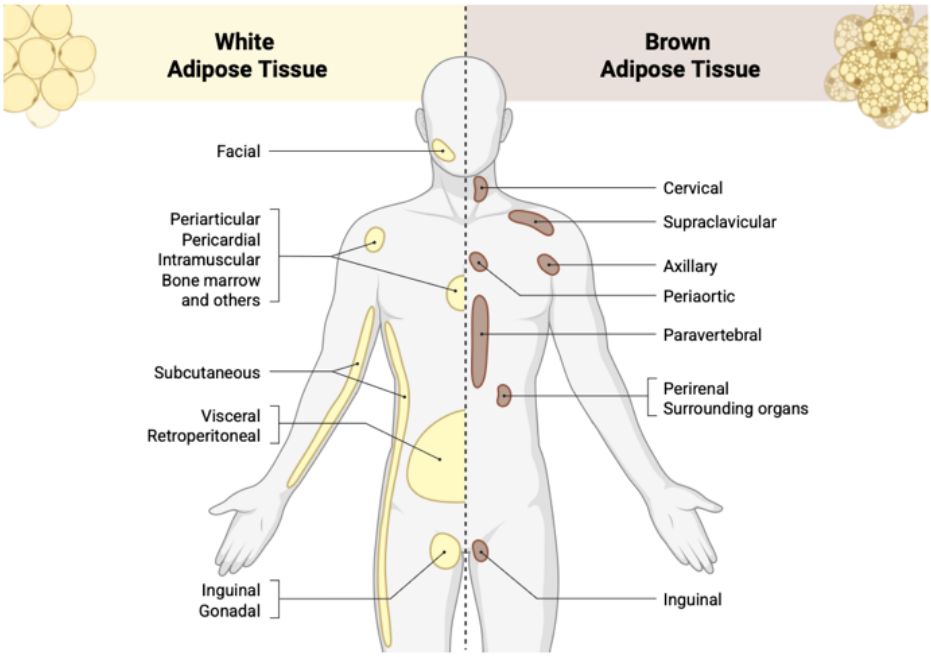


Figure 1. Anatomical sites of brown and white adipose tissue depots in humans. While WAT is widely distributed across subcutaneous and visceral regions, BAT remains restricted to specific thermogenic sites, primarily concentrated in the cervical, supraclavicular, axillary, paravertebral, and perirenal areas. Created by BioRender Template.

1.2. Adipose tissue composition

AT is composed of mature adipocytes and a heterogeneous stromal vascular fraction (SVF) (5,30). Although adipocytes account for most of the tissue volume, SVF represents a substantial and functionally relevant cellular component. This fraction includes preadipocytes, adipose stem and progenitor cells (ASCs and APCs, respectively), fibroblasts, endothelial cells (ECs) and a diverse range of immune cells (4,30–33).

The SVF serves as the functional backbone of AT, facilitating homeostasis, angiogenesis and tissue remodeling (4). Within the SVF, preadipocytes and ASCs are critical for maintaining tissue plasticity, enabling adipocyte renewal and adaptative expansion in response to metabolic demands (34). ECs contribute to vascular integrity and nutrient transport, supporting tissue growth and activity network in the extracellular matrix (ECM). Produced by fibroblasts, APCs and adipocytes, the ECM is composed of collagens (type I, III, IV and VI), laminins, fibronectin and proteoglycans and provides structural support for cell differentiation, angiogenesis and tissue remodeling (35–38).

The immune cells of AT are a critical determinant of its metabolic state, and include macrophages, T and B lymphocytes, natural killer (NK) cells, neutrophils, eosinophils, mast cells, dendritic cells and innate lymphoid cells, which modulate the inflammatory profile of the tissue and influence AT function under both physiological and pathological conditions (39,40). AT macrophages (ATMs) are the most abundant immune cells, and their polarization dictates the inflammatory state. M1-type macrophages ($CD11c^+$), classically activated and pro-inflammatory, secrete cytokines such as TNF-α and IL-6. In contrast, M2-type macrophages ($CD206^+$) are alternatively activated and anti-inflammatory (e.g. IL-10, IL-4), promoting tissue repair (5,37,41). In states of metabolic dysfunction, the balance shifts toward an M1-dominant profile, driven by the recruitment of $CD8^+$ T cells and the loss of protective regulatory T cells, ultimately contribute to chronic low-grade inflammation (3,42).

Mature adipocytes are the predominant specialized cell type within AT and play central roles in energy metabolism and endocrine signaling (37,41). Three main adipocyte subtypes have been described: white, brown and beige adipocytes (Figure 2) (41,42).

White adipocytes, which constitute the main cellular component of WAT, act as the body´s primary reservoir of energy, storing excess energy in the form of triglycerides (TGs) under anabolic conditions and releasing FFAs during periods of increased energy demand (4,5). Morphologically, white adipocytes are distinguished by the presence of a large lipid droplet and a peripherally located, flattened nucleus (Figure 2A) (4,43).

Brown adipocytes, predominantly found in BAT, are the main adipocytes responsible for heat production through NST, crucial for energy expenditure (44). Whereas white adipocytes arise from distinct mesenchymal progenitor cells residing within the SVF of AT, classical brown adipocytes originate from a $Myf5^+$ myogenic lineage. Brown adipocytes are characterized by their smaller size, multilocular lipid droplets and abundant mitochondria expressing UCP-1 (Figure 2B) (25).

Another category of thermogenic adipocytes comprises beige, or “brite” adipocytes, which have recently attracted considerable attention in obesity research (25). Beige adipocytes closely resemble classical brown adipocytes in both morphology and function (Figure 2C).

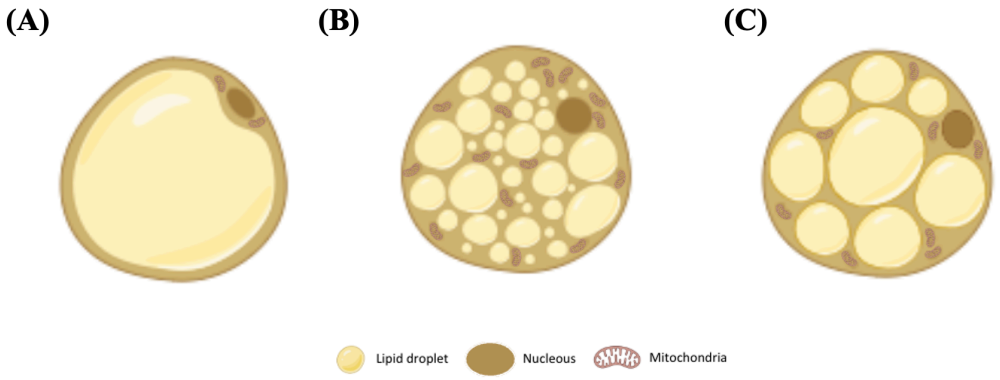


Figure 2. Appearance of adipocytes. (A) White adipocytes act as the body´s energy store, which contain a single lipid droplet, a flattened nucleus situated at the periphery, and low mitochondrial content. **(B)** Brown adipocytes are heat producers, by NST. They are characterized by multilocular lipid droplets, nucleus centrally positioned and a high number of mitochondria. **(C)** Beige adipocytes, generated through *de novo* adipogenesis or transdifferentiation of WAT, resemble brown adipocytes in both structure and function. Adapted from (5).

The emergence of beige adipocytes reflects the remarkable plasticity of WAT and characterizes the process known as WAT browning (Figure 3). Browning can occur through two distinct mechanisms: the transdifferentiation of mature white adipocytes or the de novo differentiation of APCs (Figure 3). Regardless of the underlying mechanism, browning is characterized by profound morphological, transcriptional and metabolic remodeling, whereby adipocytes acquire multilocular lipid droplets, increased mitochondrial content driven by the upregulation of peroxisome proliferator-activated receptor gamma coactivator-1α (PGC1α) and UCP-1, ultimately promoting thermogenesis and energy expenditure (42,45,46). Although transdifferentiation was initially considered the predominant mechanism of WAT browning, accumulating evidence indicates that both transdifferentiation and de novo adipogenesis contribute to beige adipocyte recruitment, with their relative contribution depending on the adipose depot, stimulus and species (25,47). De novo beige adipogenesis originates from distinct progenitor populations, including PDGFRα+/Sca1+ multipotent APCs and MYH11+ smooth muscle-like cells residing within the adipose vasculature (32,33). In contrast, classical brown adipocytes arise from a MYF5+ myogenic lineage, highlighting the distinct developmental origins of beige and classical brown adipocytes (44). Importantly, beige adipocytes exhibit high phenotypic plasticity and can undergo the reverse process, known as whitening, whereby they lose their thermogenic features and acquire a more white adipocyte-like phenotype (Figure 3) (45,48).

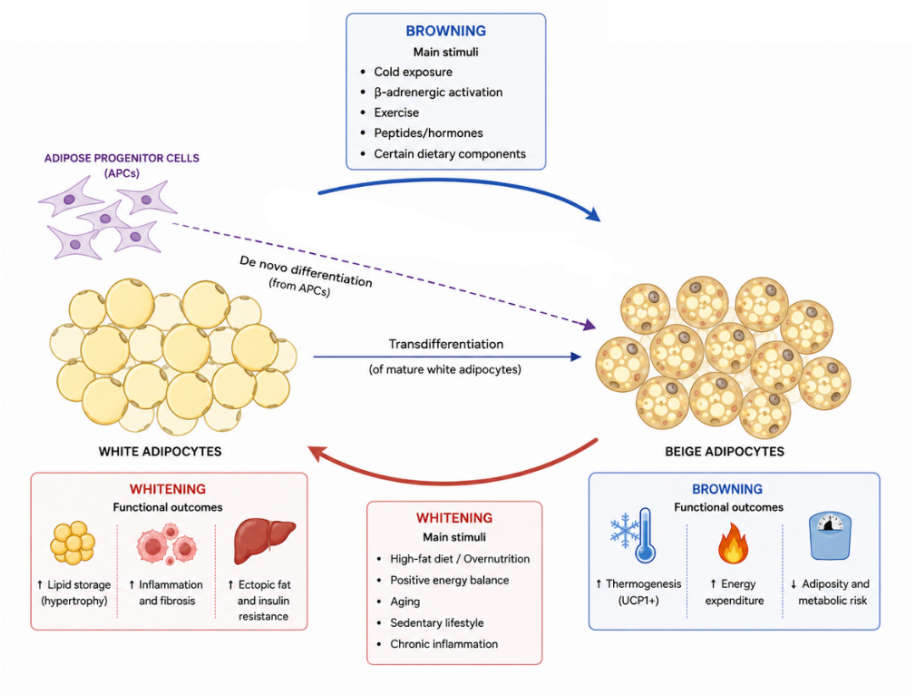


Figure 3. Adipose Tissue plasticity through browning and whitening. Browning of WAT involves the recruitment of thermogenic beige adipocytes through the transdifferentiation of mature white adipocytes or de novo differentiation of APCs. This process can be induced by several physiological and pharmacological stimulus and is associated with increased thermogenesis and energy expenditure. Conversely, whitening involves the loss of the thermogenic phenotype and acquisition of white adipocyte-like characteristics, favoring lipid storage and adipose tissue dysfunction. The balance between browning and whitening illustrates the dynamic phenotypic and metabolic plasticity of AT. Adapted from (45).

1.3. Adipose Tissue as an Endocrine Organ

Beyond its classical function as an energy storage depot, AT secretes a wide range of bioactive molecules into the circulation that communicate with other metabolically active organs such as skeletal muscle, liver, pancreas and brain, thereby contributing to the regulation of energy balance, glucose metabolism and inflammatory responses. These adipose-derived factors include hormones, cytokines, enzymes, growth factors, ECM proteins, as well as regulatory RNAs, including microRNAs (miRNAs) and messenger RNAs (mRNAs) (49,50).

Among these secretory products, adipokines represent a major class of adipose-derived signaling molecules and include factors such as leptin, adiponectin, resistin, plasminogen activator inhibitor-1 (PAI-1), MCP-1, TNF-α and IL-6, many of which have been linked to obesity and its associated metabolic complications (29,49,51).

Despite the broad range of adipokines with diverse biological functions, leptin, adiponectin and resistin are considered the principal adipokines due to their major roles in energy metabolism, insulin sensitivity and inflammatory regulation, which illustrate the central endocrine role of WAT in maintaining whole-body homeostasis (52).

Leptin is one of the most extensively characterized adipokines and its discovery in 1994 represented a breakthrough in the understanding of obesity (46). This hormone, encoded by the *LEP* gene, plays a key role in energy homeostasis by regulating appetite and energy expenditure (51). Leptin acts primarily within the central nervous system after crossing the blood-brain barrier and binding to receptors in the hypothalamus (53). Activation of leptin signaling pathways, including JAK2/STAT3, suppresses appetite by inhibiting orexigenic neurons that produce neuropeptide Y (NPY), while simultaneously stimulating anorexigenic pro-opiomelanocortin (POMC)-expressing neurons, which produce POMC-derived peptides such as α-melanocyte-stimulating hormone (α-MSH) (46). Circulating leptin concentrations are generally proportional to the amount of AT present in the body (5,54). In addition to its central effects on appetite control, leptin also acts on peripheral tissues. For example, it influences pancreatic β-cell function, modulating insulin production and secretion and thereby contributing to the regulation of glucose homeostasis (49).

Adiponectin also exerts several beneficial effects, including enhanced insulin sensitivity, anti-inflammatory activity and protection against cardiovascular diseases (CVD) (29,49,50,55). These effects are mediated, at least in part, through its actions on multiple organs involved in metabolic regulation. In the liver, it activates AMP-activated protein kinase (AMPK), which suppresses the expression of key gluconeogenic enzymes such as phosphoenolpyruvate carboxykinase and glucose-6-phosphatase, thereby reducing hepatic glucose production (49,51). In skeletal muscle, adiponectin also stimulates AMPK signaling, promoting phosphorylation of acetyl-CoA carboxylase (p-ACC), increasing FA oxidation and enhancing glucose uptake (49,51). Through these coordinated actions, adiponectin improves whole-body insulin sensitivity while also exerting anti-inflammatory effects (5). Unlike many other adipokines, circulating adiponectin levels are inversely associated with body fat mass (46).

Resistin has been shown to contribute to systemic insulin resistance by interfering with adiponectin signaling and promoting resistance to FGF21. In addition, resistin stimulates the production of pro-inflammatory mediators such as TNF-α and IL-6, as well as adhesion molecules and chemokines including intercellular adhesion molecule 1 (ICAM1) and vascular cell adhesion molecule 1 (VCAM1). These effects contribute to a pro-inflammatory environment that is associated with an increased risk of cardiometabolic disease. Interestingly, the cellular origin of resistin differs between species: in humans, it is mainly secreted by ATMs, whereas in mice, it is produced primarily by adipocytes (5,29).

BAT, similarly to WAT, also exhibits endocrine activity, by the secretion of a variety of batokines (29). Some classical adipokines, such as leptin and adiponectin, can also function as batokines, but are secreted by BAT at considerably lower levels than by WAT. Among the best-characterized batokines is FGF21, which has attracted significant interest because of its potential therapeutic relevance in metabolic diseases (5,29). Another important batokine is neuregulin-4 (NRG4), that protects against diet-induced insulin resistance and hepatic steatosis by suppressing hepatic lipogenesis (56). BAT also secretes factors such as IL-6 and vascular endothelial growth factor (VEGF), which contribute to local and systemic metabolic regulation and support processes involved in BAT adaptation, including vascular remodeling (2,20,24).

In addition to peptide-based adipokines, AT also secretes lipid-derived signaling molecules known as lipokines. These lipid metabolites, such as C16:1n7-palmitoleate, function as endocrine mediators that influence systemic metabolism by improving insulin sensitivity in skeletal muscle and reducing lipid accumulation in the liver (6,57).

1.4. Adipose Tissue Plasticity and Metabolic Adaptation

AT exhibits remarkable metabolic plasticity, enabling it to adapt its activity to changing environment and physiological demands. This flexibility is tightly regulated by hormonal and neural signals and relies on several key pathways, including adipogenesis, lipogenesis, lipolysis, thermogenesis and browning (6). Together, these processes coordinate energy storage, mobilization and expenditure, thereby contributing to AT function and systemic metabolic homeostasis.

Adipogenesis

The expansion and remodeling of AT occur through two main mechanisms: adipocyte hypertrophy, characterized by an increase in adipocyte size, and adipocyte hyperplasia, characterized by an increase in adipocyte number through adipogenesis, the process by which committed preadipocytes differentiate into mature adipocytes (6,58). While hypertrophic expansion of AT is often associated with adipose dysfunction and metabolic complications, hyperplasia represents a more adaptive mechanism that allows AT to accommodate excess energy in a metabolically healthier manner (58).

Adipogenesis thus contributes to the renewal of adipocytes in AT, supporting tissue plasticity and adaptive responses to changing metabolic demands, including the maintenance of adipocyte number and, under specific stimuli, the formation of beige adipocytes (59).

Adipogenesis involves two main stages. First, mesenchymal stem cells (MSCs) give rise to preadipocytes, which serve as APCs. In the second stage, preadipocytes undergo terminal differentiation into mature adipocytes, accompanied by morphological changes with the progressive accumulation of lipid droplets (60). Because mature adipocytes have limited proliferative capacity *in vivo*, the expansion and renewal of WAT largely depend on the proliferation and differentiation of these precursor cells (60).

Adipocyte differentiation is regulated by a network of transcription factors, with peroxisome proliferator-activated receptor gamma (PPARγ) serving as the master regulator of adipogenesis (49,61,62). The process is initiated by early factors such as CCAAT/enhancer-binding proteins β and δ (C/EBPβ and C/EBPδ), which induce PPARγ and C/EBPα, promoting the expression of adipocyte-specific genes required for maturation (49,60). Adipocyte differentiation is also controlled by a balance between factors that promote or inhibit adipogenesis. . Specific members of Kruppel-like factor (KLF) family including KLF4 and KLF5, bone morphogenetic proteins (BMPs) and early B-cell factor (EBF1) can promote adipocyte differentiation. Conversely, GATA transcription factors, KLF2, C/EBP homologous protein (CHOP), transforming growth factor-β (TGF-β) and preadipocyte factor 1 (Pref1) act as inhibitors of adipogenesis (49,61).

Lipid mobilization

As the major energy reservoir, AT plays a central role in the regulation of lipid storage and mobilization. During periods of nutrient abundance, AT stores excess energy as TGs within adipocyte lipid droplets, whereas during energy demand TGs are hydrolyzed to release FAs into the circulation (63).

Lipogenesis refers to the metabolic process responsible for TG synthesis and storage in adipocytes. This pathway includes both de *novo* FA synthesis from acetyl-CoA as well as the esterification of FAs into TGs (37,49). Insulin is a key regulator of lipogenesis by promoting glucose uptake into adipocytes, which provides substrates for lipid synthesis, while also activating lipogenic transcription factors such as sterol regulatory element-binding protein 1 (SREBP1) and carbohydrate response element-binding protein (ChREBP). These factors promote *de novo* lipogenesis and modulate both lipid and glucose metabolism in AT, thereby influencing whole-body insulin sensitivity (49).

Although adipocytes can synthesize FAs *de novo*, most FAs used for TG synthesis originate from circulating triglyceride-rich lipoproteins such as chylomicrons and very-low-density lipoproteins (VLDL). These circulating TGs are hydrolyzed by lipoprotein lipase (LPL) at the adipocyte surface, releasing FAs that are subsequently internalized by adipocytes and esterified into TGs, with diacylglycerol acyltransferase (DGAT) catalyzing the final step of TG synthesis (49,64). Efficient lipid storage in AT is essential for maintaining metabolic homeostasis. However, excessive accumulation of TGs results in adipocyte hypertrophy, contributing to the development of obesity and metabolic dysfunction (65,66).

In contrast, lipolysis is the catabolic process responsible for the hydrolysis of stored TGs into FFAs and glycerol, providing energy substrates for peripheral tissues during fasting or increased energy demand (67). Lipolysis is regulated by multiple hormonal signals that act through specific receptors on the adipocyte surface. Catecholamines released by the sympathetic nervous system, for example, stimulate lipolysis through β-adrenergic receptors (β-AR), activating cyclic AMP-dependent protein kinase A (PKA) signaling to promote TG breakdown (65,67). Other hormonal regulators, including natriuretic peptides and melanocortins can also directly stimulate lipolysis by binding to their respective receptors expressed on adipocytes (5,63,68–71). Lipolysis

process occurs through a sequential action of lipases, beginning with adipose triglyceride lipase (ATGL), which hydrolyzes TGs to diacylglycerol (DAG). Hormone-sensitive lipase (HSL) subsequently converts DAG into monoacylglycerol (MAG), and finally monoacylglycerol lipase (MGL) generates glycerol and FFAs (72,73). The FFAs released during lipolysis can be further transported to peripheral tissues, where their fate depends on the metabolic demands and stimulation. They can undergo mitochondrial β-oxidation to generate ATP, or, in BAT, they serve as substrates for thermogenesis.

Thermogenesis and browning

Thermogenesis is the process by which brown and beige adipocytes dissipate energy in the form of heat, contributing to body temperature regulation and increased energy expenditure (49,73). This process is mainly mediated by UCP-1, which uncouples oxidative phosphorylation from ATP production by dissipating the proton gradient across the inner mitochondrial membrane, thereby releasing energy as heat (74). In WAT, thermogenic capacity can also be enhanced through browning, characterized by the recruitment and activation of beige adipocytes within white adipose depots (45). Although enhancement of thermogenic AT has shown beneficial metabolic effects in experimental and human studies, its long-term efficacy and clinical applicability as a therapeutic strategy remain to be established (75).

Thermogenic activity and WAT browning can be stimulated by several physiological and pharmacological stimuli, including cold exposure, exercise, natriuretic peptides, dietary components, β-adrenergic and melanocortin signaling (45,70,74,76). Cold exposure represents one of the most extensively studies activators of thermogenic AT. In response to cold, norepinephrine released from sympathetic nerve endings binds to β-AR on adipocytes, triggering signaling pathways that stimulate lipolysis and induce the expression of thermogenic genes, such as PGC1α, Iodothyronine deiodinase type 2 (DIO-2), PRDM16 (5,65). In humans, cold-induced BAT and pharmacological β-adrenergic stimulation has been associated with increased energy expenditure and glucose uptake, as well as improvements in glucose homeostasis and insulin sensitivity (77,78).

Melanocortins also contribute to thermogenic and browning regulation through central and peripheral mechanisms. Centrally, α-MSH activates melanocortin receptors, particularly MC4R, in the hypothalamus, increasing sympathetic activity in BAT and promoting thermogenesis (79,80). In addition, peripheral administration of α-MSH has been shown to act on melanocortin receptors expressed in WAT, promoting browning and the expression of thermogenesis-associated markers (81,82).

2. Aging- Associated Remodeling and Dysfunction of Adipose Tissue

Despite its remarkable plasticity, AT is susceptible to progressive structural and functional alterations that can compromise its ability to adapt to changing physiological demands (83). This decline in AT function is increasingly recognized as a feature of chronological aging, a biological process characterized by the progressive decline in physiological function across multiple tissues and organs and associated with an increased risk of chronic diseases and mortality worldwide (83). Age-associated alterations in AT may therefore contribute to the disruption of tissue homeostasis and the development of metabolic dysfunction (84–86).

2.1. Age-Related Changes in Adipose Tissue Distribution and Architecture

Aging is accompanied by profound changes in body composition that become increasingly evident during middle age (approximately between 40 and 60 years), characterized by a progressive increase in total fat mass, a decline in lean body mass and a redistribution of AT depots (83). Age-associated AT redistribution is characterized by increased VAT and progressive loss of SAT (6,83). These alterations have important metabolic consequences, as SAT is considered metabolically protective, whereas excessive VAT accumulation is strongly associated with insulin resistance, CVD, and type 2 diabetes mellitus (T2DM) (83,87). The decline in SAT mass is accompanied by a progressive loss of its endocrine function, resulting in reduced secretion of adiponectin and other metabolically beneficial adipokines, and increased leptin levels, often accompanied by leptin resistance (46,83,87).

With aging, the adipogenic capacity of AT progressively declines, in part due to the accumulation of senescent cells (SCs) within the tissue (88). In particular, preadipocytes are particularly susceptible to senescence, exhibiting reduced

proliferative and differentiation capacity alongside decreased expression of adipogenic regulators such as PPARγ and C/EBPα (16,88). Impaired pre-adipocyte function consequently limits the formation of new adipocytes and reduces the capacity for adipocyte hyperplasia, favoring the hypertrophic expansion of existing adipocytes and compromising AT remodeling (83,84). Adipocyte hypertrophy is accompanied by local hypoxia as tissue expansion is not adequately supported by an efficient vascular network (10,46,89). In response to low oxygen levels, hypoxia-inducible factor 1α (HIF-1α), a key regulator of oxygen homeostasis, is activated and promotes a compensatory angiogenic response through the upregulation of VEGF. However, this response is often insufficient in aging and metabolic diseases, resulting in persistent hypoxia (37,89). Sustained hypoxia promotes the expression of pro-inflammatory genes and excessive ECM deposition, leading to increased tissue rigidity and fibrosis, hallmarks of dysfunctional AT (3,7,90).

The development and resolution of fibrosis depend on the balance between ECM deposition and degradation, which is tightly regulated under physiological conditions. In a healthy state, fibrosis resolution involves the activation of proteolytic enzymes, such as matrix metalloproteinases (MMPs), including MMP3 and MMP14, which promote ECM degradation and enable tissue repair and renewal (9,10). However, aging-associated metabolic dysfunction, chronic inflammation and hypoxia drive a maladaptive fibrotic response characterized by reduced MMPs activity and increased expression of tissue inhibitors of metalloproteinases (TIMPs), particularly TIMP1, thereby impairing ECM remodeling (9,91). As a result, fibrotic remodeling leads to impaired lipid storage capacity, increased tissue stiffness and reduced metabolic flexibility (7,91).

2.2. Age-Related Alterations in Adipose Tissue Metabolism

With aging, lipid handling by AT becomes progressively impaired. In particular, the reduced expandability of SAT limits its capacity to safely accommodate excess lipids, weakening its role as the primary lipid-buffering depot and promoting lipid redistribution towards VAT and other metabolic organs (92). At the same time, aging alters the regulation of lipolysis, impairing the ability of adipocytes to appropriately mobilize stored lipids in response to metabolic cues. Although total lipolytic activity

may increase with greater fat mass, adipocytes can exhibit impaired catecholamine-stimulated lipolysis and reduced responsiveness to lipolytic stimuli, contributing to metabolic inflexibility and AT dysfunction (65,68).

At the molecular level, these alterations are associated with defects in β-adrenergic signaling, including reduced β-AR expression and decreased activity of key lipolytic enzymes such as HSL and ATGL (6), thereby impairing the capacity of adipocytes to appropriately respond to metabolic demands. Impaired HSL expression and activity have been consistently observed in metabolically dysfunctional adipocytes, suggesting that defective lipolysis may represent an early feature of AT dysfunction (68,93).

The combined impairment of lipid storage and lipolytic regulation led to chronically elevated circulating FFA levels, favoring ectopic lipid deposition in peripheral tissues. This lipid overload promotes lipotoxicity, mitochondrial dysfunction, chronic inflammation, insulin resistance and apoptosis, thereby accelerating the progression of age-associated diseases (65,83,94,95). Age-related progressive mitochondrial dysfunction contributes to impaired FFAs β-oxidation and is accompanied by reduced UCP-1 expression and BAT activity, defective WAT browning and a progressive shift from a thermogenic toward a more white-like adipocyte phenotype (77). Furthermore, the age-related decline in sympathetic nervous system activity further contributes to reduced thermogenesis by attenuating β-adrenergic stimulation of the thermogenic adipocytes (46).

2.3. Inflammaging and adipaging

A key feature of aging is the persistent low-grade systemic inflammation, commonly referred to as inflammaging (2,7). This chronic inflammatory state is characterized by dysregulated production of inflammatory mediators, including pro-inflammatory cytokines and chemokines that can impair the ability of the immune system to efficiently resolve inflammation, thereby contributing to metabolic dysfunction and age-related diseases (29). AT is particularly affected by this age-associated inflammatory shift. The progressive disruption of AT homeostasis and function that accompanies aging has been referred to as adipaging, reflecting the accumulation of changes in adipocyte function, adipokine secretion, immune cell composition, and inflammatory status within AT (2). This local inflammatory milieu is accompanied by

profound alterations in adipokine secretion, including increased production of pro-inflammatory mediators such as C-reactive protein (CRP), TNF-α, IL-1β, IL-6, IL-8, leptin, resistin and MCP-1, together with reduced levels of anti-inflammatory factors such as IL-4, IL-10 and adiponectin (46).

Adipaging drives extensive immune cell remodeling within AT, characterized by changes in both the abundance and phenotype of resident immune cell population, ultimately promoting a pro-inflammatory immune microenvironment (96). Age-related increase infiltration of immune cells, such as T and B lymphocytes and macrophages, further amplifies local cytokine production and sustain chronic inflammation. One of the most prominent features of the age-related AT remodeling is the phenotype switch of resident anti-inflammatory M2 macrophages toward a pro-inflammatory M1 phenotype. These M1 macrophages impair adipocyte function through the secretion of pro-inflammatory cytokines, including TNF-α, IL-6, IL-1β and PAI-1. Their accumulation around dead or dying adipocytes also contributes to the formation of crown-like structures (CLS), a hallmark of AT dysfunction (46,90,97).

Increasing evidence suggests that oxidative stress is one of the major contributors to the development of inflammaging (96,98). Oxidative stress arises from an imbalance between the production of reactive oxygen species (ROS) and the antioxidant defense system, leading to excessive ROS accumulation and oxidative damage to cellular components (98). Mitochondria are particularly susceptible to oxidative damage, which can impair oxidative phosphorylation and ATP production while increasing ROS generation (99). Mitochondrial dysfunction can thus increase oxidative stress, while elevated ROS can activate redox-sensitive inflammatory pathways, such as NF-κB, promoting the production of pro-inflammatory mediators (100). Conversely, inflammatory cytokines can further stimulate ROS generation, establishing a self-reinforcing cycle between oxidative stress and inflammation that may exacerbate AT dysfunction during aging (96,100). Interestingly, this concept is supported by the oxidation-inflammation theory, which proposes that both oxidative stress and chronic inflammation reinforce the mechanisms driving aging and the development of age-associated diseases (101,102).

3. Obesity as a Driver of Adipose Tissue Aging

Several features of AT dysfunction associated with aging are also observed in obesity, suggesting shared mechanisms underlying the progressive loss of AT homeostasis (2).

3.1. Obesity-Induced Adipose Tissue Dysfunction

Obesity is a chronic, complex and multifactorial disease that has emerged as a major global health concern, reaching pandemic proportions (103). In adults, obesity is conventionally defined by a BMI ≥ 30 kg/m^2, although BMI alone does not fully reflect adiposity, fat distribution or metabolic health (104). Importantly, obesity extends beyond excessive body weight and is characterized by profound alterations in metabolic and tissue homeostasis, increasing the risk of several comorbidities, including CVD, T2DM and other complications (105). Obesity develops in the context of a sustained positive energy balance, in which chronic nutrient excess promotes progressive expansion and remodeling of AT (106). During chronic overnutrition, AT expands through adipocyte hypertrophy and hyperplasia to accommodate excess energy. However, when adipogenic capacity becomes impaired, the formation of new adipocytes is limited, placing greater demands on existing adipocytes and promoting their excessive hypertrophy (106,107). This maladaptive expansion can compromise local vascular support, leading to hypoxia and increased cellular stress, and ultimately contributing to AT dysfunction with consequences for both local and systemic metabolic homeostasis (108). Nutrient excess further imposes metabolic stress on adipocytes, promoting oxidative and endoplasmic reticulum stress, mitochondrial dysfunction and altered adipokine secretion (108).These stress responses activate inflammatory pathways and promote the release of pro-inflammatory mediators, while the recruitment and activation of immune cells, particularly macrophages, further amplify inflammatory signaling within AT (109,110). When sustained, this inflammatory and stress-associated environment promotes excessive ECM deposition and fibrotic remodeling of AT (111). Increased fibrosis progressively limits tissue expandability, further restricting the capacity of adipocytes to accommodate excess lipids and thereby perpetuating AT dysfunction (111,112).

3.2. Obesity as a Model of Accelerated Aging

Although aging and obesity represent distinct biological conditions, they share several cellular and molecular alterations that converge in AT dysfunction (113). Beyond these similarities, increasing evidence suggests that obesity may accelerate aging-related processes, leading to an earlier onset of age-associated chronic diseases and multimorbidity (7).

Evidence supporting this relationship has emerged from studies of epigenetic aging. Epigenetic clocks estimate biological age based on age-associated DNA methylation patterns and can therefore identify deviations between chronological age and biological age (114). In human AT, obesity has been associated with accelerated epigenetic aging, with each 10-unit increase in BMI corresponding to approximately 2.3 additional years of epigenetic age (114).

Telomere attrition provides additional evidence linking obesity with accelerated biological aging (115). Telomere shortening is a well-established feature of cellular aging and is influenced by chronic oxidative and inflammatory stress (116). A large meta-analysis of 146 144 individuals associated higher BMI with shorter leukocyte telomere length, providing further evidence of an association between obesity and biological aging (117).

These molecular features are accompanied by an earlier decline in tissue function. As described above, obesity and aging converge on several aspects of AT dysfunction, including reduced adipogenic capacity and metabolic flexibility, impaired mitochondrial and thermogenic function, altered insulin responsiveness and intercellular communication, and increased ECM remodeling and fibrosis (87,118,119). Collectively, these alterations reflect a premature loss of AT function capacity in obesity that resembles the progressive tissue dysfunction observed during aging (Figure 4).

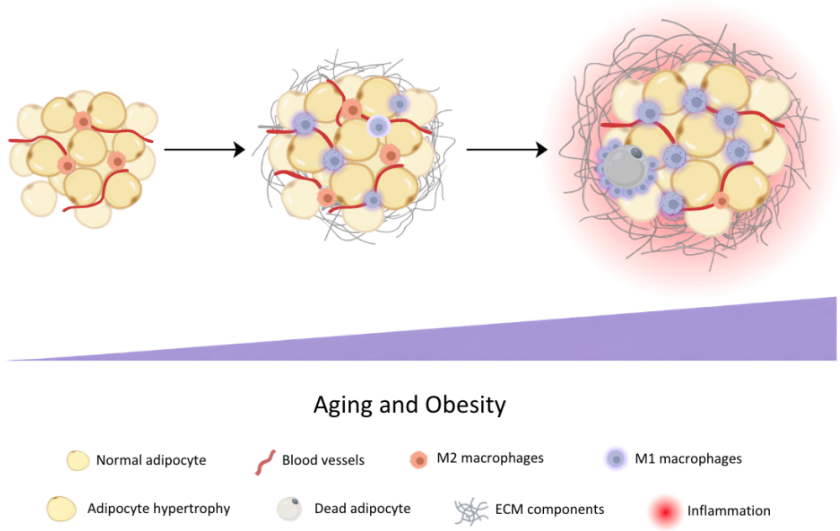


Figure 4. Adipose tissue remodeling during aging and obesity. Under health conditions, AT expansion is mediated via adipocyte hyperplasia, supported by adequate angiogenesis and balanced ECM remodeling. Resident anti-inflammatory M2 macrophages maintain tissue homeostasis and suppress inflammation. However, either the progressive expansion of AT along obesity or the metabolic stress observed during chronological aging shift this balance toward adipocyte hypertrophy, that is often accompanied by local hypoxia, due to insufficient angiogenesis. Hypoxia stabilizes HIF-1α, which promotes inflammatory genes expression and increases tissue stiffness and diminishes metabolic flexibility. Prolonged AT hypertrophy promotes the recruitment of pro-inflammatory M1 macrophages, which aggregate around dead or dying adipocytes to form CLS. Consequently, this severely dysfunction of AT contributes to significantly metabolic dysfunction, which leads to metabolic syndrome. Adapted from (46).

At the clinical level, obesity is associated with the earlier development of age-related diseases, including type 2 diabetes, hypertension, CVD, chronic kidney disease, and certain cancers, as well as with increased multimorbidity (120). Notably, the prevalence of complex multimorbidity observed at 75 years in individuals with healthy weight was already reached at approximately 55 years in individuals with obesity, representing an advancement of approximately 20 years (120). Individuals with obesity also had more than a 5-fold higher risk of simple multimorbidity and a more than 12-fold higher hazard of complex multimorbidity (120).

3.3. Therapeutic Approaches to Obesity and Adipose Tissue Dysfunction

3.3.1. Lifestyle and Pharmacological Interventions for Obesity

Obesity management requires a multifactorial approach aimed not only at reducing body weight, but also at improving metabolic health and preventing obesity-related complications. Lifestyle interventions, particularly dietary modification and physical activity are commonly recommended as first-line strategies to reduce energy intake and increase energy expenditure, respectively (152). By promoting a sustained negative energy balance, these interventions can reduce body weight and adiposity and improve metabolic parameters, including glycemic control, lipid profile and insulin sensitivity

(153). Regular exercise has also been associated with attenuation of obesity-associated inflammation (154).

Despite these beneficial effects, the complex and heterogeneous nature of obesity often requires additional therapeutic strategies to achieve sustained weight loss and metabolic improvement (156).

Among these, pharmacological therapies have become an increasingly important component of obesity management, particularly with the recent development of incretin-based treatments (157). The incretin hormones glucagon-like peptide-1 (GLP-1) and glucose-dependent insulinotropic polypeptide (GIP) are released from the gastrointestinal tract in response to nutrient intake and play an important role in glucose homeostasis by stimulating glucose-dependent insulin secretion (158). In addition to its incretin effects, GLP-1 contributes to the regulation of appetite and energy intake by promoting satiety and delaying gastric emptying, making the GLP-1 signaling pathway an important therapeutic target for obesity (157).

Accordingly, GLP-1 receptor agonists (GLP-1RAs), such as semaglutide, mimic and prolong the actions of endogenous GLP-1, whereas tirzepatide simultaneously activates GIP and GLP-1 receptors (159). Semaglutide is commercially available in Europe as Ozempic®, approved for the treatment of T2DM (160), and as Wegovy®, approved for weight management in adults with BMI $\geq$ 30 kg/m^2 or a BMI $\geq$ 27 and < 30 kg/m^2 in the presence of at least one obesity-related comorbidity (161). Tirzepatide, marked as Mounjaro®, is approved for the treatment of T2DM and for weight management under the same BMI criteria (162). These therapies have demonstrated substantial reductions in body weight and adiposity, accompanied by improvements in glycemic control and several cardiometabolic outcomes (163).

3.3.2. Bariatric Surgery

Bariatric surgery represents one of the most effective therapeutic strategies for achieving substantial weight loss, particularly when lifestyle and pharmacological interventions are ineffective to control obesity-related complications (164). According to current guidelines, bariatric surgery is recommended for individuals with a BMI $\geq$ 35 kg/m², regardless of the presence or severity of obesity-related comorbidities and should also be considered in individuals with a BMI of 30-34.9 kg/m² presenting

metabolic disease or insufficient response to non-surgical interventions (164). Procedures such as sleeve gastrectomy and Roux-en-Y gastric bypass induce marked and sustained reductions in body weight and adiposity and are associated with long-term improvements in obesity-related morbidity and mortality (165).

Substantial improvements in glucose homeostasis, insulin sensitivity, lipid metabolism and cardiovascular risk are frequently observed following surgery, together with remission or improvement of obesity-associated comorbidities such as T2DM, hypertension and dyslipidemia (166). Importantly, these metabolic benefits of bariatric surgery involve mechanisms beyond those resulting from weight loss alone, including changes in gastrointestinal physiology and enteroendocrine signaling (167). Both sleeve gastrectomy and Roux-en-Y gastric bypass alter postprandial gut hormone responses, including enhanced GLP-1 secretion, which contributes to improved glucose homeostasis (167,168). Indeed, these profound effects on metabolic health have led to the broader concept of metabolic and bariatric surgery (MBS), emphasizing that its therapeutic benefits extend beyond weight reduction (164).

3.3.3. Limitations of Current Therapeutic Approaches

Despite the substantial improvements in body weight and metabolic health achieved with current obesity therapies, long-term maintenance of these benefits remains a major challenge. Weight regain is common following lifestyle-based weight loss, reflecting the biological adaptations that oppose sustained weight reduction and favor the recovery of lost weight (169). Similarly, discontinuation of pharmacological treatment, particularly incretin-based therapies, is frequently followed by substantial weight regain and partial reversal of the cardiometabolic improvements achieved during treatment (170). Weight regain may also occur following bariatric surgery, and some metabolic benefits achieved following surgery are not necessarily permanent. Indeed, although bariatric surgery can induce remission of obesity-associated comorbidities, particularly T2DM, disease recurrence has been reported in some patients following initial remission (171,172).

Importantly, weight loss and improvement in systemic metabolic parameters do not necessarily imply complete restoration of AT homeostasis. Although substantial weight reduction can reverse several obesity-associated alterations, increasing evidence

suggests that specific cellular and molecular features of dysfunctional AT may persist after weight loss (173). The persistence of obesity-associated alterations has led to the emerging concept of an AT memory, whereby previous exposure to obesity leaves persistent molecular, cellular or epigenetic alterations that influence subsequent tissue responses (173).

Recent studies have provided evidence supporting this concept. Following weight loss, AT undergoes extensive remodeling, including reductions in adipocyte size and macrophage infiltration. However, specific obesity-associated cellular states and transcriptional programs may persist, indicating that the tissue is not necessarily restored to its pre-obesity state (169). Such persistent alterations may influence the metabolic responsiveness of AT and potentially increase susceptibility to weight regain and metabolic deterioration upon renewed nutritional excess (173).

Therefore, although current therapeutic approaches effectively reduce adiposity and improve systemic metabolic health, they may not completely reverse the cellular and molecular alterations established within dysfunctional AT. Understanding and targeting these persistent changes may provide an important complementary strategy to conventional weight-loss interventions, with the aim of promoting a more complete and durable restoration of AT homeostasis.

4. Cellular Senescence: A hallmark of Adipose Tissue Dysfunction

Cellular senescence has emerged as a key driver of AT dysfunction in both aging and obesity, affecting multiple aspects of AT metabolic function (88,119). This accumulation reflects the combined effects of increased senescence induction, driven by chronic metabolic and cellular stress, and impaired immune-mediated recognition and clearance of SCs (119). As a result, SCs progressively persist within AT, where their altered secretory profile can disrupt tissue homeostasis and exacerbate AT dysfunction. Importantly, senescence occurs in both visceral and subcutaneous adipose depots and is not restricted to a single cell population, but can affect several other cellular components, including mature adipocytes, APCs/preadipocytes, ECs and immune populations within the SVF (16). Consequently, the accumulation of SCs can compromise adipocyte function through both cell-autonomous alterations and paracrine effects on neighboring cells.

4.1. Molecular Features and Mechanisms of Cellular Senescence

Cellular senescence is characterized by a stable and irreversible cell-cycle arrest and resistance to apoptosis, while cells remain metabolically active and undergo extensive phenotypic and metabolic changes (121). A defining feature of SCs is the senescence-associated secretory phenotype (SASP), which comprises a diverse array of bioactive factors, including pro-inflammatory cytokines, chemokines, growth factors, and ECM-remodeling proteins (122,123). The composition and magnitude of the SASP vary according to the cell type and the nature and duration of the inducing stress, and its secretory profile can profoundly influence the surrounding tissue microenvironment (124,125). Among its major components are pro-inflammatory cytokines (such as IL-6, IL-8, IL-1α, and TNF-α), chemokines (e.g., MCP-1), MMPs, and growth factors (TGF-β and VEGF) (Figure 5) (126,127). The SASP is regulated by a complex network of transcriptional and signaling pathways, including transcription factors such as NF-κB, GATA binding protein 4 (GATA4) and C/EBPβ, as well p38 mitogen-activated protein kinase (MAPK), mechanistic target of rapamycin (mTOR) and the cyclic GMP-AMP synthase-stimulator of interferon genes (cGAS-STING) axis (126–131). Although transient SASP expression can contribute to tissue repair and remodeling, its persistent activation promotes inflammaging and can propagate senescence to neighboring cells through paracrine signaling (132).

A broad spectrum of morphological and molecular alterations further characterizes SCs. These include an enlarged and flattened morphology, increased lysosomal content, mitochondrial alterations and nuclear changes, including dysregulation of Lamin B1 and chromatin reorganization, which may involve the formation of Senescence-Associated Heterochromatin Foci (SAHF) (Figure 5) (132,133). These changes are accompanied by increased expression of cell-cycle regulators such as $p16^{INK4A}$ and $p21^{CIP1}$, as well as increased senescence-associated β-galactosidase (SA-β-gal) activity at pH 6.0, one of the most widely used markers of cellular senescence (Figure 5) (134). Importantly, accumulating evidence indicates that no single marker is universally specific for cellular senescence, supporting the combined assessment of multiple senescence-associated features for the identification of SCs (121,133).

Cell senescence can be triggered by multiple internal and external stressors, including persistent DNA damage, telomere shortening or dysfunction, replicative stress,

oxidative stress, epigenetic alterations and exposure to cytotoxic agents (Figure 5) (132,133). Although the molecular response varies according to the nature of the senescence-including stimulus, many of these stressors converge on the activation of the DNA Damage Response (DDR), a cellular surveillance mechanism responsible for detecting DNA lesions and coordinating DNA repair and cell-cycle checkpoints (132). When DNA damage is persistent and irreparable, sustained DDR signaling can promote the establishment of senescence, thereby preventing the proliferation of damaged cells (128). The DDR is primarily coordinated by the phosphoinositide 3-kinase-related kinases Ataxia-Telangiectasia Mutated (ATM) and ATM- and Rad3-related (ATR). While ATM is recruited to DNA double-strand breaks (DSBs), ATR responds to single-stranded DNA coated by Replication Protein A (RPA) at stalled replication forks (135,136). Activation of these kinases promotes the phosphorylation of histone H2AX (γH2AX), and activation of the checkpoints kinases CHK1 and CHK2, ultimately transmitting the damage signal to cell-cycle regulatory mechanisms (136,137).

These signaling cascades converge on two major tumor suppressor axes: the p53/$p21^{CIP1}$ and $p16^{INK4A/pRB}$ pathways (126). Activation of p53 induces the expression of the cyclin-dependent kinase inhibitor (CDKI) p21, leading to cell cycle arrest in the G1 phase (133,135,138). Concurrently, p16 inhibits CDK4/6, maintaining the retinoblastoma protein (Rb) in a hyperphosphorylated state and preventing S-phase entry (128,132,133,138). Together, these mechanisms contribute to the establishment and maintenance of the stable proliferative arrest characteristic of cellular senescence (126).

SCs can persist within tissues for prolonged periods due in part to their increased dependence on specialized Senescent Cell Anti-Apoptotic Pathways (SCAPs), which provide resistance to apoptosis through the upregulation of pro-survival pathways, including members of the B-cell lymphoma-2 (BCL-2) family and other anti-apoptotic regulators (139). This survival advantage, together with an age-associated decline in immune-mediated clearance, can promote the progressive accumulation of SCs within tissues. According to the threshold theory of cellular senescence, low numbers of these cells can be tolerated and may participate in physiological processes, whereas their excessive or persistent accumulation drives to tissue dysfunction and age-related diseases (139).

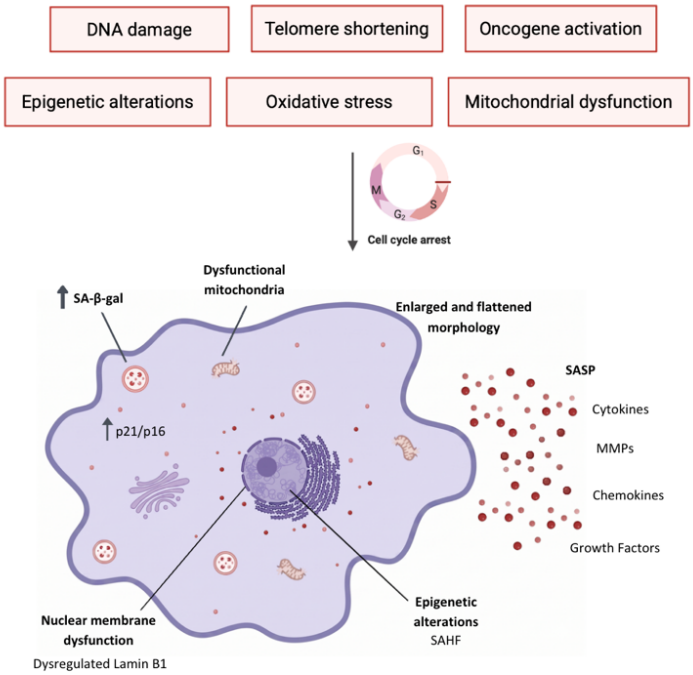


Figure 5. Inducing mechanisms and phenotypic hallmarks of cellular senescence. Internal and external factors can trigger the senescent state, including DNA damage, telomere shortening, oncogene activation, epigenetic alterations, oxidative stress and mitochondrial dysfunction. These stimuli induce persistent cell cycle arrest, leading to senescence. Senescent cells are characterized by an enlarged and flattened morphology and are associated with an increase of SA-β-gal activity, upregulated p21/p16, mitochondrial dysfunction, nuclear dysfunction characterized by dysregulated Lamin B1 and epigenetic alterations, leading to the formation of SAHF. Adapted from (144).

4.2. Cellular Senescence in Adipose Tissue

Within AT, APS and preadipocytes appear to be particularly susceptible to cellular senescence and represent an important senescent population within aging and dysfunctional AT (119). Activation of senescence-associated cell-cycle arrest restricts their proliferative capacity and impairs adipogenic differentiation, thereby limiting the generation of new functional adipocytes (119,140). This loss of adipogenic capacity may favor expansion through hypertrophy of existing adipocytes rather than

hyperplasia. Importantly, the consequences of progenitor senescence extend beyond the affected cells themselves. Senescent APCs can secrete factors such as activin A, which inhibit adipogenic differentiation of neighboring non-senescent progenitors, further exacerbating AT dysfunction (88).

Although mature adipocytes are traditionally considered post-mitotic cells, increasing evidence indicates that they can also acquire a senescence-like phenotype in response to metabolic stress (141). Under conditions such as obesity and hyperinsulinemia, mature adipocytes may re-enter a cell cycle-like program that is subsequently associated with activation of senescence-related pathways (141). Consistent with this, mature adipocytes from individuals with obesity exhibit increased expression of senescence-associated makers, including SA-β-Gal, p16, p53 and PAI-1, together with activation of stress-related signaling pathways such as JNK (142). These alterations are accompanied by a reduction in key adipogenic and metabolic regulators, including PPARγ and GLUT4, alongside impaired insulin signaling, as reflected by decreased AKT phosphorylation (142), thereby compromise adipocyte's capacity to appropriately respond to metabolic and hormonal signals.

Importantly, cellular senescence is not confined to adipocytes or their progenitor cells but can occur across multiple cellular components of AT, potentially affecting their coordinated interactions. Senescence of ECs can impair angiogenic and vascular function compromising the exchange of nutrients and lipids between the circulation and adipocytes (143,144). Senescence of immune cells adds further complexity to the relationship between cellular senescence and immune dysfunction in aging AT (16).

The accumulation of SCs across different cellular compartments can progressively reshape the AT microenvironment through the SASP. Persistent secretion of pro-inflammatory cytokines and chemokines can promote local inflammatory signaling and immune cell recruitment, contributing to the chronic low-grade inflammatory state characteristic of aged and obese AT (113,119). SASP signaling can also affect ECM remodeling through mediators such as TGF-β and MMPs, which can modify ECM turnover and contribute to the profibrotic features observed in dysfunctional AT (145,146).

At the metabolic level, AT senescence has been associated with impaired insulin signaling, altered adipokine secretion and disturbances in lipid handling, including changes in the capacity to store and mobilize lipids (147,148). Senescence-associated mitochondrial dysfunction may additionally compromise oxidative metabolism and thermogenic competence, further reducing the ability of AT to adapt to changes in energetic demand (149,150). Through these changes, together with the altered release of inflammatory mediators, adipokines and metabolites, senescent AT may contribute to systemic metabolic disturbances, including insulin resistance and ectopic lipid accumulation (143,144,151).

Overall, the presence of SCs across different AT cellular components may therefore contribute to the persistence and progression of AT dysfunction during aging and obesity (7,16). This had provided a rationale for investigating whether targeting cellular senescence can attenuate these alterations and improve AT function.

4.3. Senotherapeutic Potential and Limitations

4.3.1. Senolytic and Senomorphic Strategies

The growing recognition of cellular senescence as an important contributor to aging and age-related diseases has stimulated the development of therapeutic strategies targeting SCs (174). These approaches, collectively known as senotherapeutics, aim either to selectively eliminate SCs or to attenuate their detrimental effects on surrounding tissues (174). Senotherapeutic strategies can therefore be broadly divided into senolytics, which selectively induce the death of SCs, and senomorphics, also referred to as senostatics, which suppress or modulate the senescent phenotype, particularly the SASP, without necessarily eliminating the cells (139,174,175).

Senolytics act through multiple mechanisms, primarily targeting pro-survival pathways, particularly SCAPs, thereby inducing apoptosis of SCs (175). Several components of these pro-survival networks have been identified as potential senolytic targets, including BCL-2 family members, PI3K/AKT and tyrosine kinase signaling, FOXO4-p53 interactions and heat shock proteins (176).

In contrast, senomorphic strategies primarily modulate pathways involved in SASP production and secretion, including NF-κB, p38 MAPK, mTOR and JAK/STAT

signaling, thereby limiting chronic inflammation and the paracrine effects of senescence (174).

The therapeutic potential of senolytics has been extensively investigated in preclinical models of aging. In naturally aged mice, pharmacological clearance of SCs has been shown to reduce senescent cell (SC) burden, improve physical function and attenuate age-related tissue dysfunction, supporting the potential of senolytic strategies to extend healthspan (177–179). Additional studies have demonstrated beneficial effects in specific age-associated conditions, including preservation of bone mass and function following SC targeting (180). Together, these findings support the concept that selective elimination of SCs may represent a promising strategy to delay or alleviate multiple features of age-related dysfunction (181).

Translation of senolytic therapies into humans remains at an early stage, but initial clinical studies have shown promising results. Short-term administration of senolytics has been shown to reduce markers of SC burden in humans, while pilot clinical trials in age-related diseases have generally demonstrated acceptable tolerability without identifying major treatment-related safety concerns (175,182). However, current clinical evidence remains limited, and larger controlled trials are required to establish the long-term efficacy and safety of senolytic therapies (183).

4.3.2. Senolytic Approaches in Adipose Tissue

Among the senolytic approaches in AT, the combination dasatinib and quercetin (D+Q) is one of the most studied senolytic therapies (175). Dasatinib is a tyrosine kinase inhibitor capable of suppressing cell proliferation and inducing apoptosis, whereas quercetin is a naturally occurring flavonoid that targets multiple signaling pathways, including PI3K and BCL-2 family-related survival mechanisms (174).

Importantly, the response to senolytic treatment is highly dependent on the cellular context, as SCs are heterogeneous and may rely on different pro-survival pathways depending on cell type and senescence-inducing stimulus (183). Consequently, individual senolytic compounds do not exhibit equivalent activity across all SC populations. This heterogeneity provides a rationale for combining senolytics with complementary activity. Indeed, dasatinib shows greater efficacy against senescent preadipocytes, whereas quercetin preferentially targets senescent ECs (184). Their

combination therefore broadens the range of SC populations that can be targeted compared with either compound alone (184).

The senolytic effects of D+Q have been demonstrated in adipocyte cellular models. In senescent 3T3-L1 adipocytes, D+Q treatment promoted the selective elimination of SCs and reduced senescence-associated features, supporting its senolytic activity directly in adipocytes (185).

Beyond cellular models, D+Q has also demonstrated a reduction in SC burden in AT. In human VAT explants obtained from individuals with obesity undergoing bariatric surgery, D+Q treatment for 48 h reduces senescent-associated markers such as p16 and SA-β-gal, together with decreased SASP factor expression and AT inflammation (177). Importantly, evidence of senolytic activity has also been reported *in vivo* in humans, where a three-day oral treatment with D+Q reduced senescence-associated markers in SAT, accompanied by decreased macrophage abundance and CLS formation (175).

In mouse models, intermittent oral administration of D+Q has also been shown to improve AT and systemic metabolic function. In diet-induced obese mice, D+Q administrated by oral gavage in intermittent treatment cycles reduced AT inflammation, improved glucose tolerance and insulin sensitivity, and promoted adipogenesis (186). Similarly, in old mice, oral gavage of D+Q for three consecutive days every two weeks for three months attenuated senescence and inflammation in perigonadal WAT and improved systemic glucose and lipid metabolism (187). Notably, the metabolic improvements observed in obese mice were not accompanied by a reduction in body weight (186).

4.3.3. Limitations of Senotherapeutics Targeting Adipose Tissue Dysfunction

Despite the promising effects of senolytic interventions, important questions remain regarding the extent to which SC clearance translates into functional recovery of dysfunctional tissues. Preclinical studies have demonstrated that D+Q can effectively reduce senescence-associated markers and attenuate several age-related phenotypes, with senolytic treatment also increasing longevity (175,177). However, elimination of SCs does not necessarily imply complete restoration of tissue function.

In AT, senolytic treatment has been associated with reduced SASP signaling and inflammation, as well as improvements in systemic glucose tolerance and insulin sensitivity (186). These effects suggest that reducing the senescent and inflammatory burden can alleviate important components of AT dysfunction. Nevertheless, the direct effects of senolytic treatment on several key functional properties of AT remain poorly characterized (187). In particular, whether SC clearance is sufficient to restore adipocyte lipid handling, thermogenic capacity and metabolic flexibility has not been fully established. Similarly, although reduced senescence-associated inflammation may favor a less profibrotic environment, evidence that senolytic treatment can reverse established AT fibrosis and restore tissue plasticity remains limited (187).

Importantly, the AT improvements reported following D+Q treatment have not consistently been accompanied by changes in body weight in obese animals (186). This suggests that targeting cellular senescence, while capable of alleviating several components of AT dysfunction, may not be sufficient to reverse all features of the obese phenotype. Senolytic treatment may therefore benefit from complementary strategies that directly stimulate metabolic processes that remain impaired. Such an approach could simultaneously reduce the contribution of SCs to tissue dysfunction and promote the recovery of specific metabolic functions of AT.

Aims

Despite the beneficial effects of senolytic treatment on several features of AT dysfunction, evidence that targeting cellular senescence alone is sufficient to restore specific metabolic functions remains limited. The lack of a consistent effect of D+Q on body weight in obese animals, despite improvements in several metabolic parameters, further suggests that senolytic treatment may not fully address the metabolic consequences of obesity. Based on this rationale, the present study hypothesized that combining senolytic treatment with lipolytic stimuli could reduce senescence-associated AT dysfunction and facilitate the metabolic response to lipolytic stimulation.

D+Q were used to target SCs, whereas α-MSH (M) and isoproterenol (I) were used as lipolytic stimuli acting through melanocortin and β-adrenergic signaling, respectively (71,81,188–190). Specifically, the present study aimed to determine the effects of these interventions on cellular senescence, inflammation, oxidative stress, ECM remodeling and adipocyte metabolic function. To assess this objective, human SAT was collected during plastic surgery from individuals with a history of bariatric surgery and substantial weight loss and used to establish an *ex vivo* model of previously obese AT. This model provided an opportunity to investigate whether features of obesity-associated AT dysfunction persist despite weight loss and whether they remain amenable to therapeutic modulation. Explants were treated with D+Q, α-MSH or isoproterenol, alone or in combination, for one and two weeks to evaluate their individual and combined effects on SAT function over time.

Materials and Methods

1. Adipose Tissue Collection and treatment

Samples of human abdominal SAT were collected from thirteen female individuals aged over 40 years with a history of obesity who underwent abdominoplasty at Centro Hospitalar Universitário de São João (CHUSJ) following bariatric surgery. All the patients gave informed consent before surgery, and the project was approved by the Ethics Committee of the Faculty of Medicine of University of Porto (CE-36-2024).

At the time of abdominoplasty, thirteen participants were overweight (BMI $\geq$ 25 kg/m²), of whom two remained obese, whereas two participants were within the normal-weight range (BMI < 25 kg/m²). Despite the substantial weight loss achieved following bariatric surgery, four participants still presented obesity-associated comorbidities, including T2DM, hypertension, and dyslipidemia.

Immediately after collection, AT samples were dissected into small pieces and washed with 1x PBS. Afterwards, four explants, each approximately 10 mm in diameter and weighing 250-300 mg, were carefully placed in each of the six wells of a 6-well plate containing 4 mL of DMEM/F12 medium supplemented with 10% FBS, 1% penicillin / streptomycin solution and 0.1% amphotericin B solution. Each well corresponded to one of the six treatment conditions: (1) vehicle (V), (2) α-MSH (M), (3) isoproterenol (I), (4) dasatinib + quercetin (D+Q), (5) dasatinib + quercetin + α-MSH (D+Q+M) and (6) dasatinib + quercetin + isoproterenol (D+Q+I). A total of two 6-well plates were prepared, corresponding to the one-week and two-week treatment periods. Following 24 h of incubation at 37ºC and 5% CO_2, the medium was carefully removed from the wells and replaced with 4 mL of fresh supplemented medium containing the respective pharmacological agent or combination according to the treatment condition. Pharmacological agents were administrated at 24 h intervals according to the respective experimental condition. All pharmacological agents were initially prepared as 200x

stock solutions in their respective vehicles and subsequently diluted in the culture medium to achieve the desire final concentration. α-MSH, isoproterenol and dasatinib were prepared in sterile water, and quercetin in 40% DMSO and 60% PBS. The final concentrations in the culture medium were 1 µM for α-MSH and dasatinib, 10 µM for isoproterenol, and 20 µM for quercetin. The vehicle control received the same final volumes of sterile water, DMSO and PBS as those used in the treatment conditions. Throughout the treatment period, the culture medium was renewed daily, except when explants had been treated with only α-MSH or isoproterenol, in which case the medium was replaced every 48 h. On the final day of each treatment week period, the medium and SAT explants were collected for subsequent analyses.

The treatment protocol was conducted over a two-week period, with tissue and conditioned medium collected after either one or two weeks of treatment, as illustrated in Figure 6.

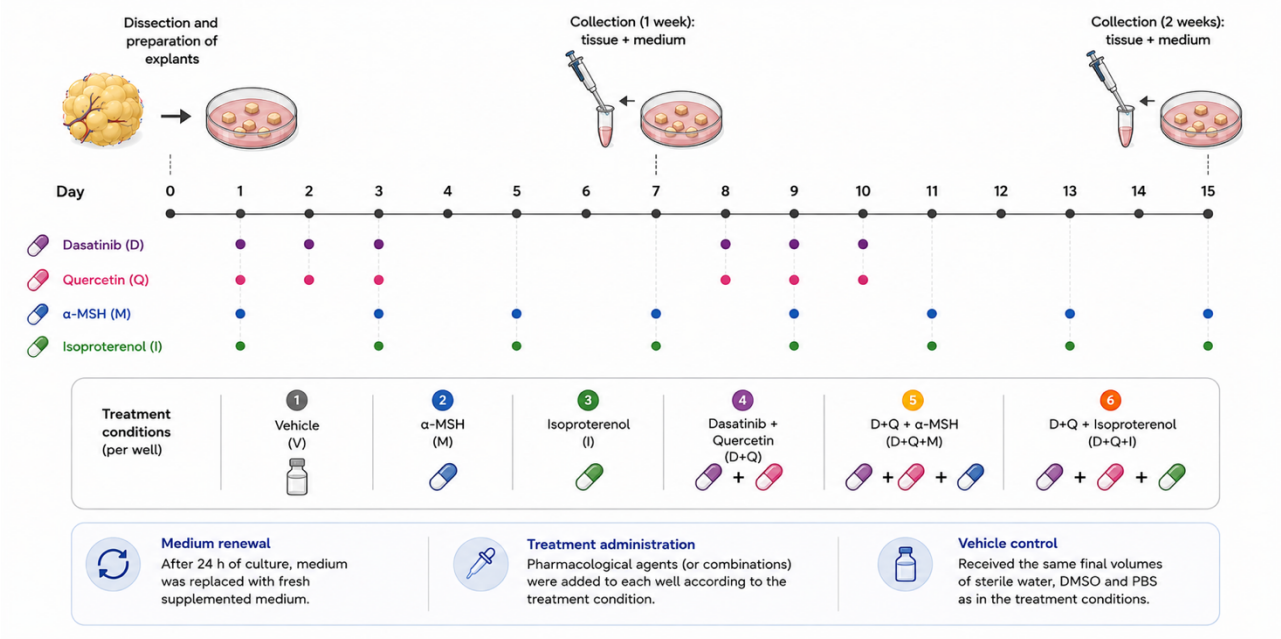


Figure 6. Schematic representation of the experimental treatment timeline of human SAT explants culture for two weeks. Explants were treated ex vivo with the senolytic combination dasatinib plus quercetin (D+Q) for three consecutive days and with the lipolytic agents α-MSH (M) or isoproterenol (I) every other day. At the end of each treatment period, tissue and culture medium were collected for subsequent analysis. Schematic representation generated with the assistance of ChatGPT (OpenAI).

The culture medium was also stored at -20 ºC and AT explants were washed with PBS, stored at - 80º or fixed in 4% paraformaldehyde (PFA) for subsequent paraffin embedding.

2. Adipose Tissue processing for paraffin embedding

SAT samples were fixed in 4% PFA for 24 hours at RT. Following fixation, tissue dehydration was performed over a graded alcohol series (70%, 80%, 90%, 97% and 100%). At each alcohol concentration, samples underwent three consecutive incubations of 1 h each, with fresh alcohol used for each incubation. On the following day, tissues were placed in cassettes and transferred to xylene through three consecutive incubations of 2 h each. The samples were subsequently transferred to 50% xylene + 50% paraffin at 65 ºC for overnight. After that, tissues were immersed in paraffin using two successive paraffin baths, with two consecutive 1 h incubations in each bath. After complete impregnation, tissues were carefully embedded in fresh paraffin and allowed to solidify at room temperature (RT), forming paraffin blocks suitable for sectioning and further histological analysis.

3. Histological evaluation of Adipose Tissue samples

Paraffin-embedded SAT samples were sectioned with 5 μm thickness using the microtome (Leica MR2145). These sections were mounted on poly-L-lysine-coated slides and dried overnight at 37ºC. Prior to staining, tissue sections were deparaffinized by incubation in xylene for 10 min, followed by 5 min incubation, and subsequently rehydrated through a graded ethanol series (100%, 90% and 70%) for 5 min each. Sections were then immersed in distilled water for 10 min to ensure complete rehydration. Following this procedure, the samples were processed according to the specific staining protocol described below.

3.1. Sirius Red staining

Tissue sections were immersed in 0.1% Red Sirius (Direct red 80, Sigma-Aldrich) prepared in 1.3% Picric Acid solution for 90 min. Following a brief rinse in acidified water containing 0.5% acetic acid, sections were dehydrated through increasing ethanol

concentrations (70%, 90%, and 100% for 5 min each), cleared with xylene for 5 min and mounted with Entellan (Sigma-Aldrich).

3.2. Computer-assisted morphometric analysis of Adipose Tissue

Adipocyte size was quantified using computer-assisted image analysis. Images were captured at 10x magnification with an Axioskop 40 light microscope equipped with an Axiocam 208 color camera (Carl Zeiss AG) and operated with ZEN 3.3 software (Carl Zeiss). Quantitative morphometric analysis was conducted with a modified version of Adiposoft, a plugin for Fiji (ImageJ), as previously described by Salazar MJ, et al. (82), which enables automated recognition and measurement of adipocyte areas.

For treatment conditions containing lipolytics (M, I, D+Q+M and D+Q+I), analysis was performed on three non-overlapping images from a single tissue section, obtained from explants of one individual. For the vehicle (V) and senolytic (D+Q) groups, two sections from two distinct individuals were analyzed (six images in total per group). The total number of adipocytes analyzed per condition was as follows: V - 943 adipocytes, M - 479 adipocytes, I - 881 adipocytes, D+Q - 1384 adipocytes, and the combined treatments D+Q+M - 669 adipocytes and D+Q+I - 729 adipocytes.

4. Glycerol Release Assay

Glycerol levels released into the culture medium were quantified at the end of one and two weeks of treatment. Briefly, 10 µL of culture medium was mixed with 40 µL of H_2O, and 100 µL of Free Glycerol Reagent (F6428; Sigma-Aldrich, Schnelldorf, Germany) in a 96-well plate. Absorbance was subsequently measured at 540 nm using an Infinite M200 microplate reader (Tecan, Männedorf, Switzerland).

5. Gene Expression Analysis

5.1. RNA extraction

RNA was extracted using TripleXtractor direct RNA Kit (GRiSP, Porto, Portugal) following the manufacturer's protocol with some slight modifications. Briefly, 150-200 mg of SAT was placed in tubes containing ceramic beads (Precellys, Montigny-le-Bretonneux, France), and 700 µL of TripleXtractor Direct Reagent was added. Tissue samples were homogenized using MagNa Lyser (Roche, Mannheim, Germany) at 6500

rpm for 45 sec and subsequently incubated for 5 min at RT. Following incubation, samples were centrifuged for 5 min at 1500 rpm. RNA purification was then performed according to the manufacturer's instructions, and RNA was eluted in 30 μL of RNase-free water. RNA concentrations and purity were assessed using the NanoDrop 2000 spectrophotometer (ThermoFisher Scientific, Waltham, MA, USA). The extracted RNA was stored at -80ºC.

5.2. Synthesis of cDNA

Complementary DNA (cDNA) was synthetized using NZY First-Strand cDNA Synthesis Kit (NZYTech), following the manufacturer's instructions. For reverse transcription, 500 ng of RNA was used. A no-reverse transcriptase (-RT) control was also prepared using RNA from the most concentrated sample. This control lacked the reverse transcriptase enzyme to monitor potential amplification from contaminating genomic DNA in qPCR.

5.3. Real- time polymerase chain reaction (qPCR)

Quantitative PCR (qPCR) was conducted in duplicates on transparent 384-well plates (Bio-Rad, Hercules, CA, USA) using the PowerTrack™ SYBR™ Green Master Mix from Applied Biosystems (Thermo Fisher Scientific, Waltham, MA, USA), 0.5 μM of each reverse and forward primers and 1 μL of cDNA. qPCR reactions were performed using CFX Opus 384 Real-Time PCR System (Bio-Rad, Hercules, CA, USA). The amplification protocol started with an initial denaturation step at 95ºC for 5 min, followed by 40 cycles consisting of denaturation at 95ºC for 15 s, annealing at 60ºC for 30 sec, and extension at 60ºC for 30 sec. To ensure the specificity of the PCR products, a melting curve analysis was performed following amplification. Gene expression levels were normalized to *importin 8 (IPO-8)* and relative expression was calculated using $2^{-\Delta CT}$ method. Primer sequences are listed in Table 1.

Table 1. List of primer sequences used in the qPCR experiments.

Gene	Annealing temperature (ºC)	Forward Sequence 5′-3′	Reverse Sequence 5′-3′
UCP-1	60	CTAACGAAGGACCAACGGCT	ACGTTCCAGGATCCAAGTCG
PGC1α	60	TCTGAGAGGGCCAAGCAAAG	TAGCTGTCTCCATCATCCCG
FN	60	AGCCGAGGTTTTAACTGCGA	CCCACTCGGTAAGTGTTCCC

IL-6	60	ACAGCCACTCACCTCTTCAG	CCATCTTTTTCAGCCATCTTT
IL-1β	60	TGGCAATGAGGATGACTTGTTC	CTGTAGTGGTGGTCGGAGATT
MMP3	60	AGGGATTAATGGAGATGCCCAC	TGAGTGAAAGAGACGCAGGGA
TIMP1	60	GCCTTCTGCAATTCCGACC	AGGTGGTCTGGTTGACTTCT
APOJ	60	GGATGAAGGACCAGTGTGACAAG	CAGCGACCTGGAGGGATTC
HO-1	60	CCAGCAAGGTGCAAGATT	CACATGGCATAAAGCCCTACA
TGF-β	60	AGGGCTACCATGCCAACTTCT	CCGGGTTATGCTGGTTGTACA
p21	60	CTGGAGACTCTCAGGGTCGAA	CCAGGACTGCAGGCTTCC
CD206	60	TTCCTTTGGACGGATGGACG	CCTCGTTTACTGTCGCAGGT
ZFAND5	60	CCCCGAAAACAGAGGTGTCA	CACATCGGCAGTCAAACCCT
IPO-8	60	CCAAGGGGTGGTGGTTCATTCT	TCTTGCCACAGCTCTTCATC

6. Protein analysis

6.1. Protein extraction and quantification

For SAT explant lysis, 100 mg of frozen tissue (stored at -80 °C) was homogenized in 200 µL of lysis buffer containing 50 mM EDTA, 50 mM Tris-HCl (pH 7.6), 10 mM NaCl, 10 mM β-glycerophosphate, and 0.25% Triton X-100, supplemented with a cocktail of phosphatase inhibitors (1:500) and protease inhibitors (1:100). Tissue disruption was performed in a MagNA Lyser (Roche, Mannheim, Germany) in tubes containing ceramic beads (Precellys, Montigny-le-Bretonneux, France) at 6500 rpm for two 30 sec cycles. The resulting lysates were further sonicated for 15 min at 4 °C using a Bioruptor device (Bioruptor™ UCD-200, Diagenode Liège, Belgium). The samples were then centrifugated at 10,000 x g for 10 min at 4 °C and the clear supernatants, located beneath the fat layer, were carefully transferred to new 1.5 mL eppendorf tubes. Protein concentration was then determined using the Bradford Reagent colorimetric assay (Bio-Rad, Hercules, CA, USA).

6.2. Western Blotting

A total of 20 µg of protein was mixed with 100 mM dithiothreitol (DTT) and gel loading buffer (50 mM Tris-base, 2 mM EDTA, 10% glycerol, 2% SDS, 0.0125% bromophenol blue, pH 8.8), denatured by sequential heating at 65 °C for 15 min and 95 °C for 5 min in a thermoblock (Thermal Shakelite, USA), and centrifuged at 10,000 × g for 5 min. Samples were then loaded onto a 12% polyacrylamide gel and separated by sodium dodecyl sulfate-polyacrylamide gel electrophoresis (SDS-PAGE) in 1x Laemmli

running buffer (25 mM Tris-base, 250 mM glycine, and 0.1% SDS, pH 8.3) at a constant electric current of 25 mA. Following electrophoresis, the proteins were transferred to a nitrocellulose membrane (Bio-Rad Hercules, CA, USA) in a transfer system (Bio-Rad Hercules, CA, USA) by setting a constant voltage of 30 V for 1 h 30 min. The membranes were then stained with Ponceau S and images were captured using a ChemiDoc™ XRS imaging system (Bio-Rad, Hercules, CA, USA). Membranes were then blocked in 5% milk powder (Molico®, Nestle, Vevey, Switzerland) in Tris-buffered saline containing 0.1% Tween (TBS-T) for 1 h at RT. After that, the membrane was incubated overnight at 4ºC on a shaker with the specific primary antibody solution diluted in 5% bovine serum albumin (BSA), 0.1% TBS-T and 0.1% NaN_3. The next day, after three 10-minute washing steps with TBS-T, the membrane was incubated with the secondary antibody diluted in 5% milk in TBS-T for 1 h at RT. The dilution factors for all antibodies, both primary and secondary, can be found in Table 2. Following another round of three 10-min washes with TBS-T, the membranes were incubated for 5 min with Clarity Western ECL Substrate (Bio-Rad, Hercules, CA, USA) according to the manufacturer´s instructions. Chemiluminescent bands were detected using the Chemi-Doc™ XRS system (Bio-Rad, Hercules, CA, USA).

Protein expression levels were quantified by densitometry and normalized to the β-actin, which served as a loading control.

Table 2. Primary and secondary antibodies and experimental conditions used for Western blotting analysis.

Primary Antibody	Reactivity	Time of incubation and dilution
Rabbit anti-human ATGL Cell Signaling Technology; #2138	Human, Mouse	1:1000 3 overnights, 4ºC
Rabbit anti-human HSL Cell Signaling Technology; #4107	Human, Mouse	
Rabbit anti-human Lamin B1 Abcam; ab16048	Human, Mouse, Rat	
Rat anti-mouse Galectin-3 Santa Cruz; #sc-23938	Human, Mouse, Rat	
Rabbit anti-human IL-6	Human	

Cell Signaling Technology; #12153		
Rabbit anti-human PAI-1 Cell Signaling Technology; #11907	Human, Monkey, Bovine	
Mouse anti-chicken β-actin Santa Cruz; sc47778	Human, Mouse, Rat, Chicken and others	
Secondary Antibody		
Goat anti-rabbit HRP antibody Invitrogen; A16096 (1:5000)	Rabbit and Rat IgG	1:5000 1 h, RT
Donkey anti-mouse HRP antibody Jackson Immunoresearch; 715-035-150 (1:5000)	Mouse IgG	

7. Statistical analysis

Data are presented as means ± SEM. Statistical comparisons were conducted using one-way analysis of variance (ANOVA) followed by Uncorrected Fisher´s LSD test in GraphPad PRISM 10 (version 10.3.1). A significance threshold of $p < 0.05$ was applied, with levels of significance indicated as follows: *p<0.05; **p<0.01; ***p<0.001; ****p<0.0001. Outlier detection was carried out with ROUT method, setting Q to 1%.

Results

To investigate whether adipose tissue (AT) dysfunction could be therapeutically modulated, an *ex vivo* model of human subcutaneous adipose tissue (SAT) explants was used. This experimental model preserves the multicellular architecture and local tissue microenvironment, allowing treatment responses to be assessed in a physiologically relevant human tissue context. SAT was obtained from individuals with a history of obesity who had undergone abdominoplasty following bariatric surgery and substantial weight loss. This population is particularly relevant because AT can retain a cellular and molecular memory of obesity even after weight loss, with alterations related to cellular senescence, inflammation, extracellular matrix (ECM) remodeling, and metabolic dysfunction. Importantly, several of these alterations overlap with key features of age-associated AT dysfunction, making this tissue a relevant model for investigating mechanisms that are shared between obesity-associated and age-related AT deterioration. Thus, this model allowed us to investigate whether residual dysfunctional phenotype could be attenuated while improving AT metabolic competence.

Based on this rationale, two complementary therapeutic strategies were investigated. The senolytic combination dasatinib and quercetin (D+Q) was used to target the senescence-associated component of AT dysfunction, whereas the lipolytic stimuli α-melanocyte-stimulating hormone (α-MSH) and isoproterenol were used to directly stimulate adipocyte metabolic activity. The combined treatments were used to determine whether targeting the dysfunctional cellular environment while simultaneously stimulating adipocyte metabolism could provide additional functional benefits. Accordingly, six experimental conditions were established: vehicle control (V), α-MSH (M), isoproterenol (I), D+Q, D+Q combined with α-MSH (D+Q+M), and D+Q combined with isoproterenol (D+Q+I). Treatment responses were evaluated after one and two weeks to assess their temporal effects on AT metabolic function.

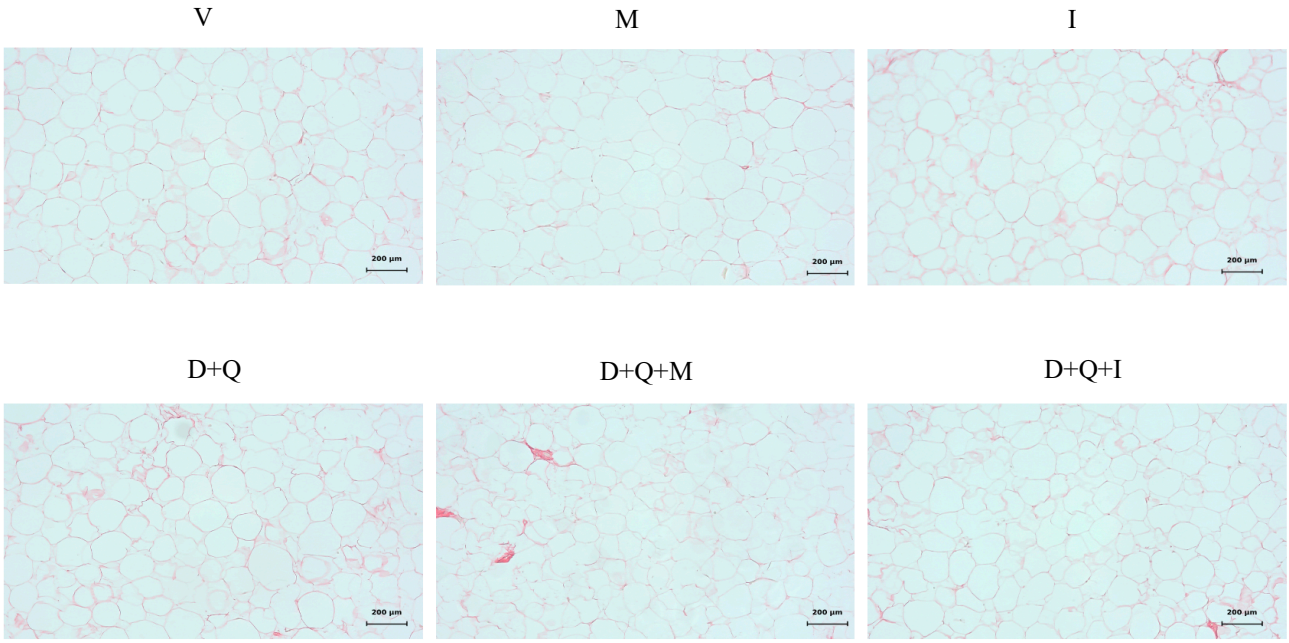
1. Senolytic and lipolytic treatment induce changes in adipocyte morphology

We first investigated whether senolytic and lipolytic treatments induces morphological changes in human SAT explants. For this purpose, tissue architecture and adipocyte

size were evaluated after two weeks of treatment, allowing the assessment of morphological changes following prolonged treatment exposure. SAT architecture was assessed in Sirius Red-stained sections (Figure 7A), and adipocyte area was quantified as a measure of adipocyte size.

After two weeks, I, D+Q, D+Q+M and D+Q+I treatments significantly decreased adipocyte area compared with vehicle, whereas no significant difference was observed following α-MSH treatment alone (Figure 7B). Adipocyte area was also significantly reduced following D+Q+M compared with α-MSH. Furthermore, D+Q+I resulted in significantly lower adipocyte area compared with isoproterenol alone (Figure 7B).

A



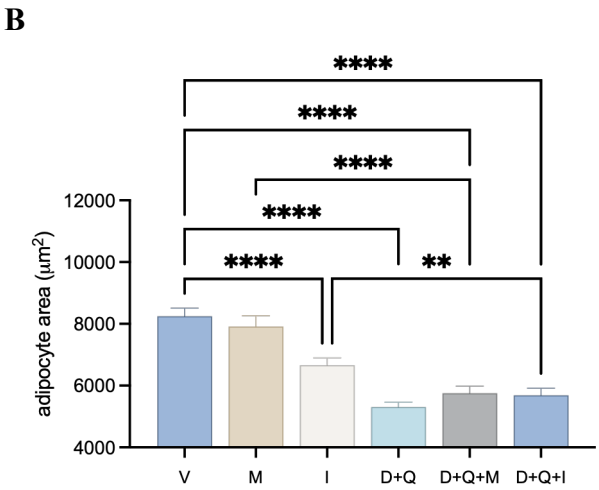


Figure 7. Effect of senolytic and lipolytic treatments on SAT morphology after two weeks of treatment. (A) Representative images of Sirius-Red-stained sections of human SAT. Scale bar = 200 µm. **(B)** Quantification of adipocyte cross-sectional area (µm²) in human SAT treated with vehicle (V), α-MSH (M), isoproterenol (I), dasatinib plus quercetin (D+Q), and the combined treatments D+Q+M and D+Q+I using a modified version of Adiposoft, a plugin for Fiji (Image J). Data are presented as mean ± SEM. Statistical significance was determined using one-way ANOVA followed by Fisher´s uncorrected LSD test. $p < 0.01$ (**), $p < 0.0001$ (****).

Adipocyte membrane boundaries were subsequently delineated using the Adiposoft plugin, providing a clearer visualization of individual adipocytes. Representative images showed well-defined adipocyte boundaries across all experimental conditions, with no apparent major structural disruption, indicating that the overall architecture of the SAT explants was preserved throughout the two-week treatment period (Figure 8).

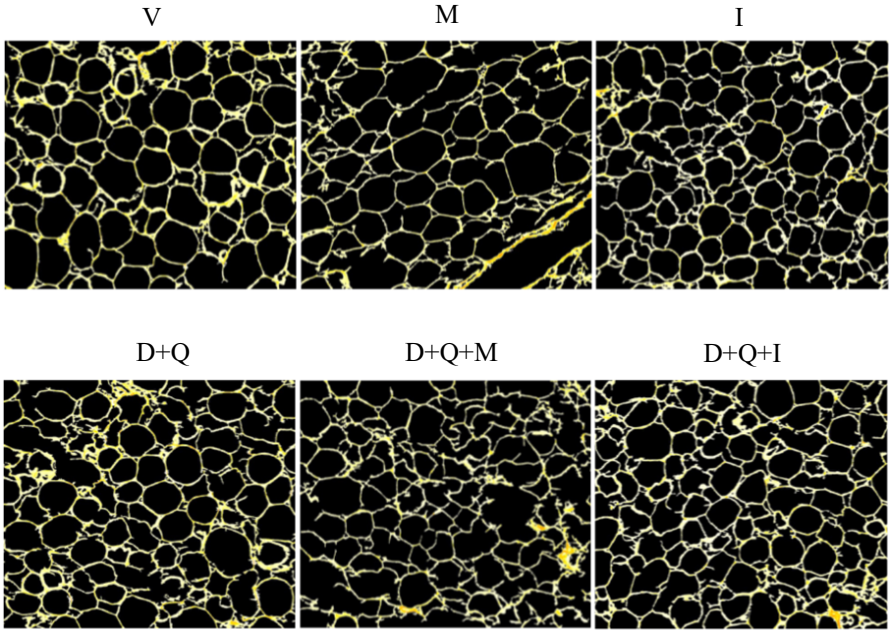


Figure 8. Structural integrity and adipocyte membrane boundaries in human SAT explants after two weeks of treatment. Representative images displaying adipocyte membrane outlines in Sirius Red–stained sections of human SAT explants treated with vehicle (V) , α-MSH (M) , isoproterenol (I) , dasatinib plus quercetin (D+Q), or the combinations D+Q+M and D+Q+I. Images were generated using the Adiposoft plugin in Fiji (ImageJ). Scale bar = 200 µm.

2. Combined senolytic and lipolytic treatment enhances AT basal lipolytic activity

The reduction in adipocyte size observed following treatment prompted us to investigate the metabolic changes associated with this morphological response. We first assessed whether the reduction in adipocyte area was accompanied by enhanced lipolytic activity by measuring glycerol release into the culture medium after one and two weeks of treatment (Figure 9).

After one week of treatment, no significant differences were observed between the experimental groups, although a trend towards increased glycerol levels was observed across all treatment's conditions compared with vehicle (Figure 9A).

In contrast, after two weeks, glycerol release was significantly increased in all treatment groups compared with vehicle. α-MSH and isoproterenol alone increase glycerol release by approximately 1.4-fold while D+Q and D+Q+M resulted in increases of approximately 1.5-fold. The highest glycerol release was observed following the combined D+Q+I treatment, reaching approximately 1.7-fold above vehicle (Figure 9B).

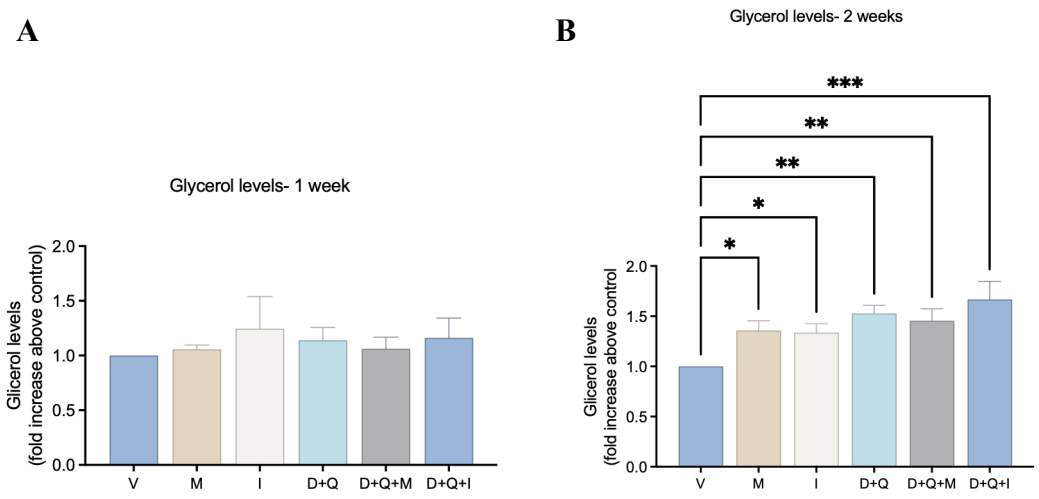


Figure 9. Effect of senolytic and lipolytic treatments on basal glycerol release from human SAT explants. Glycerol release into the culture medium was assessed after one **(A)** and two **(B)** weeks of treatment. Experimental groups included vehicle (V), α-MSH (M), isoproterenol (I), dasatinib plus quercetin (D+Q), and the combined treatments D+Q+M and D+Q+I. Glycerol levels are expressed as fold change relative to vehicle. Data are presented as mean ± SEM (n= 2-5). Statistical significance was determined using one-way ANOVA followed by Fisher´s uncorrected LSD test. $p < 0,05$ (*), $p < 0.01$ (**), $p < 0.001$ (***).

To further characterize the lipolytic profile of AT following treatment, the protein expression of the key lipolytic enzymes ATGL and HSL was evaluated.

After one week of treatment, both D+Q and D+Q+I significantly upregulated ATGL protein expression by approximately 1.5-fold compared with vehicle. A comparable, albeit non-significant, trend toward increased expression was likewise observed for D+Q+M (~1.5-fold, p = 0.0532) (Figure 10C). After 2 weeks of treatment, ATGL protein expression was significantly upregulated by D+Q (~ 2.1-fold) and D+Q+I (~ 2.3-fold) compared with vehicle. Notably, ATGL expression in the D+Q+I group was also significantly higher than with isoproterenol alone (Figure 10D).

Similarly to ATGL, HSL protein expression was significantly increased by approximately 2.1-fold and 2.7-fold after one week of D+Q and D+Q+I treatments, respectively (Figure 10E). After two weeks, HSL protein expression was significantly increased by approximately 1.8-fold, 1.9-fold and 2.1-fold following D+Q, D+Q+M and D+Q+I treatments, respectively, relative to vehicle. Furthermore, HSL levels were significantly higher with D+Q+M compared with α-MSH alone and with D+Q+I compared with isoproterenol alone (Figure 10F).

Overall, these results demonstrated that the observed increases in ATGL and HSL protein expression were primarily associated with the presence of D+Q, as α-MSH or isoproterenol alone did not significantly alter either protein compared with vehicle.

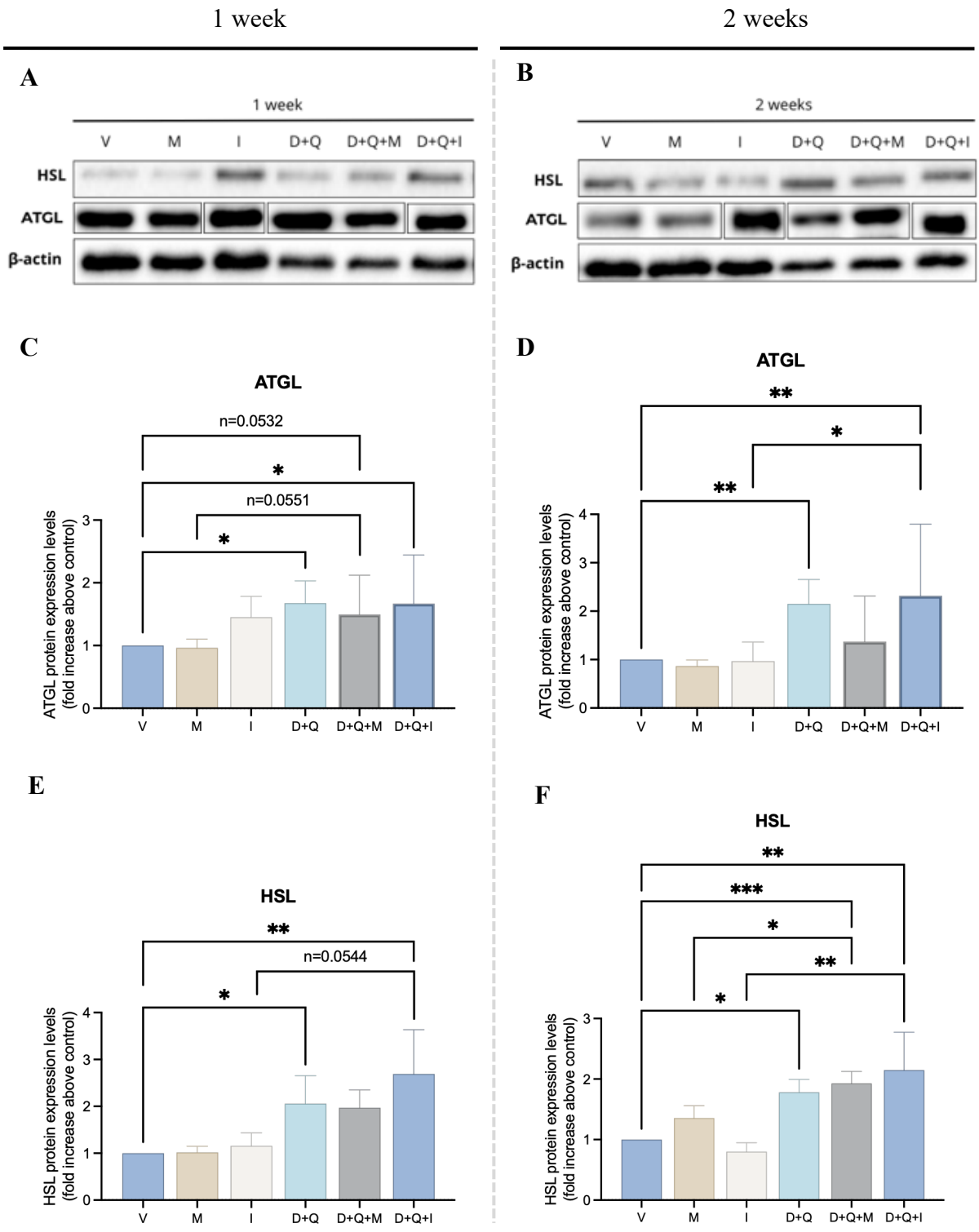


Figure 10. Effect of senolytic and lipolytic treatments on the protein expression of lipolytic enzymes in human SAT Explants. Representative Western blots of ATGL and HSL are presented after one **(A)** and two **(B)** weeks of treatment. Protein expression levels of ATGL **(C, D)** and HSL **(E, F)** were assessed by Western blotting after one and two weeks of treatment. Experimental groups included vehicle (V), α-MSH (M), isoproterenol (I), dasatinib plus quercetin (D+Q), and the combined treatments D+Q+M and D+Q+I. Protein levels were normalized to β-actin and expressed as fold change relative to vehicle. Data are presented as mean ± SEM (n = 3-13). Statistical significance was determined using one-way ANOVA followed by Fisher´s uncorrected LSD test. $p < 0{,}05$ (*), $p < 0.01$ (**), $p < 0.001$ (***).

3. Combined senolytic and lipolytic treatment restores thermogenic competence of AT

To determine whether the metabolic effects of the treatments extended beyond enhanced lipolysis, the expression of the browning- and thermogenesis-associated *UCP-1*, a key mediator of thermogenesis, and *PGC1α*, a major regulator of mitochondrial, was subsequently evaluated. After one week treatment, *UCP-1* mRNA expression was markedly increased in the groups containing D+Q (Figure 11A). D+Q alone induced an approximately 15-fold increase in *UCP-1* expression compared to vehicle, while the combined treatments D+Q+M and D+Q+I resulted in more pronounced increases of approximately 50- and 60-fold increase relative to vehicle, respectively. Furthermore, *UCP-1* expression was significantly higher following D+Q+M compared with α-MSH alone and following D+Q+I compared with isoproterenol. D+Q+M and D+Q+I also showed a tendency towards increased *UCP-1* expression compared with D+Q alone ($p = 0.0597$ and $p = 0.0551$, respectively).

After two weeks of treatment, *UCP-1* expression remained increased in the D+Q-containing groups, whereas α-MSH and isoproterenol alone showed expression levels similar to vehicle (Figure 11B). D+Q and D+Q+I induced approximately 30- and 35-fold increases in *UCP-1* expression, respectively, both reaching statistical significance compared with vehicle. D+Q+M also increased *UCP-1* expression by approximately 20-fold relative to vehicle, although this difference did not reach statistical significance ($p = 0.0653$).

Similarly, *PGC1α* mRNA expression was significantly increased following the combined D+Q+M treatment after one week of treatment, reaching approximately a 7-fold increase relative to vehicle, α-MSH and D+Q alone (Figure 11C). *PGC1α* expression following one week of D+Q+I was approximately 3-fold higher than vehicle but did not reach statical significance ($p = 0.3233$). However, this effect became more pronounced after two weeks of treatment, when *PGC1α* expression in D+Q+I group reached an approximately 5-fold increase relative to vehicle (Figure 11D), with statistically significant differences also observed compared with isoproterenol and D+Q alone. *PGC1α* expression remained elevated in the other D+Q-treated groups after two

weeks. D+Q and D+Q+M showed significantly higher *PGC1α* expression compared with vehicle and compared with vehicle and α-MSH, respectively.

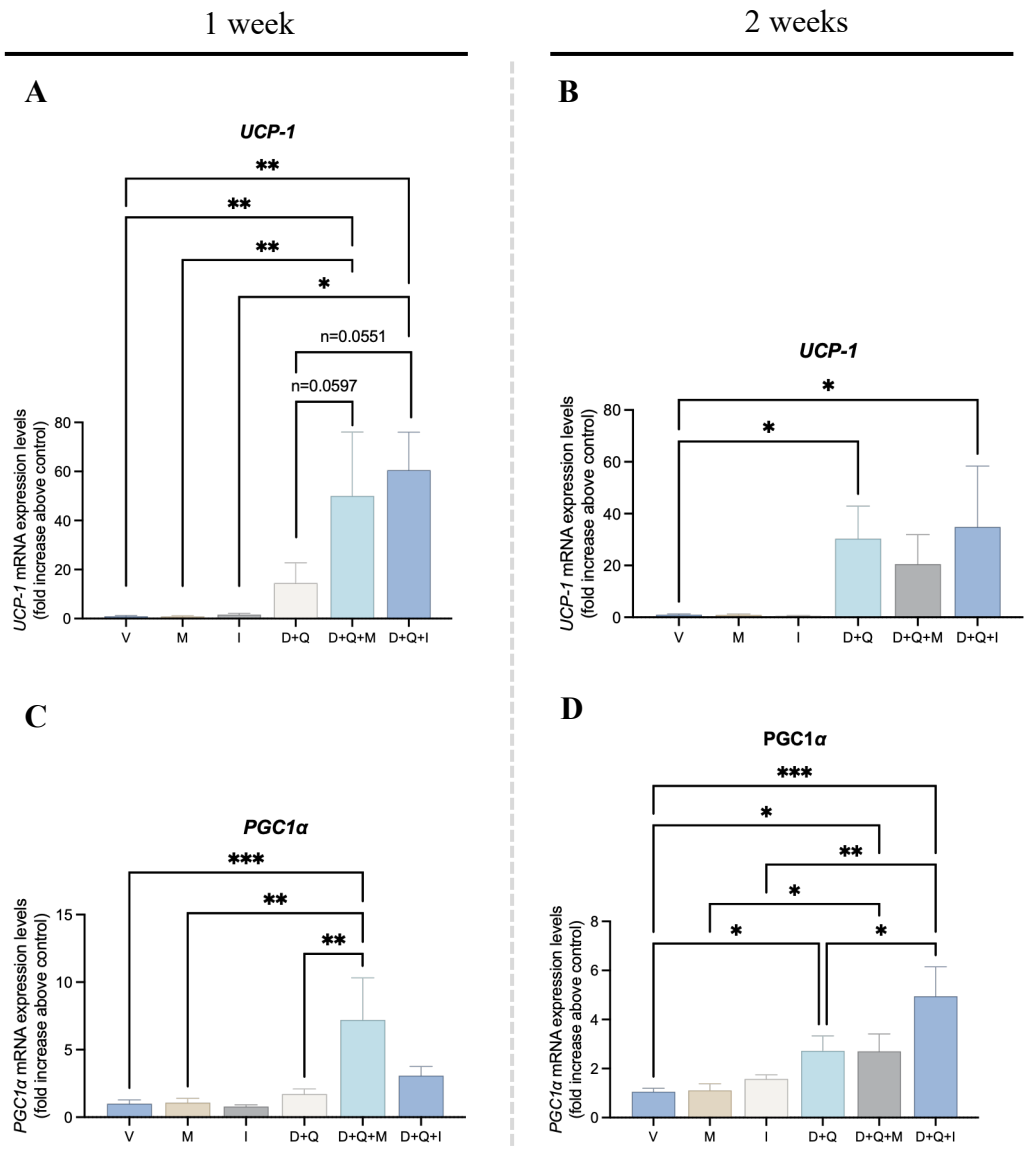


Figure 11. Effect of senolytic and lipolytic treatments on thermogenic and browning-associated markers in human SAT Explants. mRNA expression levels of *UCP-1* **(A, B)** and *PGC1α* **(C, D)** were assessed by RT-qPCR after one and two weeks of treatment. Experimental groups included vehicle (V), α-MSH (M), isoproterenol (I), dasatinib plus quercetin (D+Q) and the combined treatments D+Q+M and D+Q+I. Gene expression levels were normalized to *IPO8* and are expressed as fold change relative to vehicle. Data are presented as mean ± SEM (n = 2-10). Statistical significance was determined using one-way ANOVA followed by Fisher´s uncorrected LSD test. $p < 0,05$ (*), $p < 0.01$ (**), $p < 0.001$ (***).

Taken together, the morphological, lipolytic, and thermogenic responses observed following treatment indicate a broader modulation of the metabolic phenotype of human SAT explants, particularly in the presence of D+Q. These findings led us to

investigate whether the observed metabolic changes were accompanied by alterations in other features of AT dysfunction.

4. Senescence-associated markers show a time-dependent response to treatment

Since D+Q was used as a senolytic treatment to target SCs, it was next investigated whether the metabolic improvements observed following treatment were accompanied by changes in senescence- and SASP- associated markers, including *p21*, zinc finger AN1-type containing 5 (*ZFAND5*), *TGF-β*, PAI-1, lamin B1, and clusterin/apolipoprotein J (*APOJ*).

After two weeks of treatment, *p21* mRNA expression - a key regulator of cell cycle arrest and a commonly used marker of cellular senescence - was markedly reduced across all D+Q-containing groups, consistent with the expected senolytic clearance of SCs (Figure 12B). Specifically, D+Q and D+Q+M significantly decreased *p21* levels to approximately 0.3-fold relative to vehicle, with D+Q+M showing significantly lower expression than α-MSH alone. D+Q+I also exhibited a trend toward reduction of *p21* levels (p = 0.067). Notably, neither α-MSH nor isoproterenol alone altered *p21* expression at this time point.

Interestingly, this clearance response was not yet established at one week, where *p21* mRNA levels remained unchanged by D+Q alone. Surprisingly, a transient effect of α-MSH was observed (Figure 12A). At this earlier time point, α-MSH treatment elevated *p21* mRNA levels, reaching its highest expression in the D+Q+M combination group (∼3-fold increase), which was statistically significant compared with both vehicle and D+Q alone. In contrast, isoproterenol alone or in combination with D+Q had no impact on *p21* expression at one week.

A parallel pattern was observed for *ZFAND5*, a stress-responsive gene associated with cellular senescence. After two weeks of treatment, *ZFAND5* mRNA expression was significantly reduced in D+Q-containing groups, with D+Q and D+Q+M downregulating its expression to approximately 0.4-fold relative to vehicle (Figure 12D). D+Q+I followed a similar decreasing trend, although this reduction did not reach statistical significance (p = 0.068).

In contrast to this two-week reduction, one week of treatment revealed an overall increase in *ZFAND5* expression following lipolytic stimulation (Figure 12C). α-MSH alone significantly increased *ZFAND5* levels by approximately 1.8-fold relative to vehicle. Similarly, the combination treatments D+Q+M and D+Q+I significantly upregulated *ZFAND5* expression to approximately 1.8- and 2.1-fold compared with vehicle, respectively. In addition, *ZFAND5* expression following D+Q+I treatment was significantly higher than with D+Q alone.

A consistent response was also observed for *TGF-β*, a cytokine involved in cellular senescence and tissue remodeling. After two weeks of treatment, *TGF-β* mRNA expression tended to be reduced across D+Q-containing groups as well as with isoproterenol alone (Figure 12F); however statistical significance was only obtained for the D+Q+M group when compared to α-MSH alone.

In contrast, one week of treatment was characterized by a robust, transient induction of *TGF-β*, with the combination treatments producing the highest expression levels (Figure 12E). D+Q+M and D+Q+I significantly upregulated *TGF-β* mRNA levels by approximately 3.6-fold and 4.1-fold relative to vehicle, respectively. In comparison, α-MSH, isoproterenol and D+Q alone induced only moderate changes in *TGF-β* expression at this earlier time point.

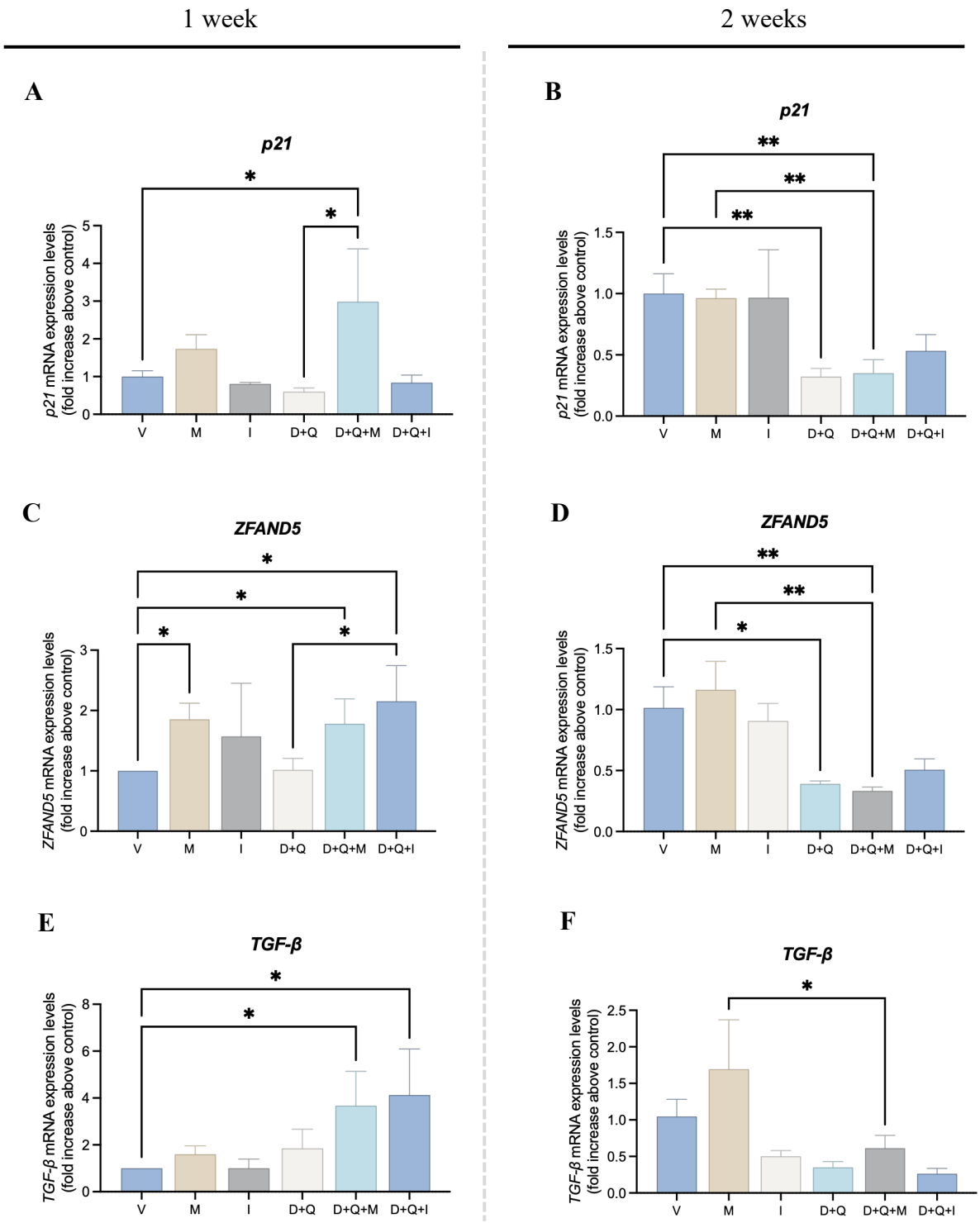


Figure 12. Effect of senolytic and lipolytic treatments on the mRNA expression of senescence-associated markers in human SAT explants. mRNA expression levels of *p21* **(A, B),** *ZFAND5* **(C, D)**, and *TGF-β* **(E, F)** were assessed by RT-qPCR after one and two weeks of treatment. Experimental groups included vehicle (V), α-MSH (M), isoproterenol (I), dasatinib plus quercetin (D+Q) and the combined treatments D+Q+M and D+Q+I. Gene expression levels were normalized to *IPO8* and are expressed as fold change relative to vehicle. Data are presented as mean ± SEM (n = 2-10). Statistical significance was determined using one-way ANOVA followed by Fisher´s uncorrected LSD test. $p < 0{,}05$ (*), $p < 0.01$ (**).

Overall, these findings reveal a time-dependent modulation of the analyzed senescence-associated markers, with distinct expression patterns observed between one and two weeks of treatment. To further characterize the effects of the treatments on other

senescence-associated features, we next evaluated the protein expression of PAI-1, a component of SASP and a primary downstream effector of TGF-β signaling pathway, and Lamin B1, a nuclear envelope protein whose dysregulation is associated with cellular senescence (Figure 13).

PAI-1 protein expression was consistently downregulated by D+Q-containing treatments across both one and two weeks. After one week, D+Q alone markedly suppressed PAI-1 levels relative to vehicle, representing the lowest expression among groups (Figure 13C). Significant reductions were likewise sustained when D+Q was combined with lipolytic agents, with D+Q+I decreasing PAI-1 relative to vehicle and D+Q+M maintaining levels significantly below those of α-MSH alone. This suppressive pattern persisted at two weeks, where PAI-1 expression continued to be reduced in the groups treated with D+Q (Figure 13D). At this later time point, α-MSH alone induced a significant 2.8-fold increase relative to vehicle; however, co-treatment with D+Q completely blunted this effect, reducing PAI-1 levels to values even below those observed with α-MSH alone. These findings align with the downstream reduction observed for *TGF-β*, suggesting that PAI-1 serves as an earlier and more sensitive reporter of the *TGF-β* signaling cascade in response to senolytic treatment.

Lamin B1 protein levels remained comparable to vehicle following α-MSH or isoproterenol monotherapies, after one week of treatment (Figure 13E). While lower expression was observed with D+Q alone or combined with isoproterenol (D+Q+I), the D+Q+M combination sustained higher Lamin B1 levels, resulting in a significant increase compared with D+Q alone. A distinct response pattern emerged after two weeks of treatment (Figure 13F). Isoproterenol alone induced the highest Lamin B1 protein expression, showing a significant 2.2-fold increase relative to vehicle, but co-treatment with D+Q (D+Q+I) significantly blunted this effect, reducing Lamin B1 expression compared with isoproterenol alone. No significant differences were observed among the remaining groups at this later time point.

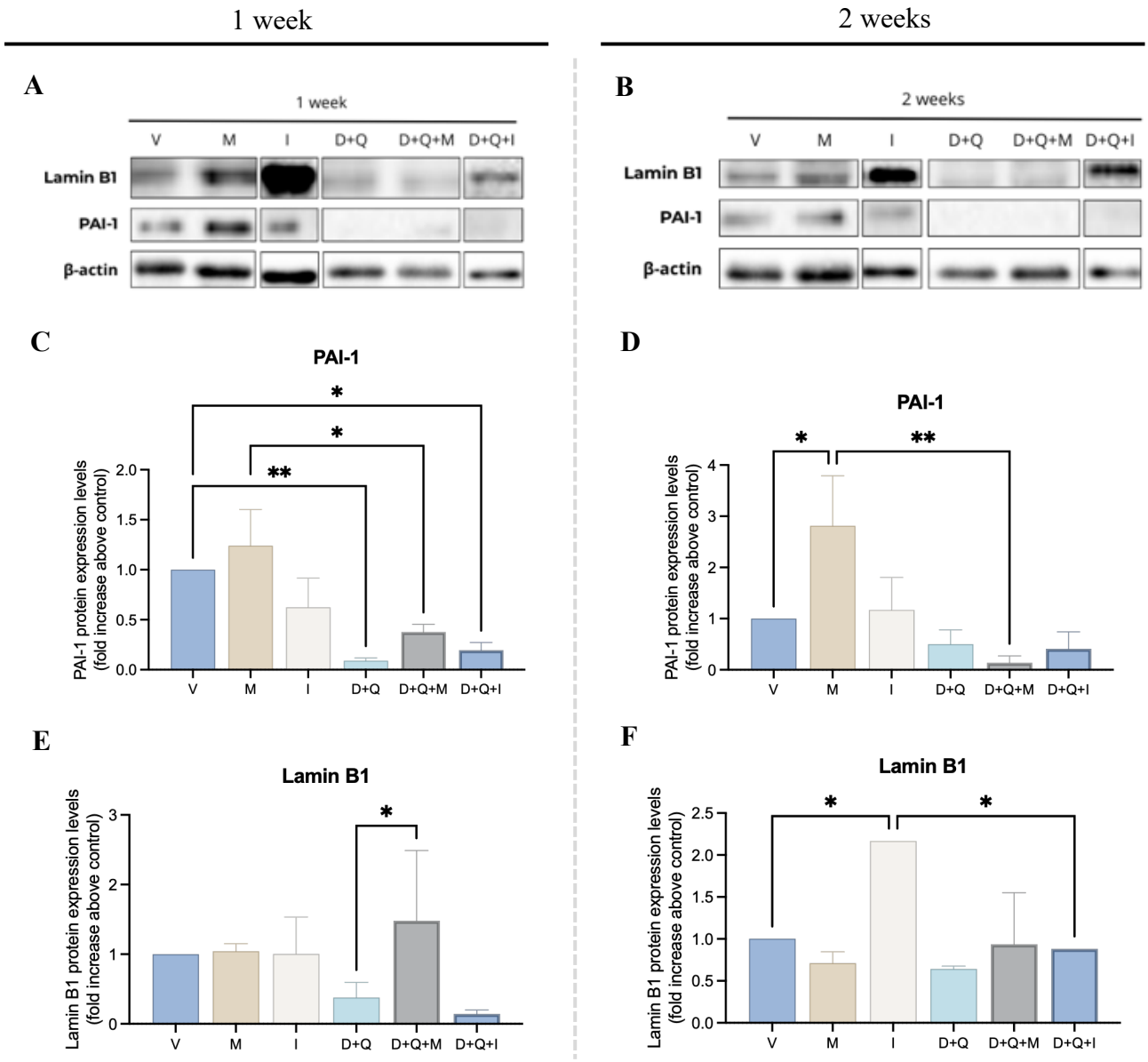


Figure 13. Effect of senolytic and lipolytic treatments on the protein expression of senescence-associated markers in human SAT Explants. Representative Western blots of PAI-1 and Lamin B1 are presented after one **(A)** and two **(B)** weeks of treatment. Protein expression levels of PAI-1 **(C, D)** and Lamin B1 **(E, F)** were assessed by Western blotting after one and two weeks of treatment. Experimental groups included vehicle (V), α-MSH (M), isoproterenol (I), dasatinib plus quercetin (D+Q) and the combined treatments D+Q+M and D+Q+I. Protein expression levels were normalized to β-actin and are expressed as fold change relative to vehicle. Data are presented as mean ± SEM (n = 2-7). Statistical significance was determined using one-way ANOVA followed by Fisher´s uncorrected LSD test. $p < 0{,}05$ (*), $p < 0.01$ (**).

In contrast to the downregulation observed for classical senescence markers, *APOJ* mRNA expression was consistently upregulated by D+Q treatments at both one and two weeks, particularly when combined with α-MSH (Figure 14A, B). At one week, D+Q+M significantly increased *APOJ* levels compared with vehicle and α-MSH alone, while D+Q+I showed a similar 3.3-fold upward trend ($p = 0.051$; Figure 14A). At two weeks, *APOJ* levels remained elevated, with D+Q+M sustaining a significant ~ 2.7-fold increase over both vehicle and α-MSH alone (Figure 14B). This unexpected

pattern suggests that APOJ modulation by D+Q+M is driven by a distinct biological mechanism rather than merely reflecting senescent cell burden. Indeed, although APOJ is frequently regarded as a senescence-associated marker, it primarily functions as an extracellular chaperone involved in cytoprotection, proteostasis, and tissue remodeling.

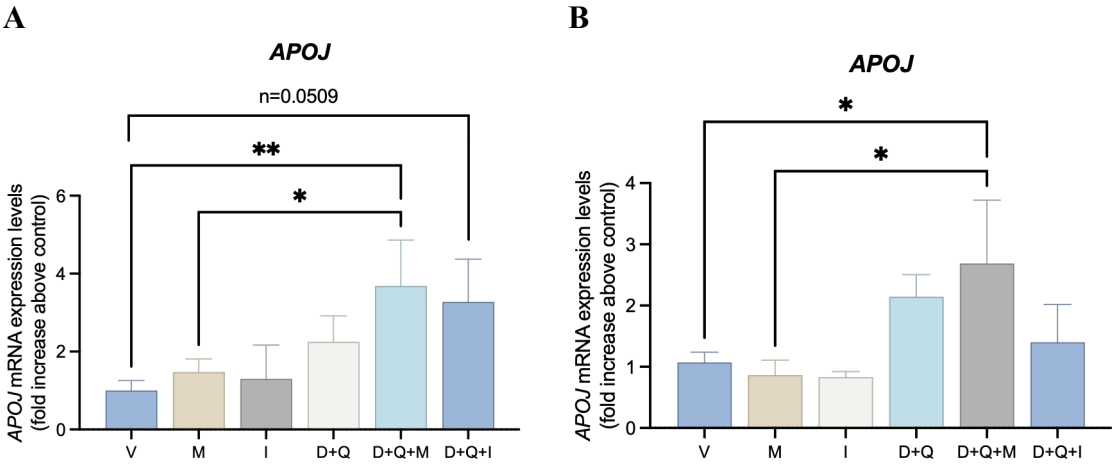


Figure 14. Effect of senolytic and lipolytic treatments on the mRNA expression of the senescence-associated marker APOJ in human SAT explants. mRNA expression levels of *APOJ* were assessed by RT-qPCR after one **(A)** and two **(B)** weeks of treatment. Experimental groups included vehicle (V), α-MSH (M), isoproterenol (I), dasatinib plus quercetin (D+Q) and the combined treatments D+Q+M and D+Q+I. Gene expression levels were normalized to *IPO8* and are expressed as fold change relative to vehicle. Data are presented as mean ± SEM (n = 3-11). Statistical significance was determined using one-way ANOVA followed by Fisher´s uncorrected LSD test. $p < 0{,}05$ (*), $p < 0.01$ (**).

5. The combination of senolytic and lipolytic agents activate cytoprotective responses

To further explore this inducible cytoprotective machinery suggested by *APOJ* results, we next analyzed the expression of heme oxygenase-1 (*HO-1*), a master antioxidant enzyme and sensor of cellular stress. Reinforcing the trend observed for APOJ, one week of treatment revealed a robust upregulation of *HO-1* mRNA expression in groups exposed to lipolytic stimulation combined with D+Q (Figure 15A). Both D+Q+M and D+Q+I significantly increased *HO-1* expression by approximately 4.5- and 6.5-fold compared with vehicle, respectively. After two weeks of treatment, *HO-1* expression also tended to remain elevated following the combined treatments, reaching approximately 2.0- and 2.5-fold relative to vehicle in the D+Q+M ($p = 0.052$) and D+Q+I groups ($p < 0.05$), respectively (Figure 15B). D+Q alone also displayed a strong trend toward increased expression relative to vehicle ($p = 0.051$).

Overall, *APOJ* and *HO-1* showed a similar expression pattern, with a more pronounced activation of protective pathways following the combined senolytic and lipolytic treatments. These results underscore an early and ongoing activation of endogenous antioxidant and cytoprotective defenses in response to combined lipolytic and senolytic stress.

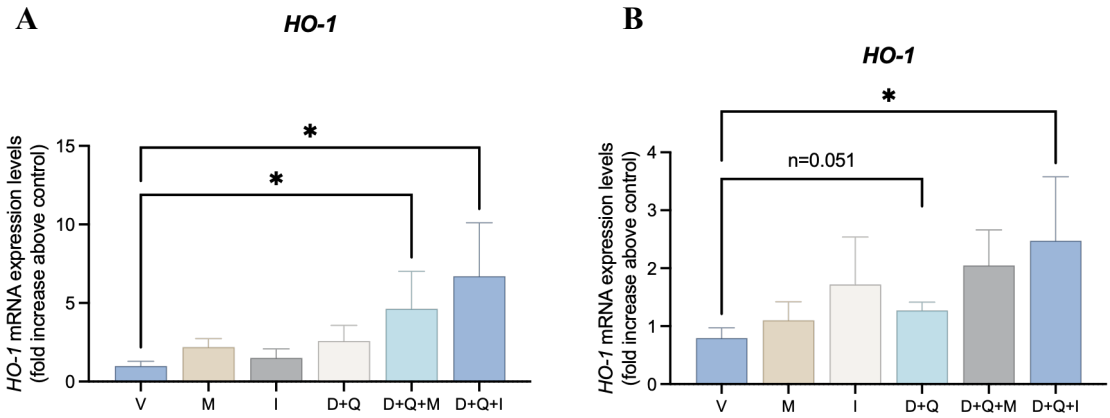


Figure 15. Effect of senolytic and lipolytic treatments on the mRNA expression of the cytoprotective marker HO-1 in human SAT Explants. mRNA expression levels of *HO-1* were assessed by RT-qPCR after one **(A)** and two **(B)** weeks of treatment. Experimental groups included vehicle (V), α-MSH (M), isoproterenol (I), dasatinib plus quercetin (D+Q) and the combined treatments D+Q+M and D+Q+I. Gene expression levels were normalized to *IPO8* and are expressed as fold change relative to vehicle. Data are presented as mean ± SEM (n = 3-11). Statistical significance was determined using one-way ANOVA followed by Fisher´s uncorrected LSD test. $p < 0{,}05$ (*).

6. Combined senolytic and lipolytic treatment modulates inflammatory and extracellular matrix remodeling markers

The increase in cytoprotective markers suggested that the treatments may influence adaptive cellular responses. Therefore, we next investigated whether these changes were accompanied by alterations in the inflammatory profile of AT by assessing the expression of inflammatory and immune markers, including IL-6, *IL-1β*, mannose receptor C-type 1 (*CD206*) and Galectin-3.

Surprisingly, the expression of IL-6, a pro-inflammatory cytokine with important roles in AT metabolism, exhibited a time-dependent induction by lipolytic monotherapies that was completely suppressed by D+Q co-treatment (Figure 16A, B, E, F). At one week, α-MSH and isoproterenol showed a strong trend toward elevated *IL-6* mRNA levels (~1.4- and 1.5-fold relative to vehicle, respectively; Figure 16A). By two weeks, this pro-inflammatory effect reached statistical significance for α-MSH, which induced a sustained 1.5-fold increase (Figure 16B). Remarkably, all D+Q-containing therapies consistently blunted this induction across both time points, with D+Q alone significantly lowering *IL-6* mRNA levels below those observed in the vehicle group.

After one week, D+Q+M and D+Q+I suppressed *IL-6* expression compared with α-MSH and isoproterenol alone, respectively (Figure 16A). Similarly, at week two, D+Q+M completely abolished the α-MSH-driven upregulation of *IL-6*, and D+Q+I maintained significantly lower levels than isoproterenol alone (Figure 16B).

This transcriptional suppression faithfully translated to the protein level: D+Q-based treatments significantly reduced IL-6 protein expression relative to vehicle at week one (Figure 16E) and sustained this reduction at week two, where D+Q+M significantly counteracted the protein elevation induced by α-MSH alone (Figure 16F).

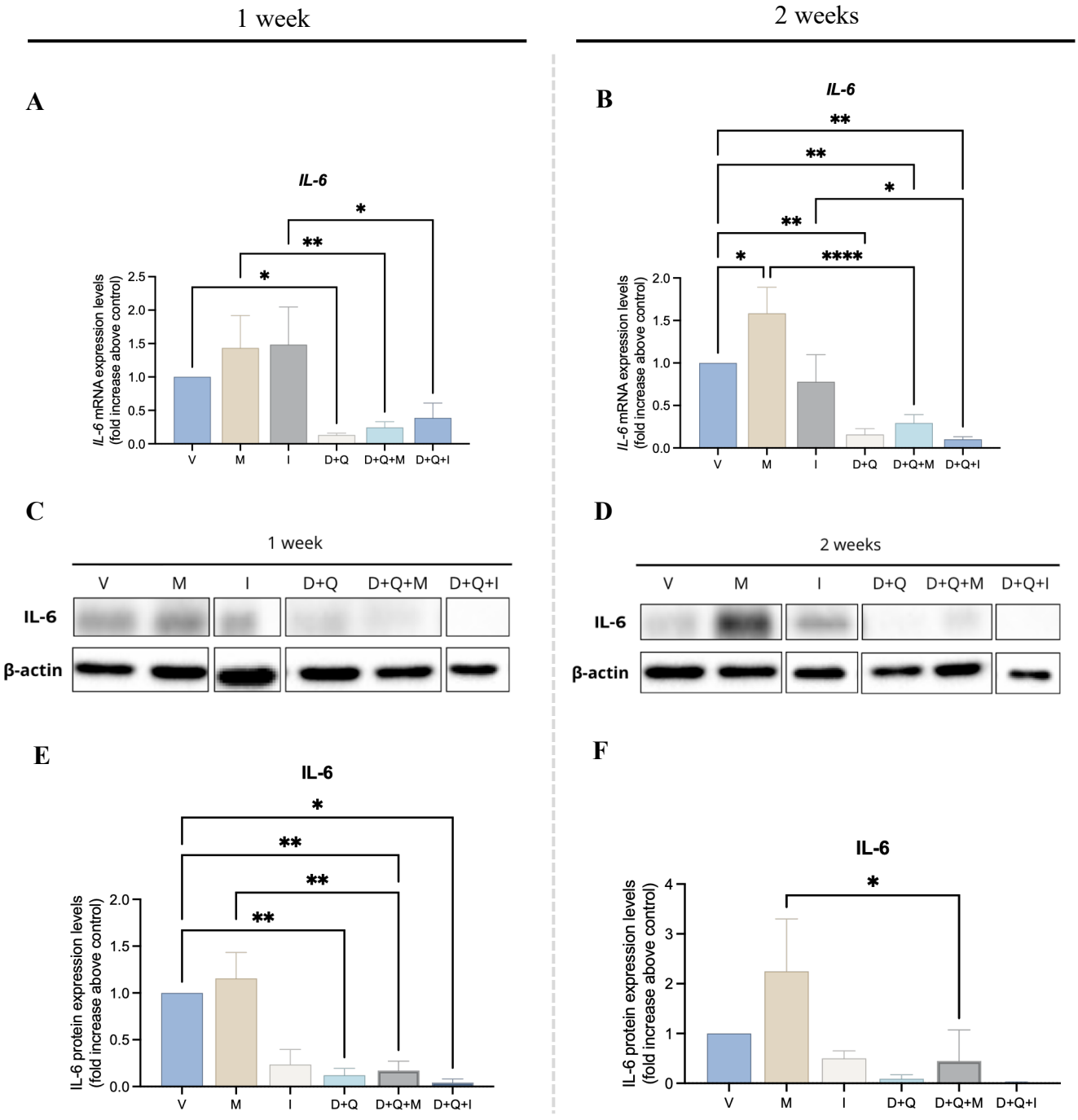
A parallel suppressive effect was observed for the pro-inflammatory cytokine *IL-1β* (Figure 16G, H). While α-MSH monotherapy trended toward a modest increase in *IL-1β* mRNA levels (~1.3-fold relative to vehicle), D+Q-containing treatments maintained robust and persistent downregulation across the entire study period. Comparing to vehicle, *IL-1β* mRNA expression was significantly suppressed by D+Q alone and by D+Q+M at one and two weeks of treatment, while D+Q+I achieved significant reduction only at week two (Figure 16H). Furthermore, co-treatment with D+Q persistently overrode the pro-inflammatory drive of both lipolytic agents, yielding markedly lower *IL-1β* levels compared with α-MSH alone (at both weeks) and isoproterenol alone (at week two).

Assessment of *CD206*, a surface marker associated with alternatively activated (M2-like) macrophages, also revealed a profound and sustained reduction in response to senolytic treatment (Figure 16I, J). Across both one and two weeks, D+Q-based therapies drastically downregulated *CD206* mRNA levels compared with vehicle: D+Q and D+Q+M reduced the expression to approximately 0.1-fold or less relative to vehicle levels, while D+Q+I suppressed levels to ~0.25-fold. In comparison with lipolytic monotherapies, D+Q+M maintained significantly lower *CD206* expression than α-MSH alone at both weeks, whereas D+Q+I displayed a strong downregulatory trend relative to isoproterenol alone at week one ($p = 0.0596$).

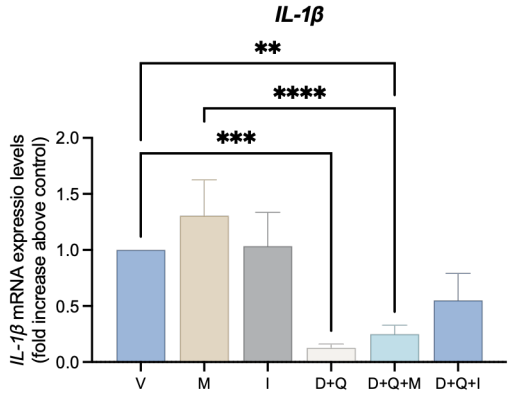
In stark contrast to the dynamic shifts observed for IL-6, *IL-1β* and *CD206*, protein expression of Galectin-3, a macrophage-derived lectin involved in CLS formation and a hallmark of AT dysfunction, remained entirely unaffected. No statistically significant

differences were detected among any experimental groups after either one week (Figure 16M) or two weeks of treatment (Figure 16N).

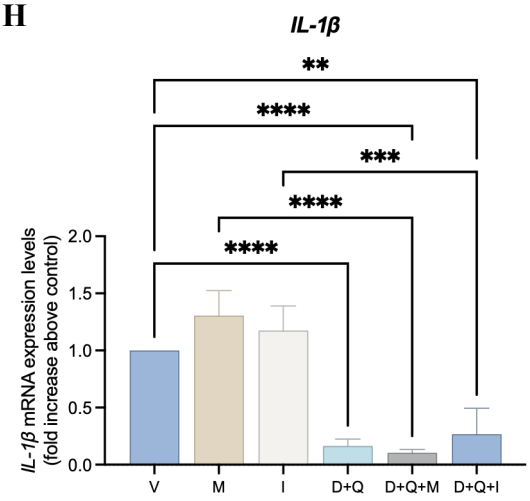
Taken together, these findings reveal that α-MSH and isoproterenol induce specific cytokine responses such as IL-6 and *IL-1β*, which may reflect metabolic crosstalk or pro-resolving signaling rather than classical inflammation. Importantly, D+Q-based treatments override these lipolytic-associated cytokine dynamics, driving a sustained shift in AT immune signaling.



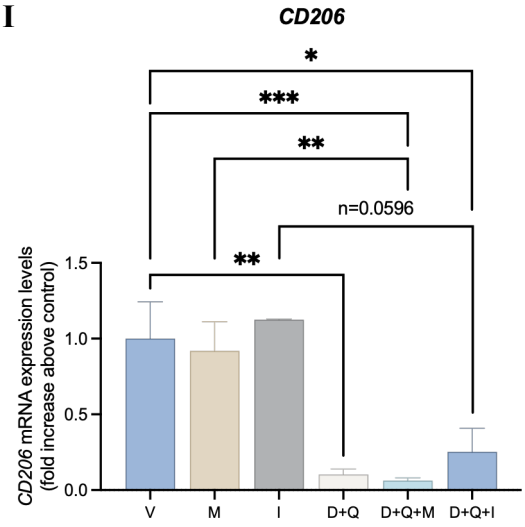
G


IL-1β
**
****
***
IL-1β mRNA expressio levels
(fold increase above control)
2.0
1.5
1.0
0.5
0.0
V
M
I
D+Q
D+Q+M
D+Q+I

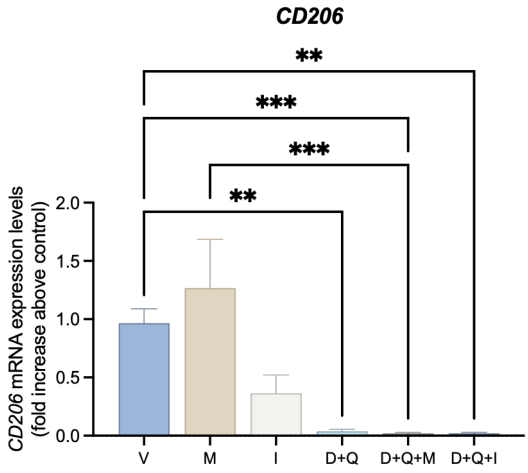
H


IL-1β
**
****
***
****
****
IL-1β mRNA expression levels
(fold increase above control)
2.0
1.5
1.0
0.5
0.0
V
M
I
D+Q
D+Q+M
D+Q+I

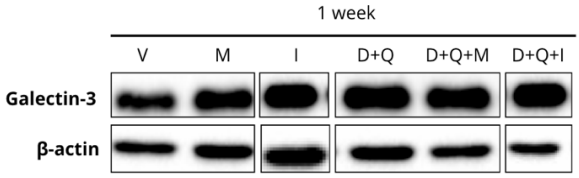
I


CD206
*
***
**
n=0.0596
**
CD206 mRNA expression levels
(fold increase above control)
1.5
1.0
0.5
0.0
V
M
I
D+Q
D+Q+M
D+Q+I

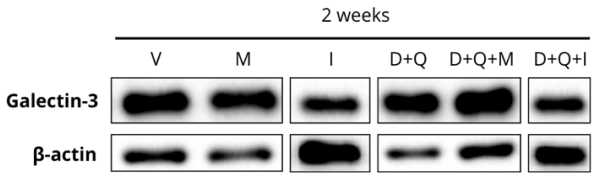
J


CD206
**
***
***
**
CD206 mRNA expression levels
(fold increase above control)
2.0
1.5
1.0
0.5
0.0
V
M
I
D+Q
D+Q+M
D+Q+I

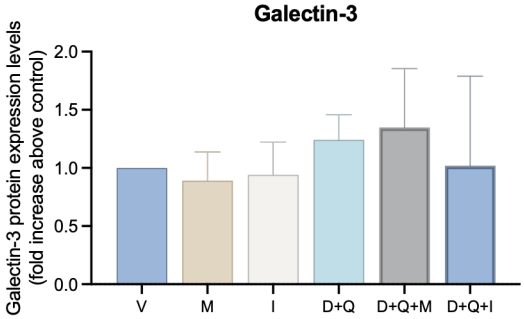
K


1 week
V
M
I
D+Q
D+Q+M
D+Q+I
Galectin-3
β-actin

L


2 weeks
V
M
I
D+Q
D+Q+M
D+Q+I
Galectin-3
β-actin

M


Galectin-3
Galectin-3 protein expression levels
(fold increase above control)
2.0
1.5
1.0
0.5
0.0
V
M
I
D+Q
D+Q+M
D+Q+I

N

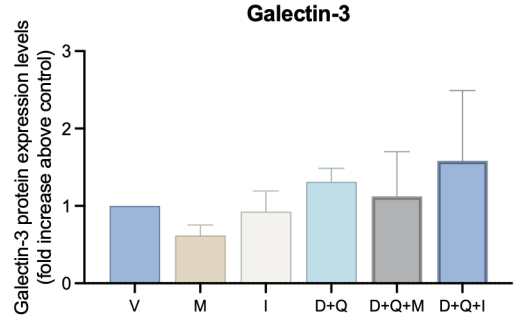

Galectin-3
Galectin-3 protein expression levels
(fold increase above control)
3
2
1
0
V
M
I
D+Q
D+Q+M
D+Q+I

Figure 16. **Effect of senolytic and lipolytic treatments on inflammatory and immune-related markers in human SAT Explants.** mRNA expression levels of *IL-6* **(A, B),** *IL-1β* **(G, H)** and *CD206* **(I, J)**, were assessed by RT-qPCR after one and two weeks of treatment. Protein expression levels of IL-6 **(E, F)**, and Galectin-3 **(M, N)** were assessed by Western blotting after one and two weeks of treatment. Representative Western blots of IL-6 **(C, D)** and Galectin-3 **(K, L)** are shown after one and two weeks of treatment. Gene expression levels were normalized to *IPO8*, while protein expression levels were normalized to β-actin, and are all expressed as fold change relative to vehicle. Experimental groups included vehicle (V), α-MSH (M), isoproterenol (I), dasatinib plus quercetin (D+Q) and the combined treatments D+Q+M and D+Q+I. Data are presented as mean ± SEM (n = 2-10). Statistical significance was determined using one-way ANOVA followed by Fisher´s uncorrected LSD test. $p < 0,05$ (*), $p < 0.01$ (**), $p < 0.001$ (***), $p < 0.0001$ (****).

Senescence and chronic inflammation, hallmarks of pathological AT expansion observed in both obesity and aging, are associated with excessive ECM deposition, initially serving to restrict tissue growth but ultimately contributing to tissue fibrosis and dysfunction. Therefore, it was next investigated whether changes observed following combined senotherapeutic treatment were accompanied by alterations in ECM remodeling by evaluating the key markers involved in AT ECM structure and turnover, including fibronectin (*FN*), *MMP3* and *TIMP1*.

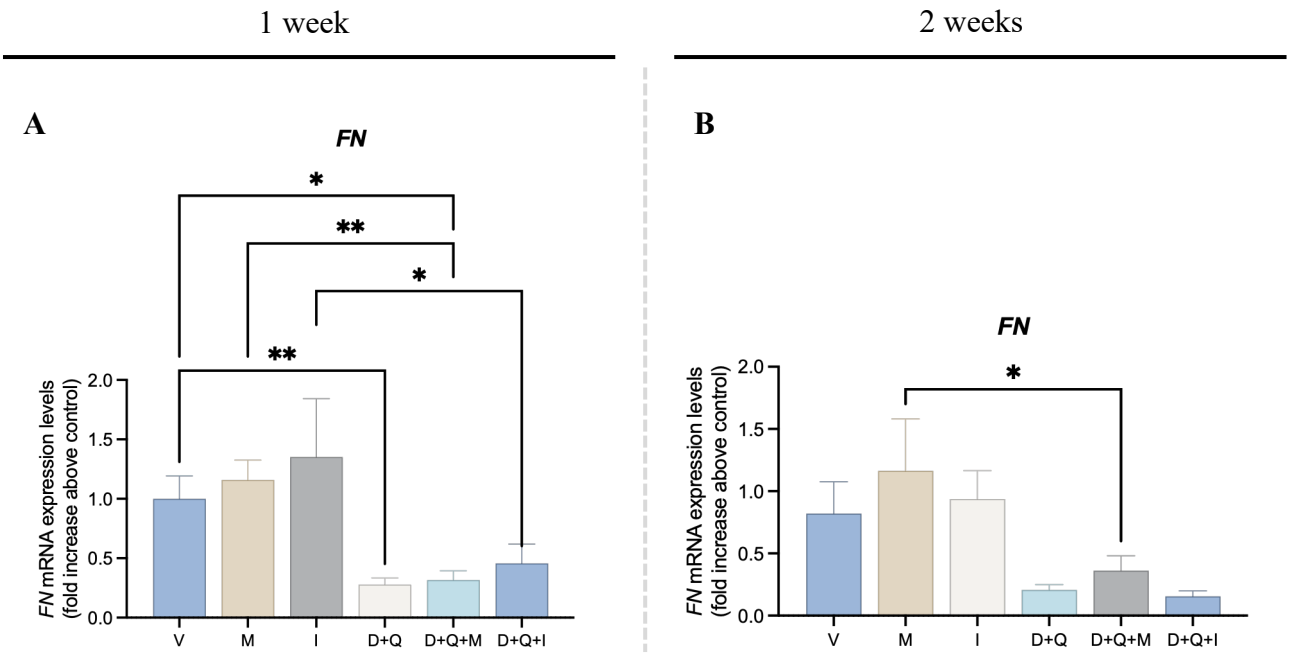
Expression of *FN*, a major matrix glycoprotein involved in tissue fibrosis, was persistently downregulated in D+Q-containing groups at both time points (Figure 17A, B). At one week, D+Q significantly reduced *FN* expression compared with vehicle, while D+Q+M resulted in significantly lower expression compared with both vehicle and α-MSH. D+Q+I also significantly reduced *FN* expression compared with isoproterenol (Figure 17A). This suppressive pattern was sustained for two weeks (Figure 17B), where D+Q-treated groups maintained lower *FN* expression than vehicle and lipolytic monotherapies, with D+Q+M achieving a significant reduction compared with α-MSH alone.

MMP3, an enzyme responsible for ECM degradation and remodeling, alongside its endogenous inhibitor, *TIMP1*, were next examined (Figure 17C, D, E, F). At one week, α-MSH monotherapy induced a marked upregulation of both genes, elevating *MMP3* expression to approximately 2.0-fold and *TIMP1* to 1.7-fold relative to vehicle (Figures 17C and E). In contrast, D+Q-based treatments prevented this effect: D+Q+M significantly suppressed both *MMP3* and *TIMP1* mRNA levels relative to α-MSH alone. By week two, this suppressive effect became even more pronounced across all D+Q-containing groups (Figure 17D, F). *MMP3* mRNA expression was significantly reduced by D+Q alone, D+Q+M, and D+Q+I relative to vehicle, with the lowest levels recorded in the combination treatments (Figure 17D). Similarly, *TIMP1* expression was

markedly suppressed by all D+Q-containing treatments relative to vehicle (Figure 17F) and showed significant reductions compared with their respective lipolytic monotherapies.

To assess the relative balance between ECM degradation and its inhibition, we analyzed the *MMP3/TIMP1* expression ratio (Figure 17G, H). At one week, D+Q-containing treatments shifted the balance toward a lower ratio, with D+Q+M inducing a significant reduction relative to both vehicle and α-MSH alone, while D+Q+I displayed a strong downward trend compared with vehicle ($p = 0.0515$; Figure 17G). By week two, despite the significant independent reductions observed in both *MMP3* and *TIMP1* transcript levels, no statistically significant alterations were detected in the *MMP3/TIMP1* ratio among any experimental groups (Figure 17H).

Taken together, these findings demonstrate that D+Q-based treatments were associated with an overall reduction in the expression of key ECM components and remodeling enzymes, while the reduced *MMP3/TIMP1* ratio indicated a shift in the balance of ECM turnover towards reduced proteolytic activity.



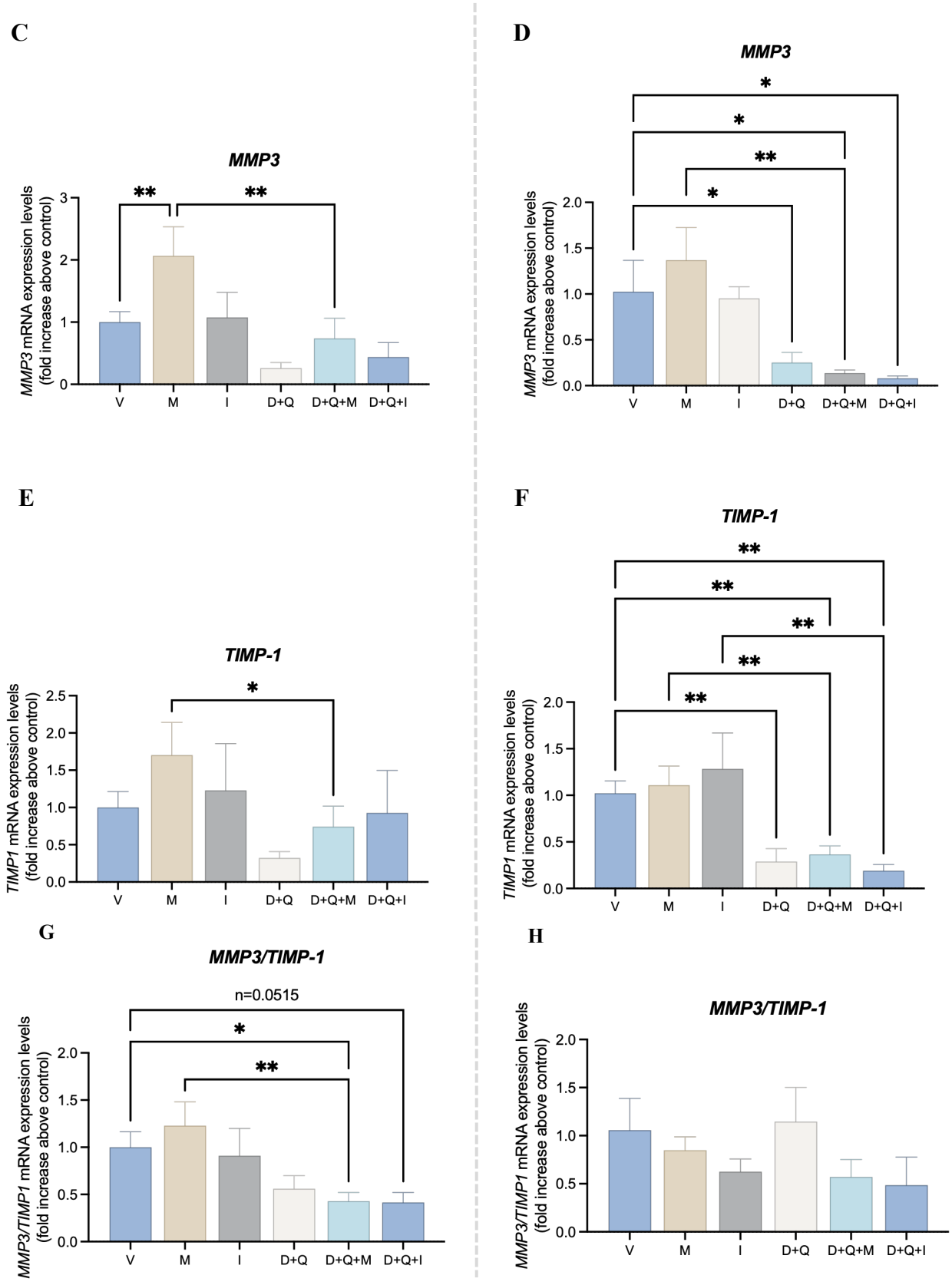


Figure 17. Effect of senolytic and lipolytic treatments on ECM remodeling in human SAT Explants. mRNA expression levels of *FN* **(A, B),** *MMP3* **(C, D)**, and *TIMP1* **(E, F)**, as well as the *MMP3/TIMP1* ratio **(G, H)** were assessed by RT-qPCR after one and two weeks of treatment. Experimental groups included vehicle (V), α-MSH (M), isoproterenol (I), dasatinib plus quercetin (D+Q) and the combined treatments D+Q+M and D+Q+I. Gene expression levels were normalized to *IPO8* and are expressed as fold change relative to vehicle. Data are presented as mean ± SEM (n = 3-11). Statistical significance was determined using one-way ANOVA followed by Fisher´s uncorrected LSD test. $p < 0{,}05$ (*), $p < 0.01$ (**).

7. Integrated transcriptional response of human SAT explants to treatment

To provide a broader view of the transcriptional changes described above, the expression profiles obtained after one and two weeks of treatment were integrated into heatmaps (Figure 18). By bringing together these individual responses, the heatmaps revealed distinct treatment-specific transcriptional signatures and highlighted how these patterns evolved over time. (Figure 18).

After one week of treatment, the integrated transcriptional profile already revealed changes across most of the genes analyzed (Figure 18A). Combining D+Q with lipolytic stimuli resulted in a broader and more pronounced response compared with D+Q alone, characterized by increased expression of thermogenesis- and cytoprotection-associated genes, together with reduced expression of several inflammation- and ECM remodeling-associated genes. These findings indicate a greater contribution of lipolytic stimulation to the transcriptional response during the early phase of D+Q treatment.

The transcriptional profile after two weeks revealed a more distinct and coordinated treatment-dependent pattern compared with the first week (Figure 18B). D+Q-containing treatments showed the most coordinated transcriptional response, characterized by increased expression of thermogenesis-associated genes together with an overall reduction in several markers associated with cellular senescence, inflammation, and ECM remodeling, while combining D+Q with lipolytic stimulation (D+Q+M and D+Q+I) produced limited additional transcriptional changes compared with D+Q alone, highlighting the predominant response associated with prolonged D+Q treatment (Figure 18B).

Notably, at one week, α-MSH alone also upregulated a broad set of genes classically associated with cellular senescence. However, their modulation occurred alongside evidence of increased lipolytic and thermogenic activity, suggesting that these changes may reflect an adaptive response to the metabolic stimulation induced by α-MSH rather than a direct promotion of senescence. The early transcriptional response to α-MSH is therefore consistent with coordinated metabolic reprogramming, stress adaptation, and tissue remodeling. Moreover, α-MSH and isoproterenol in the presence of D+Q elicited distinct transcriptional responses between one and two weeks of treatment, suggesting

that the response to metabolic stimulation may be shaped by the underlying tissue microenvironment and its progressive remodeling during D+Q treatment. Importantly, comparison of gene expression levels between vehicle-treated explants after one and two weeks revealed no significant differences for most of the analyzed genes, with *CD206* representing the only exception (Figure 19). This finding indicates that, overall, the transcriptional changes observed between one and two weeks were not primarily attributable to time in culture, supporting their association with treatment-dependent effects.

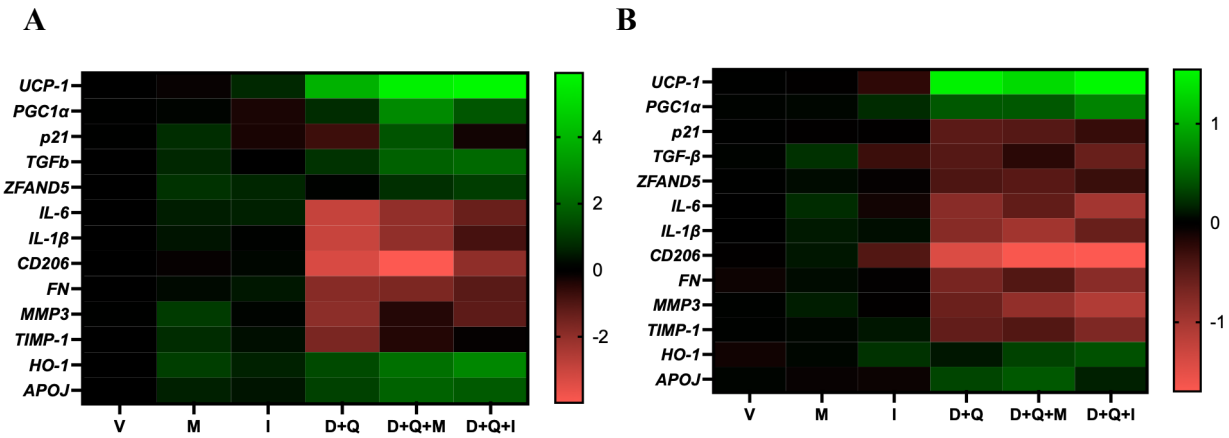


Figure 18. Integrated heatmap analysis of gene expression profiles in human SAT Explants following senolytic and lipolytic treatment. Heatmap showing the relative expression profiles of genes associated with thermogenesis (UCP-1 and PGC1α), senescence and stress response (*p21*, *TGF-β* and *ZFAND5*), cytoprotection (*HO-1* and *APOJ*), inflammation and immune response (*IL-6*, *IL-1β* and *CD206*) and ECM remodeling (*FN*, *MMP3*, *TIMP1*) after one **(A)** and two **(B)** weeks of treatment. Experimental groups included vehicle (V), α-MSH (M), isoproterenol (I), dasatinib plus quercetin (D+Q) and the combined treatments D+Q+M and D+Q+I (n = 2-11). The color scale represents relative gene expression, with green indicating higher and red indicating lower expression.

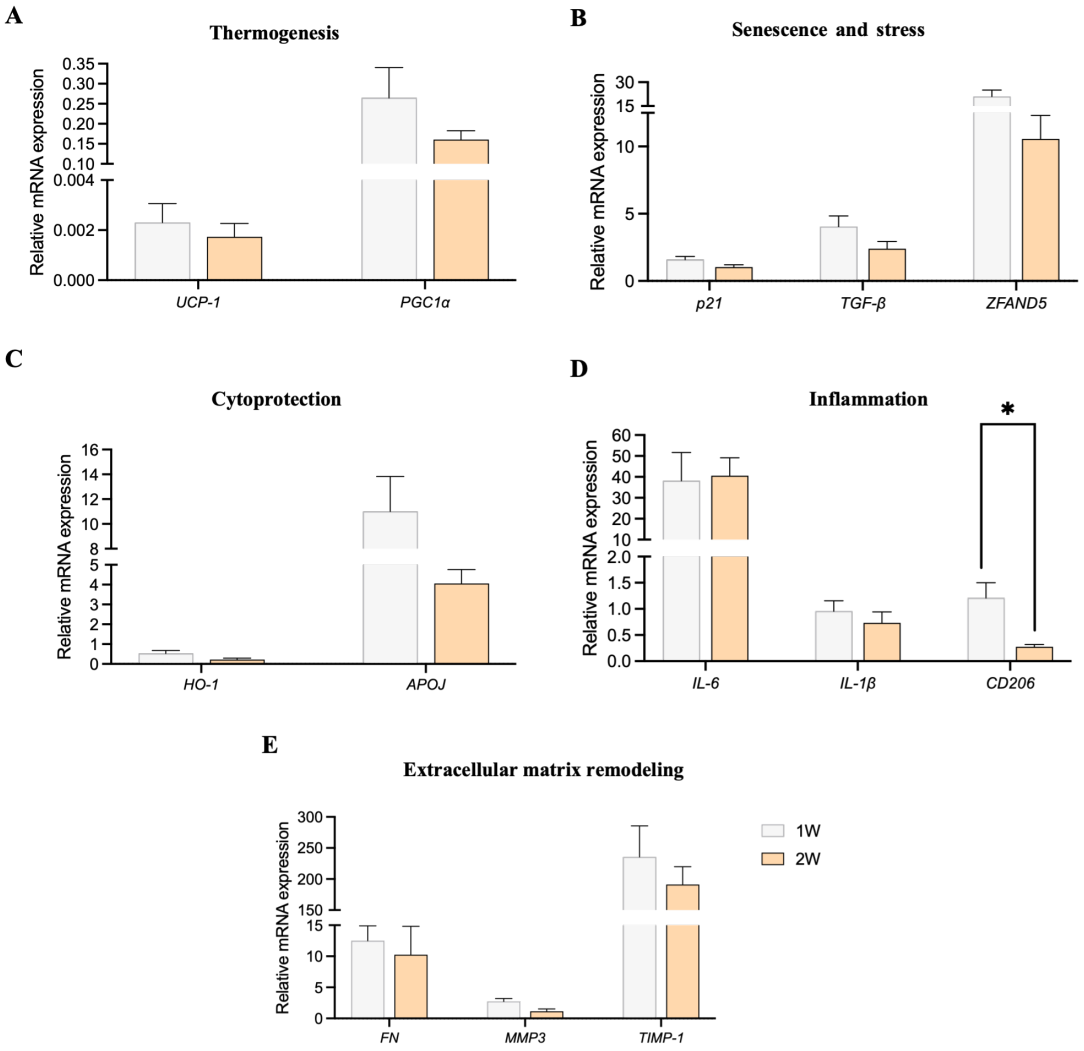


Figure 19. Gene expression stability in vehicle-treated in human SAT Explants during the culture period. Relative mRNA expression levels of genes associated with thermogenesis (*UCP-1* and *PGC1α*) **(A),** senescence and stress response (*p21*, *TGF-β* and *ZFAND5*) **(B)**, cytoprotection (*HO-1* and *APOJ*) **(C)**, inflammation and immune response (*IL-6*, *IL-1β* and *CD206*) **(D)** and extracellular matrix remodeling (*FN*, *MMP3*, *TIMP1*) **(E)**, were compared between vehicle-treated explants after one (1W) and two weeks (2W) of culture. Gene expression levels were assessed by RT-qPCR and normalized to *IPO8*. Data are presented as mean ± SEM (n = 2-11). No statistically significant differences were observed between the two time points for most of the analyzed genes, with *CD206* being the only gene showing a significant difference between 1W and 2W. Statistical significance was determined using Multiple Unpaired t-test. $p < 0,05$ (*).

Discussion

AT is a dynamic endocrine organ with a central role in energy homeostasis and metabolic regulation. Its remarkable plasticity enables continuous adaptation to changes in energy availability and metabolic demand. However, this capacity becomes progressively impaired under conditions such as aging and obesity. Both are associated with extensive AT remodeling and the establishment of a chronic low grade inflammatory state, often referred to as adipaging (2). A hallmark of this dysfunctional environment is the progressive accumulation of SCs, which through the secretion of SASP factors, can exacerbate local inflammation and impair key metabolic functions, including lipolysis, thermogenesis and adipogenesis, further compromising AT homeostasis. In this study, clearance of SCs from ex-obese human SAT revealed a time-dependent reduction in senescence-, inflammatory-, and tissue-remodeling-associated responses and a concomitant activation of lipolytic, thermogenic and cytoprotective programs. The addition of lipolytic stimuli accelerated these metabolic adaptations after one week, whereas after two weeks senolytics alone were sufficient to elicit comparable responses. This temporal shift suggests that prolonged senolytic treatment progressively alleviates the dysfunctional tissue environment, allowing metabolic adaptation to emerge in the absence of additional lipolytic stimulation.

Although *ex vivo* culture provides a valuable model to investigate AT responses while preserving tissue architecture and cellular interactions, evidence regarding long-term AT explant viability remains limited. However, Schopow et al. demonstrated that tissue integrity, morphology, and composition remained preserved after 14 days of treatment (191) Consistent with these observations, several findings in the present study support the preservation of tissue integrity and cellular responsiveness throughout the two-week culture period. Histological analysis showed preserved adipocyte morphology after two weeks of culture, with well-defined cell boundaries and no evident signs of tissue deterioration (Figure 8). Furthermore, gene expression in vehicle-treated explants did not differ significantly between one and two weeks for most of the genes analyzed, supporting the overall stability of the explants over time (Figure 19). Importantly, SAT explants remained responsive to pharmacological stimulation after two weeks of culture, as α-MSH and isoproterenol were still able to modulate the expression of several lipolytic and inflammatory markers. Moreover, treatment-induced responses

were marker-specific, with some genes being upregulated, others downregulated, and others remaining unchanged, rather than displaying a generalized decline in gene expression. Together, these observations provide no evidence of a generalized culture-induced deterioration of the explants and support the maintenance of biologically active and responsive SAT explants throughout the experimental period.

Lipolysis represents a central metabolic function of adipocytes, allowing the mobilization of stored TG into FAs and glycerol in response to energetic demands. In the present study, D+Q treatment was associated with an overall enhancement of the lipolytic phenotype of SAT explants from ex-obese individuals, supported by both functional and molecular data. This effect became more evident after prolonged treatment, with increased basal lipolytic activity and sustained elevation of ATGL and HSL protein levels (Figures 9 and 10), accompanied by a reduction in adipocyte size (Figure 7). Given that adipocyte hypertrophy is a characteristic of dysfunctional AT and is associated with impaired metabolic function and a pro-inflammatory tissue environment (192), the reduction in adipocyte size may reflect improved lipid mobilization and a shift towards a more metabolically active adipocyte phenotype.

Interestingly, the increased ATGL and HSL protein levels following D+Q suggest that senolytic treatment may enhance the underlying lipolytic capacity of the tissue. In contrast, α-MSH or isoproterenol increased glycerol release without altering ATGL or HSL abundance, suggesting that their effects on lipolytic activity may involve regulation of the existing lipolytic machinery. However, the addition of α-MSH or isoproterenol did not further increase glycerol release beyond the effects observed with D+Q alone. This may be related, at least in part, to the fact that glycerol release was measured after 24 h of treatment, which primarily reflects the chronic effect of the interventions on basal lipolytic activity rather than the acute response to lipolytic stimulation. Moreover, α-MSH and isoproterenol were administered in serum-containing medium, where the presence of hormones, growth factors, nutrients and other bioactive components may further influence adipocyte metabolism and potentially attenuate the specific effects of exogenous lipolytic agonists (193). Assessment of the acute response, typically evaluated after a short stimulation period, would therefore be valuable to determine whether chronic D+Q treatment also alters the adipocyte responsiveness to lipolytic stimulation. This could be complemented by

evaluating HSL phosphorylation, a rapid and transient marker of lipolytic activation (194).

The metabolic changes associated with D+Q were not restricted to lipid mobilization. The concomitant induction of *UCP-1* and *PGC1α* indicates activation of a thermogenic and browning-associated program, consistent with the acquisition of a more metabolically active adipocyte phenotype (5,45,81,105). Notably, this response was strongly dependent on treatment duration. At one week, the most pronounced induction of thermogenic markers occurred when D+Q was combined with α-MSH or isoproterenol, whereas after two weeks D+Q alone elicited a comparable response (Figure 11). Lipolytic stimulation therefore appears to provide an additional metabolic stimulus during the early phase of treatment, while prolonged senolytic treatment is sufficient to achieve a similar thermogenic response. The lack of induction by α-MSH or isoproterenol alone further suggests that these stimuli, despite their established metabolic and thermogenic effects, were insufficient to induce a detectable thermogenic phenotype in this *ex vivo* WAT model in the absence of senolytic treatment. Given that UCP-1 expression in WAT reflects the acquisition of a beige/thermogenic phenotype, the absence of a significant response to either stimulus alone may indicate that the functional state of the tissue limits its capacity to undergo thermogenic reprogramming. Although both α-MSH and isoproterenol have previously been associated with activation of thermogenic pathways (81,82,195), their effects may depend on the functional state of the tissue in which the stimulus is applied.

This temporal pattern is particularly relevant when considered together with the changes observed in senescence-, inflammatory-, and tissue-remodeling-associated pathways. Rather than acting as a direct thermogenic stimulus, D+Q may progressively modify the tissue environment in a manner that increases its capacity to support metabolic adaptation. At one week, when the dysfunctional environment may still constrain adipocyte plasticity, the addition of a lipolytic stimulus resulted in a more pronounced thermogenic response. With prolonged D+Q treatment, the progressive reduction of senescence-associated AT dysfunction may create a more permissive metabolic environment, allowing adipocytes to recover their responsiveness, rendering additional lipolytic stimulation less necessary over time. Thus, the requirement for a complementary metabolic stimulus appears to diminish with treatment duration.

Consistent with this interpretation, senescence- and stress-associated pathways also evolved over the course of treatment. *p21*, *ZFAND5* and *TGF-β* markers showed an early increase in response to α-MSH-containing treatments, particularly when combined with D+Q, whereas after two weeks, D+Q-containing treatments were generally associated with lower expression (Figure 12). Importantly, these markers should not be interpreted independently as direct measures of SC abundance. p21, for example, is a classical mediator of cell-cycle arrest but also participates in adipocyte differentiation, hypertrophy, apoptosis resistance, and cellular stress responses (196). Inoue et al. showed that p21 contributes to the later stages of adipocyte differentiation, as reduced p21 expression was accompanied by decreased levels of adipogenic transcription factors C/EBPα and PPARγ (197). Additionally, cellular stress and DNA damage can activate p53/p21 pathway as part of the DNA damage response, without resulting in permanent senescence (126). Its transient increase at one week may therefore reflect an early stress or tissue-adaptation response rather than an increase in SC burden. The subsequent reduction following prolonged D+Q treatment is more compatible with attenuation of a senescence-associated phenotype (Figure 12B).

Beyond *p21*, the changes observed in *ZFAND5* and *TGF-β*/PAI-1 signaling should also be interpreted considering their broader biological functions. ZFAND5 contributes to proteostasis through activation of the 26S proteasome, enhancing the degradation of ubiquitinated proteins and thereby contributing to cellular protein turnover (198). This function may be particularly relevant in the context of aging and cellular senescence, which are characterized by a progressive loss of proteostasis and accumulation of damaged or misfolded proteins (199,200). In addition, ZFAND5 has been implicated in the regulation of inflammatory signaling, including NF-κB-related pathways, further linking its function to cellular responses within a pro-inflammatory environment (201). Its early induction by the lipolytic agents (Figure 12C) may therefore represent an adaptive response to the increased metabolic and cellular demands associated with sustained lipolytic stimulation, potentially involving enhanced protein turnover. The subsequent reduction in *ZFAND5* expression after prolonged D+Q treatment (Figure 12D) may reflect a reduced need for this adaptive response as D+Q progressively alleviates tissue dysfunction.

TGF-β is likewise involved in multiple processes relevant to dysfunctional AT, including cell proliferation, differentiation, tissue repair and ECM remodeling (202,203). In AT, TGF-β expression is elevated during obesity and has been associated with ECM accumulation and fibrosis (204). In response to tissue injury, fibrotic remodeling can initially represent a reparative mechanism, promoting ECM deposition to maintain tissue structural integrity. However, when sustained, excessive ECM accumulation can compromise tissue architecture and contribute to AT dysfunction. In this context, *FN*, *MMP3* and *TIMP1* were generally reduced following D+Q-containing treatments (Figure 16). Rather than indicating a simple shift towards increased or decreased ECM degradation, the coordinated reduction in *MMP3* and *TIMP1* after two weeks, together with reduced *FN*, is more consistent with an overall attenuation of ECM turnover. FN is an important component of the ECM involved in matrix organization, cell adhesion and tissue remodeling, and alterations in FN deposition have been associated with fibrotic remodeling of dysfunctional AT (205). At one week, α-MSH alone increased both *MMP3* and *TIMP1* without markedly altering their relative balance (Figure 16C and E), suggesting a coordinated remodeling response rather than a clear increase in net proteolytic activity.

This remodeling response was further reflected in the TGF-β/PAI-1 axis. PAI-1 is a well-established downstream target of TGF-β/SMAD signaling and contributes to tissue remodeling by inhibiting plasminogen activators and thereby regulating extracellular proteolysis and ECM turnover (206,207). Importantly, PAI-1 is also recognized as a senescence-associated factor and a component of the SASP, linking tissue remodeling with cellular senescence (208). The early induction of *TGF-β* (Figure 12E), together with the increase in PAI-1 following lipolytic stimulation (Figure 13C and D), may therefore reflect activation of remodeling-associated pathways in response to metabolic stimulation within a still dysfunctional tissue environment.

Conversely, the tendency towards lower *TGF-β*/PAI-1 signaling following prolonged D+Q treatment, together with the coordinated reduction in *FN*, *MMP3* and *TIMP1*, is consistent with an attenuation of the profibrotic environment and a shift towards a less remodeling-intensive state. Importantly, these molecular changes do not establish reversal of fibrosis but rather indicate attenuation of pathways associated with ECM remodeling. Indeed, sustained TGF-β expression has also been associated with cellular

senescence through mechanisms involving ROS production, cell-cycle arrest and SASP signaling (209). Moreover, reduced TGF-β signaling has been associated with enhanced beige adipogenesis (210,211), which agrees with the increased expression of thermogenic and browning-related markers observed after two weeks of treatment.

The response to α-MSH further supports the influence of the tissue context on these remodeling pathways. The increase in PAI-1 induced by α-MSH was strongly attenuated in the presence of D+Q (Figure 13C and D), indicating that senolytic treatment may limit the remodeling response elicited by metabolic stimulation. Importantly, this effect occurred despite continued exposure to α-MSH, suggesting that the cellular environment in which metabolic stimulation occurs influences the extent to which remodeling-associated pathways are engaged. Thus, while metabolic stimulation in a dysfunctional tissue environment may initially activate remodeling-associated responses, alleviation of this environment by D+Q appears to reduce the need for such compensatory responses.

The lack of a consistent response in Lamin B1 further illustrates the importance of interpreting individual senescence-associated markers within the broader molecular context. Lamin B1 is a major structural component of the nuclear lamina that plays essential roles in maintaining nuclear architecture, chromatin organization, DNA replication, DNA damage responses, and gene regulation (133,212,213). Although reduced Lamin B1 is commonly associated with cellular senescence, its regulation is dependent on cell type, tissue context and the mechanisms driving senescence (212,214). In previous work from our group, CuSO4-induced senescence in 3T3-L1 cells was associated with nuclear lamina destabilization and increased rather than decreased Lamin B1 levels (215). The absence of a clear treatment-dependent response in the present explant model (Figure 13E and F) therefore does not necessarily contradict the changes observed in other senescence-associated pathways but rather reinforces the limitations of using individual markers as surrogate measures of the senescent state.

The coordinated reduction in inflammatory-associated signals following D+Q further supports an overall attenuation of the dysfunctional tissue environment. D+Q reduced the expression of several inflammatory mediators, including IL-6 and *IL-1β* (Figure

16A-H), consistent with previous evidence for an anti-inflammatory effect of senolytic treatment in AT (177,186). The response to α-MSH was more complex, particularly for IL-6, which increased significantly after two weeks (Figure 16B and F). Although IL-6 is widely recognized as a pro-inflammatory cytokine and a component of the SASP, its biological effects are highly context-dependent, extending beyond inflammation to the regulation of glucose and lipid metabolism (216). A well-established example is exercise, during which IL-6, considered a myokine, is released by skeletal muscle and contributes to metabolic and anti-inflammatory signaling (217). Importantly, IL-6 has also been implicated in the regulation of AT lipid metabolism, with studies in humans demonstrating increased lipolysis, FA oxidation and glycerol release from subcutaneous AT following IL-6 stimulation (216). The increase observed following α-MSH may therefore reflect a metabolic response rather than simply an exacerbation of inflammation. Its attenuation in the presence of D+Q further suggests that, as tissue dysfunction is alleviated, the need for additional metabolic stimulation may progressively diminish.

Taken together, these findings suggest that α-MSH alone activates multiple pathways in metabolically compromised AT, whereas dysfunctional microenvironment persists. Rather than simply stimulating lipolysis, α-MSH may promote a broader metabolic response involving coordinated changes in proteostasis, inflammatory signaling and tissue remodeling. In this context, the early induction of stress-responsive genes such as *ZFAND5* and *p21* may reflect an adaptive response to the increased cellular and metabolic demands of stimulation, while the subsequent changes in TGF-β/PAI-1 signaling may reflect engagement of pathways involved in ECM turnover and tissue remodeling. By alleviating the dysfunctional tissue environment, D+Q attenuated these responses, suggesting that improved tissue homeostasis reduces the need for additional remodeling and stress-responsive pathways during metabolic stimulation.

Changes in macrophage abundance and phenotype provide additional evidence of alterations in the tissue microenvironment, although these findings require careful interpretation. Macrophage accumulation is an important feature of dysfunctional AT and contributes to the establishment and maintenance of chronic low-grade inflammation (218). AT macrophages comprise a heterogeneous population of immune cells that perform diverse functions, including immune surveillance, lipid handling,

tissue homeostasis and remodeling. Although ATMs have traditionally been classified into M1-like and M2-like phenotypes, with M1-like macrophages generally associated with pro-inflammatory responses and M2-like macrophages with anti-inflammatory functions, tissue-resident ATMs can display intermediate or distinct functional states that are not adequately captured by this binary classification (219,220). In the present study, *CD206* expression decreased following D+Q-containing treatments (Figure 16I and J). However, CD206 is not an exclusive marker of anti-inflammatory M2-like macrophages and is also expressed by resident ATMs involved in tissue maintenance and remodeling (109,221). Its reduction should therefore not be interpreted as evidence of a shift towards a more inflammatory macrophage phenotype, particularly given the concomitant reduction in inflammatory markers. Rather, it may reflect changes in macrophage abundance or functional state within the tissue. Interestingly, *CD206* was the only marker showing a significant difference between vehicle-treated explants after one and two weeks of culture (Supplementary Figure 1D), suggesting that macrophage populations may undergo specific changes during prolonged *ex vivo* maintenance.

The interpretation of these changes is particularly relevant in the context of post-bariatric SAT. Recent evidence has shown that substantial weight loss markedly reduces macrophage infiltration in human SAT but does not completely reverse obesity-associated macrophage activation and metabolic reprogramming, suggesting the persistence of a cellular memory of the previous obese state (169,222). Thus, SAT obtained from post-bariatric individuals may retain macrophage populations with persistent functional alterations despite substantial weight loss.

In this context, the further decrease in *CD206* observed following D+Q-containing treatments may reflect changes in the abundance or activity of resident macrophages as the tissue microenvironment becomes less dysfunctional. Interestingly, $CD206^{+}$ M2-like macrophages have been shown to reduce the AT microenvironment through TGF-β signaling, with depletion of these cells resulting in reduced TGF-β signaling and smaller adipocytes (223). This observation is particularly relevant in the present study given the concomitant reduction in *CD206* and *TGF-β* expression, together with the reduction in adipocyte size observed following D+Q-containing treatments.

Consistent with this idea, Galectin-3, which is highly expressed by AT macrophages surrounding damaged or dead adipocytes within CLS, remained largely unchanged

following treatment (Figure 16M and N). CLS are a characteristic feature of dysfunctional AT and are associated with obesity-related inflammation and adipocyte dysfunction (224,225). The absence of a clear treatment effect may reflect the characteristics of the post-weight-loss tissue and the extent of pre-existing macrophage remodeling. Indeed, previous studies have shown that substantial weight loss following bariatric surgery markedly reduces CLS density in human SAT, whereas dispersed macrophage populations may remain relatively stable (177,186). Therefore, CLS-associated macrophage activity may already be reduced in SAT obtained following bariatric surgery, potentially limiting the detection of further treatment-induced changes in Galectin-3 expression.

Alongside the attenuation of inflammatory and remodeling-associated pathways, D+Q-containing treatments induced cytoprotective responses, particularly involving *APOJ* and *HO-1* (Figure 14 and 15). Both proteins have functions that extend beyond senescence and are strongly associated with cellular adaptation to stress. APOJ/clusterin acts as a molecular chaperone involved in proteostasis (226). In its secreted form, APOJ binds misfolded proteins, prevents their aggregation and facilitates their clearance, thereby contributing to extracellular protein quality control (226,227). Moreover, its expression can be induced in response to different forms of cellular stress, including oxidative stress (228). In the present study, the increased *APOJ* expression observed following D+Q-containing treatments (Figure 14), particularly when combined with the lipolytic agents, may therefore reflect the activation of cytoprotective and proteostatic mechanisms associated with treatment-induced metabolic and tissue remodeling, rather than an increase in SC burden.

HO-1 is likewise a stress-inducible antioxidant enzyme with cytoprotective, anti-inflammatory and antioxidant functions (229,230). HO-1-related pathways have also been associated with attenuation of cellular senescence and suppression of SASP-associated inflammation, further supporting a protective role in dysfunctional AT (231). Notably, HO-1 has also been linked to mitochondrial function and AT browning, with experimental studies associating HO-1-related pathways with increased thermogenic activity and improved metabolic function in AT (231,232). As *APOJ*, *HO-1* expression was predominantly increased following D+Q-containing treatments, mainly when combined with the lipolytic agents (Figure 15). Hence, the concurrent

induction of *APOJ* and *HO-1* may therefore reflect activation of cytoprotective mechanisms that support proteostasis, cellular adaptation and metabolic remodeling.

Taken together, the metabolic, inflammatory, remodeling and cytoprotective responses support a time-dependent effect in which senolytic treatment progressively reshapes the tissue environment of dysfunctional SAT. Although relatively modest transcriptional changes were observed after one week, a more coordinated profile emerged after two weeks, characterized by reduced expression of markers associated with cellular senescence, inflammation and ECM remodeling, together with increased expression of thermogenesis- and cytoprotection-associated markers (Figure 18). These transcriptional changes were accompanied by broader functional and morphological adaptations, including enhanced basal lipolytic capacity and reduced adipocyte size. Notably, the addition of α-MSH or isoproterenol produced a broader early metabolic and cytoprotective response after one week of treatment, but its apparent advantage became less evident after prolonged D+Q treatment (Figure 18). This temporal pattern may indicate that, while additional metabolic stimulation can enhance the early response of a dysfunctional tissue, prolonged targeting of senescence may be sufficient to support metabolic adaptation as features of the dysfunctional microenvironment are attenuated. Importantly, the present findings do not establish a direct causal relationship between SC clearance and metabolic recovery. Rather, they provide evidence that targeting senescence is associated with coordinated changes in the tissue environment and in several components of adipocyte metabolic function, supporting senotherapy as a potential complementary strategy for improving the functional state of metabolically compromised AT.

The potential relevance of this approach may extend beyond obesity- and age-associated AT dysfunction to conditions in which tissue alterations persist despite substantial metabolic improvement, particularly following weight loss. Importantly, marked weight loss does not necessarily result in complete restoration of AT homeostasis. Recent evidence from human SAT showed that weight loss markedly reversed several obesity-associated alterations, including adipocyte hypertrophy, cellular senescence, fibrosis and inflammation, while promoting a more metabolically active adipocyte phenotype (169). Particularly, Miranda et al. showed that myeloid cell abundance was substantially reduced, from approximately 31% in obesity to 18%

following weight loss, approaching the 14% observed in lean individuals (169). However, despite this overall recovery, obesity-induced macrophage activation states persisted after weight loss, suggesting that these cells may retain an epigenetically programmed memory of the previous obese state (169). Such persistent macrophage activation may contribute to incomplete metabolic recovery and has been proposed as a potential mechanism predisposing to weight regain and long-term metabolic dysfunction (169).

These observations highlight the broader potential of the treatment strategy investigated in the present study, both to mitigate the progressive deterioration of AT associated with aging and as a complementary approach to target residual AT dysfunction following substantial weight loss induced by bariatric surgery or pharmacological therapies.

Study limitations and future perspectives

Despite the promising findings, some limitations should be acknowledged. First, the use of human SAT explants introduces considerable biological variability due to differences in donor characteristics, including age, sex, BMI, medication, and metabolic history. Although this variability reflects the heterogeneity of human AT and contributes to the translational relevance of the model, the relatively small sample size may have limited statistical power, particularly for outcomes showing trends rather than statistically significance differences. The availability of human AT was dependent on elective surgical procedures, making sample collection particularly challenging. Larger cohorts would therefore be important to confirm the present findings and determine whether donor characteristics influence treatment responsiveness.

A further limitation is that several biological processes were inferred from changes in gene and protein expression rather than directly assessed through functional or mechanistic approaches. In particular, the present data support attenuation of senescence-, inflammatory- and ECM remodeling-associated pathways but do not directly quantify SC abundance or establish that the observed metabolic effects result from SC clearance. Similarly, glycerol release was assessed after 24 h and therefore primarily reflects basal lipolytic activity rather than the acute response to α-MSH or isoproterenol. Future studies should therefore combine direct assessment of SC burden with functional measurements of acute and basal lipolysis, mitochondrial function and oxidative metabolism to further define the mechanisms underlying the observed responses. Functional and morphological analyses of adipocyte browning and thermogenesis would also help establish whether the molecular changes observed are accompanied by corresponding changes in tissue phenotype. Transcriptomic, metabolomic and secretomic approaches could additionally provide a more comprehensive characterization of the pathways and factors involved in the response to senolytic and metabolic stimulation, potentially identifying novel mechanisms and biomarkers associated with treatment responsiveness.

The present study was restricted to SAT obtained from individuals who had undergone substantial weight loss following bariatric surgery. Although this represents a particularly relevant model for investigating persistent features of AT dysfunction after

weight loss, it remains unclear whether the observed responses are applicable to other metabolic states or adipose depots. Future studies comparing post-bariatric individuals, individuals with active obesity and non-obese individuals across different age groups would help determine whether metabolic history and aging influences responsiveness to senolytic treatments. Given the more pronounced AT dysfunction in active obese or aged individuals, greater responsiveness to both senolytic and lipolytic stimuli than observed in the present study would be expected, with the strongest effects potentially arising from their combined application. Extending these analyses to VAT would also be relevant given its distinct cellular, metabolic and inflammatory characteristics and its stronger association with obesity-related metabolic complications.

Finally, although the *ex vivo* explant model represents an important advantage by preserving native tissue architecture and interactions between adipocytes and stromal, immune and vascular-associated cells more effectively than conventional monoculture systems, it does not reproduce the complex systemic environment *in vivo*, including endocrine, neural, vascular and immune interactions that may influence AT responses to treatment. Complementary *in vivo* studies using models of diet-induced obesity, such as high-fat diet (HFD)-fed mice, and naturally aged mice would be valuable to determine whether the metabolic and tissue-remodeling effects observed here are maintained under physiological conditions.

Overall, further validation in larger cohorts and complementary experimental models will be necessary to establish the therapeutic potential of combining senolytic treatment with metabolic stimulation. Of particular interest is whether targeting senescence not only improves specific components of AT function but also restores the capacity of dysfunctional AT to respond appropriately to subsequent metabolic stimuli.

Conclusions

The present study demonstrates that targeting cellular senescence with dasatinib and quercetin (D+Q) modulates the metabolic and molecular profile of human SAT obtained from individuals following substantial weight loss. D+Q was associated with increased lipolytic capacity, reduced adipocyte size and attenuation of inflammatory and ECM remodeling-associated pathways, while prolonged treatment was accompanied by increased expression of thermogenic and browning-related markers. These findings indicate that senolytic treatment can improve specific components of the metabolic competence of previously obese AT and modify features of its dysfunctional tissue environment.

The addition of α-MSH or isoproterenol enhanced the early metabolic response to D+Q, particularly with respect to thermogenic and cytoprotective pathways. However, after two weeks, D+Q alone elicited comparable thermogenic responses, suggesting that the contribution of additional metabolic stimulation diminishes with prolonged senolytic treatment. The distinct temporal responses further indicate that the metabolic effects of lipolytic stimulation depend, at least in part, on the functional state of the tissue in which the stimulus is applied.

Importantly, SAT from individuals who had undergone substantial weight loss retained molecular features associated with AT dysfunction, supporting the concept that previous obesity may leave a persistent molecular and cellular imprint on AT. Within this context, targeting cellular senescence may represent a complementary strategy to weight loss, not only by attenuating components of the dysfunctional tissue environment but also by improving the capacity of AT to engage metabolic responses.

Overall, these findings support senolytic treatment as a potential approach to improve the functional state and metabolic responsiveness of previously obese AT. By targeting persistent senescence-associated features, senolytic therapy may represent a promising therapeutic strategy to promote a healthier AT environment following established weight-loss interventions, including bariatric surgery and pharmacological therapies, potentially supporting the long-term maintenance of weight-loss benefits. Further studies are required to establish the underlying mechanisms and determine whether these effects translate into improved AT function *in vivo*.

References

1. Rosen ED, Spiegelman BM. What we talk about when we talk about fat. Cell. Elsevier B.V.; 2014. p. 20–44. doi:10.1016/j.cell.2013.12.012 PubMed PMID: 24439368.
2. Pérez LM, Pareja-Galeano H, Sanchis-Gomar F, Emanuele E, Lucia A, Gálvez BG. 'Adipaging': ageing and obesity share biological hallmarks related to a dysfunctional adipose tissue. Journal of Physiology. Blackwell Publishing Ltd; 2016. p. 3187–207. doi:10.1113/JP271691 PubMed PMID: 26926488.
3. Kawai T, Autieri M V., Scalia R. Adipose tissue inflammation and metabolic dysfunction in obesity. Am J Physiol Cell Physiol. 2021 Mar 1;320(3):C375–91. doi:10.1152/ajpcell.00379.2020 PubMed PMID: 33356944.
4. Maniyadath B, Zhang Q, Gupta RK, Mandrup S. Adipose tissue at single-cell resolution. Cell Metabolism. Cell Press; 2023. p. 386–413. doi:10.1016/j.cmet.2023.02.002 PubMed PMID: 36889280.
5. An SM, Cho SH, Yoon JC. Adipose Tissue and Metabolic Health. Diabetes and Metabolism Journal. Korean Diabetes Association; 2023. p. 595–611. doi:10.4093/dmj.2023.0011 PubMed PMID: 37482656.
6. Sakers A, De Siqueira MK, Seale P, Villanueva CJ. Adipose-tissue plasticity in health and disease. Cell. Elsevier B.V.; 2022. p. 419–46. doi:10.1016/j.cell.2021.12.016 PubMed PMID: 35120662.
7. Reyes-Farias M, Fos-Domenech J, Serra D, Herrero L, Sánchez-Infantes D. White adipose tissue dysfunction in obesity and aging. Biochemical Pharmacology. Elsevier Inc.; 2021. doi:10.1016/j.bcp.2021.114723 PubMed PMID: 34364887.
8. Song MG, Lee HJ, Jin BY, Gutierrez-Aguilar R, Shin KH, Choi SH, et al. Depot-specific differences in angiogenic capacity of adipose tissue in differential susceptibility to diet-induced obesity. Mol Metab. 2016 Nov 1;5(11):1113–20. doi:10.1016/j.molmet.2016.09.001 PubMed PMID: 27818937.
9. Marcelin G, Gautier EL, Clément K. Adipose Tissue Fibrosis in Obesity: Etiology and Challenges. Annu Rev Physiol. 2025;39:48. doi:10.1146/annurev-physiol-060721

10. Sun K, Kusminski CM, Scherer PE. Adipose tissue remodeling and obesity. Journal of Clinical Investigation. 2011. p. 2094–101. doi:10.1172/JCI45887 PubMed PMID: 21633177.
11. Iacobini C, Vitale M, Haxhi J, Menini S, Pugliese G. Impaired Remodeling of White Adipose Tissue in Obesity and Aging: From Defective Adipogenesis to Adipose Organ Dysfunction. Cells. Multidisciplinary Digital Publishing Institute (MDPI); 2024. doi:10.3390/cells13090763 PubMed PMID: 38727299.
12. Ibrahim MM. Subcutaneous and visceral adipose tissue: Structural and functional differences. Obesity Reviews. Blackwell Publishing Ltd; 2010. p. 11–8. doi:10.1111/j.1467-789X.2009.00623.x PubMed PMID: 19656312.
13. Lé B, Wajchenberg O. Subcutaneous and Visceral Adipose Tissue: Their Relation to the Metabolic Syndrome [Internet]. 2000. Available from: https://academic.oup.com/edrv/article/21/6/697/2424212 doi:10.1210/edrv.21.6.0415
14. Item F, Konrad D. Visceral fat and metabolic inflammation: The portal theory revisited. Obesity Reviews. 2012 Dec;13(SUPPL.2):30–9. doi:10.1111/j.1467-789X.2012.01035.x PubMed PMID: 23107257.
15. Zwick RK, Guerrero-Juarez CF, Horsley V, Plikus M V. Anatomical, Physiological, and Functional Diversity of Adipose Tissue. Cell Metabolism. Cell Press; 2018. p. 68–83. doi:10.1016/j.cmet.2017.12.002 PubMed PMID: 29320711.
16. Frasca D, Blomberg BB. Adipose tissue, immune aging, and cellular senescence. Seminars in Immunopathology. Springer Science and Business Media Deutschland GmbH; 2020. p. 573–87. doi:10.1007/s00281-020-00812-1 PubMed PMID: 32785750.
17. Darcy J, Tseng YH. ComBATing aging—does increased brown adipose tissue activity confer longevity? GeroScience. Springer International Publishing; 2019. p. 285–96. doi:10.1007/s11357-019-00076-0 PubMed PMID: 31230192.
18. Mattson MP. Perspective: Does brown fat protect against diseases of aging? Ageing Research Reviews. 2010. p. 69–76. doi:10.1016/j.arr.2009.11.004 PubMed PMID: 19969105.
19. Yoneshiro T, Aita S, Matsushita M, Okamatsu-Ogura Y, Kameya T, Kawai Y, et al. Age-related decrease in cold-activated brown adipose tissue and

accumulation of body fat in healthy humans. Obesity. 2011 Sep;19(9):1755–60. doi:10.1038/oby.2011.125 PubMed PMID: 21566561.

20. Dong M, Lin J, Lim W, Jin W, Lee HJ. Role of brown adipose tissue in metabolic syndrome, aging, and cancer cachexia. Frontiers of Medicine. Higher Education Press; 2018. p. 130–8. doi:10.1007/s11684-017-0555-2 PubMed PMID: 29119382.
21. Li H, Li J, Song C, Yang H, Luo Q, Chen M. Brown adipose tissue: a potential target for aging interventions and healthy longevity. Biogerontology. Springer Science and Business Media B.V.; 2024. p. 1011–24. doi:10.1007/s10522-024-10137-3 PubMed PMID: 39377866.
22. Zhang F, Hao G, Shao M, Nham K, An Y, Wang Q, et al. An Adipose Tissue Atlas: An Image-Guided Identification of Human-like BAT and Beige Depots in Rodents. Cell Metab. 2018 Jan 9;27(1):252-262.e3. doi:10.1016/j.cmet.2017.12.004 PubMed PMID: 29320705.
23. Cohen P, Kajimura S. The cellular and functional complexity of thermogenic fat. Nature Reviews Molecular Cell Biology. Nature Research; 2021. p. 393–409. doi:10.1038/s41580-021-00350-0 PubMed PMID: 33758402.
24. Nirengi S, Stanford K. Brown adipose tissue and aging: A potential role for exercise. Experimental Gerontology. Elsevier Inc.; 2023. doi:10.1016/j.exger.2023.112218 PubMed PMID: 37224933.
25. Wang W, Seale P. Control of brown and beige fat development. Nature Reviews Molecular Cell Biology. Nature Publishing Group; 2016. p. 691–702. doi:10.1038/nrm.2016.96 PubMed PMID: 27552974.
26. Liu X, Zheng Z, Zhu X, Meng M, Li L, Shen Y, et al. Brown adipose tissue transplantation improves whole-body energy metabolism. Cell Research. 2013. p. 851–4. doi:10.1038/cr.2013.64 PubMed PMID: 23649313.
27. Zhu Z, Spicer EG, Gavini CK, Goudjo-Ako AJ, Novak CM, Shi H. Enhanced sympathetic activity in mice with brown adipose tissue transplantation (transBATation). Physiol Behav. 2014 Feb 10;125:21–9. doi:10.1016/j.physbeh.2013.11.008 PubMed PMID: 24291381.
28. Xiaomeng Liu SWYYMMZZMDJLQZCZXYTHLLYHLZDWJZHJLJRSWJ. Brown Adipose Tissue Transplantation Reverses Obesity in Ob/Ob Mice. Endocrinology . 2015 Jul 1;156(7):2461–9.

29. Chait A, den Hartigh LJ. Adipose Tissue Distribution, Inflammation and Its Metabolic Consequences, Including Diabetes and Cardiovascular Disease. Frontiers in Cardiovascular Medicine. Frontiers Media S.A.; 2020. doi:10.3389/fcvm.2020.00022 PubMed PMID: 32158768.
30. Koenen M, Hill MA, Cohen P, Sowers JR. Obesity, Adipose Tissue and Vascular Dysfunction. Circulation Research. Lippincott Williams and Wilkins; 2021. p. 951–68. doi:10.1161/CIRCRESAHA.121.318093 PubMed PMID: 33793327.
31. Gesta S, Tseng YH, Kahn CR. Developmental Origin of Fat: Tracking Obesity to Its Source. Cell. Elsevier B.V.; 2007. p. 242–56. doi:10.1016/j.cell.2007.10.004 PubMed PMID: 17956727.
32. Choudhery MS, Niaz A, Arif T, Mahmood R. Adipose tissue as a living drug: Stromal vascular fraction and adipose tissue-derived stem cells in regenerative medicine. World J Stem Cells. 2025 Dec 26;17(12). doi:10.4252/wjsc.v17.i12.114170
33. Liao X, Zhou H, Deng T. The composition, function, and regulation of adipose stem and progenitor cells. Journal of Genetics and Genomics. Institute of Genetics and Developmental Biology; 2022. p. 308–15. doi:10.1016/j.jgg.2022.02.014 PubMed PMID: 35240306.
34. Smith U, Li Q, Rydén M, Spalding KL. Cellular senescence and its role in white adipose tissue. International Journal of Obesity. Springer Nature; 2021. p. 934–43. doi:10.1038/s41366-021-00757-x PubMed PMID: 33510393.
35. Sun K, Tordjman J, Clément K, Scherer PE. Fibrosis and adipose tissue dysfunction. Cell Metabolism. Cell Press; 2013. p. 470–7. doi:10.1016/j.cmet.2013.06.016 PubMed PMID: 23954640.
36. Gregoire FM, Smas CM, Sul S. Understanding Adipocyte Differentiation. PHYSIOLOGICAL REVIEWS. 1998.
37. Hafidi M El, Buelna-Chontal M, Sánchez-Muñoz F, Carbó R. Adipogenesis: A necessary but harmful strategy. International Journal of Molecular Sciences. MDPI AG; 2019. doi:10.3390/ijms20153657 PubMed PMID: 31357412.
38. Corvera S. Cellular Heterogeneity in Adipose Tissues. Annual Review of Physiology. Annual Reviews Inc.; 2021. p. 257–78. doi:10.1146/annurev-physiol-031620-095446 PubMed PMID: 33566675.

39. Lu J, Zhao J, Meng H, Zhang X. Adipose tissue-resident immune cells in obesity and type 2 diabetes. Frontiers in Immunology. Frontiers Media S.A.; 2019. doi:10.3389/fimmu.2019.01173 PubMed PMID: 31191541.
40. Michailidou Z, Gomez-Salazar M, Alexaki VI. Innate Immune Cells in the Adipose Tissue in Health and Metabolic Disease. Journal of Innate Immunity. S. Karger AG; 2022. p. 4–30. doi:10.1159/000515117 PubMed PMID: 33849008.
41. Kado T, Nishimura A, Tobe K. History and future perspectives of adipose tissue macrophage biology. Frontiers in Pharmacology. Frontiers Media SA; 2024. doi:10.3389/fphar.2024.1373182
42. Ni Y, Ni L, Zhuge F, Xu L, Fu Z, Ota T. Adipose Tissue Macrophage Phenotypes and Characteristics: The Key to Insulin Resistance in Obesity and Metabolic Disorders. Obesity. Blackwell Publishing Inc.; 2020. p. 225–34. doi:10.1002/oby.22674 PubMed PMID: 31903735.
43. Schoettl T, Fischer IP, Ussar S. Heterogeneity of adipose tissue in development and metabolic function. Journal of Experimental Biology. Company of Biologists Ltd; 2018. doi:10.1242/jeb.162958 PubMed PMID: 29514879.
44. Wang X, Xu M, Li Y. Adipose Tissue Aging and Metabolic Disorder, and the Impact of Nutritional Interventions. Nutrients. MDPI; 2022. doi:10.3390/nu14153134 PubMed PMID: 35956309.
45. Bartelt A, Heeren J. Adipose tissue browning and metabolic health. Nature Reviews Endocrinology. Nature Publishing Group; 2014. p. 24–36. doi:10.1038/nrendo.2013.204 PubMed PMID: 24146030.
46. Rodrigues AR, Salazar MJ, Gouveia AM. Obesity and Adipose Tissue Remodeling. Recent Advances in Obesity Research. 2020. doi:10.2174/9789811442636120010006
47. Sanchez-Gurmaches J, Hung CM, Guertin DA. Emerging Complexities in Adipocyte Origins and Identity. Trends Cell Biol. 2016 May;26(5):313–26. doi:10.1016/j.tcb.2016.01.004
48. Zoico E, Rubele S, De Caro A, Nori N, Mazzali G, Fantin F, et al. Brown and beige adipose tissue and aging. Front Endocrinol (Lausanne). 2019;10(JUN). doi:10.3389/fendo.2019.00368
49. Luo L, Liu M. Adipose tissue in control of metabolism. Journal of Endocrinology. BioScientifica Ltd.; 2016. p. R77–99. doi:10.1530/JOE-16-0211 PubMed PMID: 27935822.

50. Coelho M, Oliveira T, Fernandes R. Biochemistry of adipose tissue: An endocrine organ. Archives of Medical Science. 2013. p. 191–200. doi:10.5114/aoms.2013.33181 PubMed PMID: 23671428.
51. Ouchi N, Parker JL, Lugus JJ, Walsh K. Adipokines in inflammation and metabolic disease. Nature Reviews Immunology. 2011. p. 85–97. doi:10.1038/nri2921 PubMed PMID: 21252989.
52. Conde J, Scotece M, Gómez R, López V, Gómez-Reino JJ, Lago F, et al. Adipokines: Biofactors from white adipose tissue. A complex hub among inflammation, metabolism, and immunity. BioFactors. 2011 Nov 28;37(6):413–20. doi:10.1002/biof.185
53. Obradovic M, Sudar-Milovanovic E, Soskic S, Essack M, Arya S, Stewart AJ, et al. Leptin and Obesity: Role and Clinical Implication. Frontiers in Endocrinology. Frontiers Media S.A.; 2021. doi:10.3389/fendo.2021.585887
54. Picó C, Palou M, Pomar CA, Rodríguez AM, Palou A. Leptin as a key regulator of the adipose organ. Reviews in Endocrine and Metabolic Disorders. Springer; 2022. p. 13–30. doi:10.1007/s11154-021-09687-5 PubMed PMID: 34523036.
55. Funcke JB, Scherer PE. Beyond adiponectin and leptin: Adipose tissue-derived mediators of inter-organ communication. Journal of Lipid Research. American Society for Biochemistry and Molecular Biology Inc.; 2019. p. 1648–97. doi:10.1194/jlr.R094060 PubMed PMID: 31209153.
56. Gavaldà-Navarro A, Villarroya J, Cereijo R, Giralt M, Villarroya F. The endocrine role of brown adipose tissue: An update on actors and actions. Reviews in Endocrine and Metabolic Disorders. Springer; 2022. p. 31–41. doi:10.1007/s11154-021-09640-6 PubMed PMID: 33712997.
57. Cao H, Gerhold K, Mayers JR, Wiest MM, Watkins SM, Hotamisligil GS. Identification of a Lipokine, a Lipid Hormone Linking Adipose Tissue to Systemic Metabolism. Cell. 2008 Sep 19;134(6):933–44. doi:10.1016/j.cell.2008.07.048 PubMed PMID: 18805087.
58. Wang QA, Tao C, Gupta RK, Scherer PE. Tracking adipogenesis during white adipose tissue development, expansion and regeneration. Nat Med. 2013 Oct;19(10):1338–44. doi:10.1038/nm.3324 PubMed PMID: 23995282.
59. Shamsi F, Wang CH, Tseng YH. The evolving view of thermogenic adipocytes — ontogeny, niche and function. Nat Rev Endocrinol. 2021 Dec 8;17(12):726–44. doi:10.1038/s41574-021-00562-6

60. Carrageta DF, Oliveira PF, Monteiro MP, Alves MG. Adipocyte Specific Signaling. In: Tissue-Specific Cell Signaling. Springer International Publishing; 2020. p. 409–36. doi:10.1007/978-3-030-44436-5_15
61. Sarjeant K, Stephens JM. Adipogenesis. Cold Spring Harb Perspect Biol. 2012 Sep;4(9). doi:10.1101/cshperspect.a008417 PubMed PMID: 22952395.
62. Cowherd RM, Lyle RE, Mcgehee REU. Molecular regulation of adipocyte differentiation. CELL & DEV ELOPMENTAL BI OLOGY. 1999. doi:10.1006/scdb.1998.0276
63. Frühbeck G, Méndez-Giménez L, Fernández-Formoso JA, Fernández S, Rodríguez A. Regulation of adipocyte lipolysis. Nutr Res Rev. 2014;27(1):63–93. doi:10.1017/S095442241400002X PubMed PMID: 24872083.
64. Kersten S. Physiological regulation of lipoprotein lipase. Biochimica et Biophysica Acta - Molecular and Cell Biology of Lipids. Elsevier; 2014. p. 919–33. doi:10.1016/j.bbalip.2014.03.013 PubMed PMID: 24721265.
65. Yang A, Mottillo EP. Adipocyte lipolysis: From molecular mechanisms of regulation to disease and therapeutics. Biochemical Journal. Portland Press Ltd; 2020. p. 985–1008. doi:10.1042/BCJ20190468 PubMed PMID: 32168372.
66. Cho CH, Patel S, Rajbhandari P. Adipose tissue lipid metabolism: lipolysis. Current Opinion in Genetics and Development. Elsevier Ltd; 2023. doi:10.1016/j.gde.2023.102114 PubMed PMID: 37738733.
67. Zhang S, Williams KJ, Verlande-Ferrero A, Chan AP, Su GB, Kershaw EE, et al. Acute activation of adipocyte lipolysis reveals dynamic lipid remodeling of the hepatic lipidome. J Lipid Res. 2024 Feb 1;65(2). doi:10.1016/j.jlr.2023.100434 PubMed PMID: 37640283.
68. Lafontan M, Langin D. Lipolysis and lipid mobilization in human adipose tissue. Progress in Lipid Research. 2009. p. 275–97. doi:10.1016/j.plipres.2009.05.001 PubMed PMID: 19464318.
69. Tansey JT, Sztalryd C, Hlavin EM, Kimmel AR, Londos C. The central role of perilipin A in lipid metabolism and adipocyte lipolysis. IUBMB Life. 2004. p. 379–85. doi:10.1080/15216540400009968 PubMed PMID: 15545214.
70. Moro C. Natriuretic peptides and fat metabolism. Current Opinion in Clinical Nutrition and Metabolic Care. 2013. p. 645–9. doi:10.1097/MCO.0b013e32836510ed PubMed PMID: 23945222.

71. Rodrigues AR, Almeida H, Gouveia AM. α-MSH signalling via melanocortin 5 receptor promotes lipolysis and impairs re-esterification in adipocytes. Biochim Biophys Acta Mol Cell Biol Lipids. 2013 Jul;1831(7):1267–75. doi:10.1016/j.bbalip.2013.04.008 PubMed PMID: 24046867.

72. Schweiger M, Schreiber R, Haemmerle G, Lass A, Fledelius C, Jacobsen P, et al. Adipose triglyceride lipase and hormone-sensitive lipase are the major enzymes in adipose tissue triacylglycerol catabolism. Journal of Biological Chemistry. 2006 Dec 29;281(52):40236–41. doi:10.1074/jbc.M608048200 PubMed PMID: 17074755.

73. Kaur S, Auger C, Jeschke MG. Adipose Tissue Metabolic Function and Dysfunction: Impact of Burn Injury. Frontiers in Cell and Developmental Biology. Frontiers Media S.A.; 2020. doi:10.3389/fcell.2020.599576

74. Thyagarajan B, Foster MT. Beiging of white adipose tissue as a therapeutic strategy for weight loss in humans. Hormone Molecular Biology and Clinical Investigation. Walter de Gruyter GmbH; 2017. doi:10.1515/hmbci-2017-0016 PubMed PMID: 28672737.

75. Carpentier AC, Blondin DP, Virtanen KA, Richard D, Haman F, Turcotte ÉE. Brown Adipose Tissue Energy Metabolism in Humans. Front Endocrinol (Lausanne). 2018 Aug 7;9. doi:10.3389/fendo.2018.00447

76. Townsend KL, Tseng YH. Recent insights into development, metabolic function and therapeutic potential [Internet]. 2012. doi:10.4161/adip.1.1.18951

77. Saito M, Okamatsu-Ogura Y, Matsushita M, Watanabe K, Yoneshiro T, Nio-Kobayashi J, et al. High incidence of metabolically active brown adipose tissue in healthy adult humans: Effects of cold exposure and adiposity. Diabetes. 2009 Jul;58(7):1526–31. doi:10.2337/db09-0530 PubMed PMID: 19401428.

78. Barbatelli G, Murano I, Madsen L, Hao Q, Jimenez M, Kristiansen K, et al. The emergence of cold-induced brown adipocytes in mouse white fat depots is determined predominantly by white to brown adipocyte transdifferentiation. Am J Physiol Endocrinol Metab. 2010 Jun;298(6). doi:10.1152/ajpendo.00600.2009 PubMed PMID: 20354155.

79. Yasuda T, Masaki T, Kakuma T, Yoshimatsu H. Hypothalamic Melanocortin System Regulates Sympathetic Nerve Activity in Brown Adipose Tissue. Exp Biol Med. 2004 Mar 29;229(3):235–9. doi:10.1177/153537020422900303

80. Ellacott KLJ, Cone RD. The role of the central melanocortin system in the regulation of food intake and energy homeostasis: Lessons from mouse models. Philosophical Transactions of the Royal Society B: Biological Sciences. 2006;361(1471):1265–74. doi:10.1098/rstb.2006.1861 PubMed PMID: 16815803.

81. Rodrigues AR, Salazar MJ, Rocha-Rodrigues S, Gonçalves IO, Cruz C, Neves D, et al. Peripherally administered melanocortins induce mice fat browning and prevent obesity. Int J Obes. 2019 May 1;43(5):1058–69. doi:10.1038/s41366-018-0155-5 PubMed PMID: 30018312.

82. Salazar MJ, Rodrigues AR, Sousa M, Magalhães J, Neves D, Almeida H, et al. Characterization of α-msh browning effect in diverse mice white adipose tissue depots. J Mol Endocrinol. 2021;66(1):23–34. doi:10.1530/JME-20-0002 PubMed PMID: 33151902.

83. Ou MY, Zhang H, Tan PC, Zhou SB, Li QF. Adipose tissue aging: mechanisms and therapeutic implications. Cell Death and Disease. Springer Nature; 2022. doi:10.1038/s41419-022-04752-6 PubMed PMID: 35379822.

84. Al-Regaiey K. Crosstalk between adipogenesis and aging: role of polyphenols in combating adipogenic-associated aging. Immunity and Ageing . BioMed Central Ltd; 2024. doi:10.1186/s12979-024-00481-w

85. Saccon TD, Nagpal R, Yadav H, Cavalcante MB, Nunes ADDC, Schneider A, et al. Senolytic Combination of Dasatinib and Quercetin Alleviates Intestinal Senescence and Inflammation and Modulates the Gut Microbiome in Aged Mice. Journals of Gerontology - Series A Biological Sciences and Medical Sciences. 2021 Nov 1;76(11):1895–905. doi:10.1093/gerona/glab002 PubMed PMID: 33406219.

86. Whytock KL, Divoux A, Sun Y, Pino MF, Yu G, Jin CA, et al. Aging human abdominal subcutaneous white adipose tissue at single cell resolution. Aging Cell. 2024 Nov 1;23(11). doi:10.1111/acel.14287 PubMed PMID: 39141531.

87. Camell CD. Adipose tissue microenvironments during aging: Effects on stimulated lipolysis. Biochim Biophys Acta Mol Cell Biol Lipids. 2022 May 1;1867(5). doi:10.1016/j.bbalip.2022.159118 PubMed PMID: 35131468.

88. Narasimhan A, Flores RR, Camell CD, Bernlohr DA, Robbins PD, Niedernhofer LJ. Cellular Senescence in Obesity and Associated Complications: a New

Therapeutic Target. Current Diabetes Reports. Springer; 2022. p. 537–48. doi:10.1007/s11892-022-01493-w PubMed PMID: 36239841.

89. Hammarstedt A, Gogg S, Hedjazifar S, Nerstedt A, Smith U. Impaired Adipogenesis and Dysfunctional Adipose Tissue in Human Hypertrophic Obesity. Physiol Rev. 1911;98. doi:10.1152/physrev
90. Liu F, He J, Wang H, Zhu D, Bi Y. Adipose Morphology: a Critical Factor in Regulation of Human Metabolic Diseases and Adipose Tissue Dysfunction [Internet]. doi:10.1007/s11695-020-04983-6/Published
91. Debari MK, Abbott RD. Adipose tissue fibrosis: Mechanisms, models, and importance. International Journal of Molecular Sciences. MDPI AG; 2020. p. 1–24. doi:10.3390/ijms21176030 PubMed PMID: 32825788.
92. Virtue S, Vidal-Puig A. Adipose tissue expandability, lipotoxicity and the Metabolic Syndrome — An allostatic perspective. Biochimica et Biophysica Acta (BBA) - Molecular and Cell Biology of Lipids. 2010 Mar;1801(3):338–49. doi:10.1016/j.bbalip.2009.12.006
93. Langin D, Dicker A, Tavernier G, Hoffstedt J, Mairal A, Rydén M, et al. Adipocyte Lipases and Defect of Lipolysis in Human Obesity. Diabetes. 2005 Nov 1;54(11):3190–7. doi:10.2337/diabetes.54.11.3190
94. Chen B, Li T, Wu Y, Song L, Wang Y, Bian Y, et al. Lipotoxicity: A New Perspective in Type 2 Diabetes Mellitus. Diabetes, Metabolic Syndrome and Obesity . Dove Medical Press Ltd; 2025. p. 1223–37. doi:10.2147/DMSO.S511436
95. Cavaliere G, Cimmino F, Trinchese G, Catapano A, Petrella L, D'Angelo M, et al. From Obesity-Induced Low-Grade Inflammation to Lipotoxicity and Mitochondrial Dysfunction: Altered Multi-Crosstalk between Adipose Tissue and Metabolically Active Organs. Antioxidants. MDPI; 2023. doi:10.3390/antiox12061172
96. Ajoolabady A, Pratico D, Tang D, Zhou S, Franceschi C, Ren J. Immunosenescence and inflammaging: Mechanisms and role in diseases. Ageing Res Rev. 2024 Nov;101:102540. doi:10.1016/j.arr.2024.102540
97. Cinti S, Mitchell G, Barbatelli G, Murano I, Ceresi E, Faloia E, et al. Adipocyte death defines macrophage localization and function in adipose tissue of obese mice and humans. J Lipid Res. 2005 Nov;46(11):2347–55. doi:10.1194/jlr.M500294-JLR200 PubMed PMID: 16150820.

98. Liguori I, Russo G, Curcio F, Bulli G, Aran L, Della-Morte D, et al. Oxidative stress, aging, and diseases. Clin Interv Aging. 2018 Apr;Volume 13:757–72. doi:10.2147/CIA.S158513

99. Sun N, Youle RJ, Finkel T. The Mitochondrial Basis of Aging. Mol Cell. 2016 Mar;61(5):654–66. doi:10.1016/j.molcel.2016.01.028

100. Morgan MJ, Liu Z gang. Crosstalk of reactive oxygen species and NF-κB signaling. Cell Res. 2011 Jan 28;21(1):103–15. doi:10.1038/cr.2010.178

101. Fuente M, Miquel J. An Update of the Oxidation-Inflammation Theory of Aging: The Involvement of the Immune System in Oxi-Inflamm-Aging. Curr Pharm Des. 2009 Sep 1;15(26):3003–26. doi:10.2174/138161209789058110

102. Xia S, Zhang X, Zheng S, Khanabdali R, Kalionis B, Wu J, et al. An Update on Inflamm-Aging: Mechanisms, Prevention, and Treatment. J Immunol Res. 2016;2016:1–12. doi:10.1155/2016/8426874

103. Goossens GH. The Metabolic Phenotype in Obesity: Fat Mass, Body Fat Distribution, and Adipose Tissue Function. Obes Facts. 2017 Jul 1;10(3):207–15. doi:10.1159/000471488 PubMed PMID: 28564650.

104. World Health Organization. World Health Organization. 2025. Obesity and overweight.

105. Giroud M, Jodeleit H, Prentice KJ, Bartelt A, Forsythe I, Chan J. The Journal of Physiology Adipocyte function and the development of cardiometabolic disease. J Physiol. 2022;600:1189–208. doi:10.1113/JP281979#support-information-section

106. De Fano M, Bartolini D, Tortoioli C, Vermigli C, Malara M, Galli F, et al. Adipose Tissue Plasticity in Response to Pathophysiological Cues: A Connecting Link between Obesity and Its Associated Comorbidities. Int J Mol Sci. 2022 May 14;23(10):5511. doi:10.3390/ijms23105511

107. Lecoutre S, Rebière C, Maqdasy S, Lambert M, Dussaud S, Abatan JB, et al. Enhancing adipose tissue plasticity: progenitor cell roles in metabolic health. Nat Rev Endocrinol. 2025 May 6;21(5):272–88. doi:10.1038/s41574-024-01071-y

108. Longo M, Zatterale F, Naderi J, Parrillo L, Formisano P, Raciti GA, et al. Adipose Tissue Dysfunction as Determinant of Obesity-Associated Metabolic Complications. Int J Mol Sci. 2019 May 13;20(9):2358. doi:10.3390/ijms20092358

109. Russo L, Lumeng CN. Properties and functions of adipose tissue macrophages in obesity. Immunology. 2018 Dec 19;155(4):407–17. doi:10.1111/imm.13002
110. Schleh MW, Caslin HL, Garcia JN, Mashayekhi M, Srivastava G, Bradley AB, et al. Metaflammation in obesity and its therapeutic targeting. Sci Transl Med. 2023 Nov 22;15(723). doi:10.1126/scitranslmed.adf9382
111. Crewe C, An YA, Scherer PE. The ominous triad of adipose tissue dysfunction: inflammation, fibrosis, and impaired angiogenesis. Journal of Clinical Investigation. 2017 Jan 3;127(1):74–82. doi:10.1172/JCI88883
112. Carobbio S, Pellegrinelli V, Vidal-Puig A. Adipose Tissue Function and Expandability as Determinants of Lipotoxicity and the Metabolic Syndrome. In. 2017. p. 161–96. doi:10.1007/978-3-319-48382-5_7
113. Palmer AK, Kirkland JL. Aging and adipose tissue: potential interventions for diabetes and regenerative medicine. Exp Gerontol. 2016 Dec;86:97–105. doi:10.1016/j.exger.2016.02.013
114. de Toro-Martín J, Guénard F, Tchernof A, Hould FS, Lebel S, Julien F, et al. Body mass index is associated with epigenetic age acceleration in the visceral adipose tissue of subjects with severe obesity. Clin Epigenetics. 2019 Dec 2;11(1):172. doi:10.1186/s13148-019-0754-6
115. Mundstock E, Sarria EE, Zatti H, Mattos Louzada F, Kich Grun L, Herbert Jones M, et al. Effect of obesity on telomere length: Systematic review and meta-analysis. Obesity. 2015 Nov;23(11):2165–74. doi:10.1002/oby.21183
116. López-Otín C, Blasco MA, Partridge L, Serrano M, Kroemer G. The Hallmarks of Aging. Cell. 2013 Jun;153(6):1194–217. doi:10.1016/j.cell.2013.05.039
117. Gielen M, Hageman GJ, Antoniou EE, Nordfjall K, Mangino M, Balasubramanyam M, et al. Body mass index is negatively associated with telomere length: a collaborative cross-sectional meta-analysis of 87 observational studies. Am J Clin Nutr. 2018 Sep;108(3):453–75. doi:10.1093/ajcn/nqy107
118. Trim W, Turner JE, Thompson D. Parallels in immunometabolic adipose tissue dysfunction with ageing and obesity. Frontiers in Immunology. Frontiers Media S.A.; 2018. doi:10.3389/fimmu.2018.00169
119. Tchkonia T, Morbeck DE, Von Zglinicki T, Van Deursen J, Lustgarten J, Scrable H, et al. Fat tissue, aging, and cellular senescence. Aging Cell. 2010. p. 667–84. doi:10.1111/j.1474-9726.2010.00608.x PubMed PMID: 20701600.

120. Kivimäki M, Strandberg T, Pentti J, Nyberg ST, Frank P, Jokela M, et al. Body-mass index and risk of obesity-related complex multimorbidity: an observational multicohort study. Lancet Diabetes Endocrinol. 2022 Apr;10(4):253–63. doi:10.1016/S2213-8587(22)00033-X
121. Busetto L, Dicker D, Frühbeck G, Halford JCG, Sbraccia P, Yumuk V, et al. A new framework for the diagnosis, staging and management of obesity in adults. Nat Med. 2024 Sep 5;30(9):2395–9. doi:10.1038/s41591-024-03095-3
122. Yannakoulia M, Poulimeneas D, Mamalaki E, Anastasiou CA. Dietary modifications for weight loss and weight loss maintenance. Metabolism. 2019 Mar;92:153–62. doi:10.1016/j.metabol.2019.01.001
123. Engin B, Willis SA, Malaikah S, Sargeant JA, Yates T, Gray LJ, et al. The effect of exercise training on adipose tissue insulin sensitivity: A systematic review and meta-analysis. Obesity Reviews. 2022 Jul 23;23(7). doi:10.1111/obr.13445
124. McGowan B, Ciudin A, Baker JL, Busetto L, Dicker D, Frühbeck G, et al. Framework for the pharmacological treatment of obesity and its complications from the European Association for the Study of Obesity (EASO). Nat Med. 2025 Oct 2;31(10):3229–32. doi:10.1038/s41591-025-03765-w
125. Astrup A. Reflections on the discovery GLP-1 as a satiety hormone: Implications for obesity therapy and future directions. Eur J Clin Nutr. 2024 Jul 18;78(7):551–6. doi:10.1038/s41430-024-01460-6
126. Holst JJ. GLP-1 physiology in obesity and development of incretin-based drugs for chronic weight management. Nat Metab. 2024 Aug 19;6(10):1866–85. doi:10.1038/s42255-024-01113-9
127. Ansari S, Khoo B, Tan T. Targeting the incretin system in obesity and type 2 diabetes mellitus. Nat Rev Endocrinol. 2024 Aug 17;20(8):447–59. doi:10.1038/s41574-024-00979-9
128. European Medicines Agency. Ozempic: EPAR – Product Information. Amsterdam; 2026.
129. European Medicines Agency. Wegovy: EPAR – Product Information. Amsterdam; 2026.
130. European Medicines Agency. Mounjaro: EPAR – Product Information. Amsterdam; 2026.
131. Wilding JPH, Batterham RL, Calanna S, Davies M, Van Gaal LF, Lingvay I, et al. Once-Weekly Semaglutide in Adults with Overweight or Obesity. New

England Journal of Medicine. 2021 Mar 18;384(11):989–1002. doi:10.1056/NEJMoa2032183

132. Eisenberg D, Shikora SA, Aarts E, Aminian A, Angrisani L, Cohen R V., et al. 2022 American Society for Metabolic and Bariatric Surgery (ASMBS) and International Federation for the Surgery of Obesity and Metabolic Disorders (IFSO): Indications for Metabolic and Bariatric Surgery. Surgery for Obesity and Related Diseases. 2022 Dec;18(12):1345–56. doi:10.1016/j.soard.2022.08.013
133. Syn NL, Cummings DE, Wang LZ, Lin DJ, Zhao JJ, Loh M, et al. Association of metabolic–bariatric surgery with long-term survival in adults with and without diabetes: a one-stage meta-analysis of matched cohort and prospective controlled studies with 174 772 participants. The Lancet. 2021 May;397(10287):1830–41. doi:10.1016/S0140-6736(21)00591-2
134. Kim K, Sandoval DA. Endocrine Function after Bariatric Surgery. In: Comprehensive Physiology. Wiley; 2017. p. 783–98. doi:10.1002/cphy.c160019
135. Svane MS, Bojsen-Møller KN, Madsbad S, Holst JJ. Updates in weight loss surgery and gastrointestinal peptides. Current Opinion in Endocrinology & Diabetes and Obesity. 2015 Feb;22(1):21–8. doi:10.1097/MED.0000000000000131
136. Hindsø M, Svane MS, Hedbäck N, Holst JJ, Madsbad S, Bojsen-Møller KN. The role of GLP-1 in postprandial glucose metabolism after bariatric surgery: a narrative review of human GLP-1 receptor antagonist studies. Surgery for Obesity and Related Diseases. 2021 Jul;17(7):1383–91. doi:10.1016/j.soard.2021.01.041
137. Miranda AMA, McAllan L, Mazzei G, Andrew I, Davies I, Ertugrul M, et al. Selective remodelling of the adipose niche in obesity and weight loss. Nature. 2025 Aug 21;644(8077):769–79. doi:10.1038/s41586-025-09233-2
138. Wilding JPH, Batterham RL, Davies M, Van Gaal LF, Kandler K, Konakli K, et al. Weight regain and cardiometabolic effects after withdrawal of semaglutide: The STEP 1 trial extension. Diabetes Obes Metab. 2022 Aug 19;24(8):1553–64. doi:10.1111/dom.14725
139. Moriconi D, Manca ML, Anselmino M, Rebelos E, Bellini R, Taddei S, et al. Predictors of type 2 diabetes relapse after Roux-en-Y Gastric Bypass: A ten-year follow-up study. Diabetes Metab. 2022 Jan;48(1):101282. doi:10.1016/j.diabet.2021.101282

140. Conte C, Lapeyre-Mestre M, Hanaire H, Ritz P. Diabetes Remission and Relapse After Bariatric Surgery: a Nationwide Population-Based Study. Obes Surg. 2020 Dec 31;30(12):4810–20. doi:10.1007/s11695-020-04924-3
141. Hinte LC, Castellano-Castillo D, Ghosh A, Melrose K, Gasser E, Noé F, et al. Adipose tissue retains an epigenetic memory of obesity after weight loss. Nature. 2024 Dec 12;636(8042):457–65. doi:10.1038/s41586-024-08165-7
142. Gorgoulis V, Adams PD, Alimonti A, Bennett DC, Bischof O, Bishop C, et al. Cellular Senescence: Defining a Path Forward. Cell. 2019 Oct;179(4):813–27. doi:10.1016/j.cell.2019.10.005
143. Coppé JP, Desprez PY, Krtolica A, Campisi J. The Senescence-Associated Secretory Phenotype: The Dark Side of Tumor Suppression. Annual Review of Pathology: Mechanisms of Disease. 2010 Jan 1;5(1):99–118. doi:10.1146/annurev-pathol-121808-102144
144. Tchkonia T, Zhu Y, van Deursen J, Campisi J, Kirkland JL. Cellular senescence and the senescent secretory phenotype: therapeutic opportunities. Journal of Clinical Investigation. 2013 Mar 1;123(3):966–72. doi:10.1172/JCI64098
145. Tripathi U, Misra A, Tchkonia T, Kirkland JL. Impact of Senescent Cell Subtypes on Tissue Dysfunction and Repair: Importance and Research Questions. Mech Ageing Dev. 2021 Sep;198:111548. doi:10.1016/j.mad.2021.111548
146. Han X, Lei Q, Xie J, Liu H, Li J, Zhang X, et al. Potential Regulators of the Senescence-Associated Secretory Phenotype During Senescence and Aging. The Journals of Gerontology: Series A. 2022 Nov 21;77(11):2207–18. doi:10.1093/gerona/glac097
147. Kumari R, Jat P. Mechanisms of Cellular Senescence: Cell Cycle Arrest and Senescence Associated Secretory Phenotype. Frontiers in Cell and Developmental Biology. Frontiers Media S.A.; 2021. doi:10.3389/fcell.2021.645593
148. Roger L, Tomas F, Gire V. Mechanisms and regulation of cellular senescence. International Journal of Molecular Sciences. MDPI; 2021. doi:10.3390/ijms222313173 PubMed PMID: 34884978.
149. Herranz N, Gil J. Mechanisms and functions of cellular senescence. Journal of Clinical Investigation. American Society for Clinical Investigation; 2018. p. 1238–46. doi:10.1172/JCI95148 PubMed PMID: 29608137.

150. Loo TM, Miyata K, Tanaka Y, Takahashi A. Cellular senescence and senescence-associated secretory phenotype via the cGAS-STING signaling pathway in cancer. Cancer Science. Blackwell Publishing Ltd; 2020. p. 304–11. doi:10.1111/cas.14266 PubMed PMID: 31799772.
151. Kang C, Xu Q, Martin TD, Li MZ, Demaria M, Aron L, et al. The DNA damage response induces inflammation and senescence by inhibiting autophagy of GATA4. Science (1979). 2015 Sep 25;349(6255). doi:10.1126/science.aaa5612 PubMed PMID: 26404817.
152. Saito Y, Yamamoto S, Chikenji TS. Role of cellular senescence in inflammation and regeneration. Inflammation and Regeneration. BioMed Central Ltd; 2024. doi:10.1186/s41232-024-00342-5 PubMed PMID: 38831382.
153. Huang W, Hickson LTJ, Eirin A, Kirkland JL, Lerman LO. Cellular senescence: the good, the bad and the unknown. Nature Reviews Nephrology. Nature Research; 2022. p. 611–27. doi:10.1038/s41581-022-00601-z PubMed PMID: 35922662.
154. Hernandez-Segura A, Nehme J, Demaria M. Hallmarks of Cellular Senescence. Trends in Cell Biology. Elsevier Ltd; 2018. p. 436–53. doi:10.1016/j.tcb.2018.02.001 PubMed PMID: 29477613.
155. Ernst P, Heidel FH. Molecular mechanisms of senescence and implications for the treatment of myeloid malignancies. Cancers. MDPI AG; 2021. p. 1–18. doi:10.3390/cancers13040612
156. Zhang Y, Jiang Y, Yang X, Huang Y, Pan A, Liao Y. Adipose tissue senescence: Biological changes, hallmarks and therapeutic approaches. Mech Ageing Dev. 2024 Dec;222:111988. doi:10.1016/j.mad.2024.111988
157. Ajoolabady A, Pratico D, Bahijri S, Tuomilehto J, Uversky VN, Ren J. Hallmarks of cellular senescence: biology, mechanisms, regulations. Exp Mol Med. 2025 Jul 10;57(7):1482–91. doi:10.1038/s12276-025-01480-7
158. Foti R, Storti G, Palmesano M, Scioli MG, Fiorelli E, Terriaca S, et al. Senescence in Adipose-Derived Stem Cells: Biological Mechanisms and Therapeutic Challenges. Int J Mol Sci. 2024 Aug 1;25(15):8390. doi:10.3390/ijms25158390
159. Di Micco R, Krizhanovsky V, Baker D, d'Adda di Fagagna F. Cellular senescence in ageing: from mechanisms to therapeutic opportunities. Nature

Reviews Molecular Cell Biology. Nature Research; 2021. p. 75–95. doi:10.1038/s41580-020-00314-w PubMed PMID: 33328614.

160. Chaib S, Tchkonia T, Kirkland JL. Cellular senescence and senolytics: the path to the clinic. Nature Medicine. Nature Research; 2022. p. 1556–68. doi:10.1038/s41591-022-01923-y PubMed PMID: 35953721.
161. Xu M, Palmer AK, Ding H, Weivoda MM, Pirtskhalava T, White TA, et al. Targeting senescent cells enhances adipogenesis and metabolic function in old age. Elife. 2015 Dec 19;4. doi:10.7554/eLife.12997
162. Li Q, Hagberg CE, Silva Cascales H, Lang S, Hyvönen MT, Salehzadeh F, et al. Obesity and hyperinsulinemia drive adipocytes to activate a cell cycle program and senesce. Nat Med. 2021 Nov 4;27(11):1941–53. doi:10.1038/s41591-021-01501-8
163. Nerstedt A, Smith U. The impact of cellular senescence in human adipose tissue. J Cell Commun Signal. 2023 Sep 17;17(3):563–73. doi:10.1007/s12079-023-00769-4
164. Cai Y, Song W, Li J, Jing Y, Liang C, Zhang L, et al. The landscape of aging. Sci China Life Sci. 2022 Dec 2;65(12):2354–454. doi:10.1007/s11427-022-2161-3
165. Zhang H, Zhou H, Shen X, Lin X, Zhang Y, Sun Y, et al. The role of cellular senescence in metabolic diseases and the potential for senotherapeutic interventions. Frontiers in Cell and Developmental Biology. Frontiers Media SA; 2023. doi:10.3389/fcell.2023.1276707
166. Rabhi N, Desevin K, Belkina AC, Tilston-Lunel A, Varelas X, Layne MD, et al. Obesity-induced senescent macrophages activate a fibrotic transcriptional program in adipocyte progenitors. Life Sci Alliance. 2022 May 18;5(5):e202101286. doi:10.26508/lsa.202101286
167. Gasek NS, Kuchel GA, Kirkland JL, Xu M. Strategies for targeting senescent cells in human disease. Nat Aging. 2021 Oct 7;1(10):870–9. doi:10.1038/s43587-021-00121-8
168. Camell CD, Sander J, Spadaro O, Lee A, Nguyen KY, Wing A, et al. Inflammasome-driven catecholamine catabolism in macrophages blunts lipolysis during ageing. Nature. 2017 Oct 27;550(7674):119–23. doi:10.1038/nature24022

169. Palmer AK, Gustafson B, Kirkland JL, Smith U. Cellular senescence: at the nexus between ageing and diabetes. Diabetologia. 2019 Oct 27;62(10):1835–41. doi:10.1007/s00125-019-4934-x

170. Berry DC, Jiang Y, Arpke RW, Close EL, Uchida A, Reading D, et al. Cellular Aging Contributes to Failure of Cold-Induced Beige Adipocyte Formation in Old Mice and Humans. Cell Metab. 2017 Jan;25(1):166–81. doi:10.1016/j.cmet.2016.10.023

171. Liu Z, Wu KKL, Jiang X, Xu A, Cheng KKY. The role of adipose tissue senescence in obesity- and ageing-related metabolic disorders. Clin Sci. 2020 Jan 31;134(2):315–30. doi:10.1042/CS20190966

172. Burton DGA, Faragher RGA. Obesity and type-2 diabetes as inducers of premature cellular senescence and ageing. Biogerontology. 2018 Dec 27;19(6):447–59. doi:10.1007/s10522-018-9763-7

173. Zhang L, Pitcher LE, Prahalad V, Niedernhofer LJ, Robbins PD. Targeting cellular senescence with senotherapeutics: senolytics and senomorphics. FEBS Journal. John Wiley and Sons Inc; 2023. p. 1362–83. doi:10.1111/febs.16350 PubMed PMID: 35015337.

174. Hickson LTJ, Langhi Prata LGP, Bobart SA, Evans TK, Giorgadze N, Hashmi SK, et al. Senolytics decrease senescent cells in humans: Preliminary report from a clinical trial of Dasatinib plus Quercetin in individuals with diabetic kidney disease. EBioMedicine. 2019 Sep 1;47:446–56. doi:10.1016/j.ebiom.2019.08.069 PubMed PMID: 31542391.

175. Alum EU, Izah SC, Uti DE, Ugwu OPC, Betiang PA, Basajja M, et al. Targeting Cellular Senescence for Healthy Aging: Advances in Senolytics and Senomorphics. Drug Design, Development and Therapy. Dove Medical Press Ltd; 2025. p. 8489–522. doi:10.2147/DDDT.S543211 PubMed PMID: 40994903.

176. Xu M, Pirtskhalava T, Farr JN, Weigand BM, Palmer AK, Weivoda MM, et al. Senolytics improve physical function and increase lifespan in old age. Nat Med. 2018 Aug 1;24(8):1246–56. doi:10.1038/s41591-018-0092-9 PubMed PMID: 29988130.

177. Xu Q, Fu Q, Li Z, Liu H, Wang Y, Lin X, et al. The flavonoid procyanidin C1 has senotherapeutic activity and increases lifespan in mice. Nat Metab. 2021 Dec 6;3(12):1706–26. doi:10.1038/s42255-021-00491-8

178. Baker DJ, Wijshake T, Tchkonia T, LeBrasseur NK, Childs BG, van de Sluis B, et al. Clearance of p16Ink4a-positive senescent cells delays ageing-associated disorders. Nature. 2011 Nov 2;479(7372):232–6. doi:10.1038/nature10600

179. Farr JN, Xu M, Weivoda MM, Monroe DG, Fraser DG, Onken JL, et al. Targeting cellular senescence prevents age-related bone loss in mice. Nat Med. 2017 Sep 1;23(9):1072–9. doi:10.1038/nm.4385

180. Baker DJ, Childs BG, Durik M, Wijers ME, Sieben CJ, Zhong J, et al. Naturally occurring p16Ink4a-positive cells shorten healthy lifespan. Nature. 2016 Feb 3;530(7589):184–9. doi:10.1038/nature16932

181. Nambiar A, Kellogg D, Justice J, Goros M, Gelfond J, Pascual R, et al. Senolytics dasatinib and quercetin in idiopathic pulmonary fibrosis: results of a phase I, single-blind, single-center, randomized, placebo-controlled pilot trial on feasibility and tolerability. EBioMedicine. 2023 Apr;90:104481. doi:10.1016/j.ebiom.2023.104481

182. Kirkland JL, Tchkonia T. Senolytic drugs: from discovery to translation. Journal of Internal Medicine. Blackwell Publishing Ltd; 2020. p. 518–36. doi:10.1111/joim.13141 PubMed PMID: 32686219.

183. Zhu Y, Tchkonia T, Pirtskhalava T, Gower AC, Ding H, Giorgadze N, et al. The Achilles' heel of senescent cells: from transcriptome to senolytic drugs. Aging Cell. 2015 Aug 22;14(4):644–58. doi:10.1111/acel.12344

184. Lee G, Kim YY, Jang H, Han JS, Nahmgoong H, Park YJ, et al. SREBP1c-PARP1 axis tunes anti-senescence activity of adipocytes and ameliorates metabolic imbalance in obesity. Cell Metab. 2022 May;34(5):702-718.e5. doi:10.1016/j.cmet.2022.03.010

185. Palmer AK, Xu M, Zhu Y, Pirtskhalava T, Weivoda MM, Hachfeld CM, et al. Targeting senescent cells alleviates obesity-induced metabolic dysfunction. Aging Cell. 2019 Jun 1;18(3). doi:10.1111/acel.12950 PubMed PMID: 30907060.

186. Islam MT, Tuday E, Allen S, Kim J, Trott DW, Holland WL, et al. Senolytic drugs, dasatinib and quercetin, attenuate adipose tissue inflammation, and ameliorate metabolic function in old age. Aging Cell. 2023 Feb 1;22(2). doi:10.1111/acel.13767 PubMed PMID: 36637079.

187. Miller CN, Yang JY, England E, Yin A, Baile CA, Rayalam S. Isoproterenol increases uncoupling, glycolysis, and markers of beiging in mature 3T3-L1

adipocytes. PLoS One. 2015 Sep 21;10(9). doi:10.1371/journal.pone.0138344 PubMed PMID: 26390217.

188. Fujimoto Y, Hashimoto O, Shindo D, Sugiyama M, Tomonaga S, Murakami M, et al. Metabolic changes in adipose tissues in response to β3-adrenergic receptor activation in mice. J Cell Biochem. 2019 Jan 1;120(1):821–35. doi:10.1002/jcb.27443 PubMed PMID: 30191605.
189. Picó C, Bonet ML, Palou A. Stimulation of uncoupling protein synthesis in white adipose tissue of mice treated with the β3-adrenergic agonist CGP-12177. Cell Mol Life Sci. 1998 Feb 6;54(2):191–5. doi:10.1007/s000180050142
190. Carswell KA, Lee MJ, Fried SK. Culture of Isolated Human Adipocytes and Isolated Adipose Tissue. In. 2012. p. 203–14. doi:10.1007/978-1-61779-367-7_14
191. Klöting N, Blüher M. Adipocyte dysfunction, inflammation and metabolic syndrome. Rev Endocr Metab Disord. 2014 Dec 26;15(4):277–87. doi:10.1007/s11154-014-9301-0
192. Schweiger M, Eichmann TO, Taschler U, Zimmermann R, Zechner R, Lass A. Measurement of Lipolysis. In. 2014. p. 171–93. doi:10.1016/B978-0-12-800280-3.00010-4
193. Martin S, Okano S, Kistler C, Fernandez-Rojo MA, Hill MM, Parton RG. Spatiotemporal Regulation of Early Lipolytic Signaling in Adipocytes. Journal of Biological Chemistry. 2009 Nov;284(46):32097–107. doi:10.1074/jbc.M109.002675
194. Sidossis L, Kajimura S. Brown and beige fat in humans: Thermogenic adipocytes that control energy and glucose homeostasis. Journal of Clinical Investigation. American Society for Clinical Investigation; 2015. p. 478–86. doi:10.1172/JCI78362 PubMed PMID: 25642708.
195. Yan J, Chen S, Yi Z, Zhao R, Zhu J, Ding S, et al. The role of p21 in cellular senescence and aging-related diseases. Mol Cells. 2024 Nov;47(11):100113. doi:10.1016/j.mocell.2024.100113
196. Inoue N, Yahagi N, Yamamoto T, Ishikawa M, Watanabe K, Matsuzaka T, et al. Cyclin-dependent Kinase Inhibitor, p21WAF1/CIP1, Is Involved in Adipocyte Differentiation and Hypertrophy, Linking to Obesity, and Insulin Resistance. Journal of Biological Chemistry. 2008 Jul;283(30):21220–9. doi:10.1074/jbc.M801824200

197. Lee D, Takayama S, Goldberg AL. ZFAND5/ZNF216 is an activator of the 26S proteasome that stimulates overall protein degradation. Proceedings of the National Academy of Sciences. 2018 Oct 9;115(41). doi:10.1073/pnas.1809934115

198. Lee D, Zhu Y, Colson L, Wang X, Chen S, Tkacik E, et al. Molecular mechanism for activation of the 26S proteasome by ZFAND5. Mol Cell. 2023 Aug;83(16):2959-2975.e7. doi:10.1016/j.molcel.2023.07.023

199. Klaips CL, Jayaraj GG, Hartl FU. Pathways of cellular proteostasis in aging and disease. Journal of Cell Biology. 2018 Jan 2;217(1):51–63. doi:10.1083/jcb.201709072

200. Huang J, Teng L, Li L, Liu T, Li L, Chen D, et al. ZNF216 Is an A20-like and IκB Kinase γ-Interacting Inhibitor of NFκB Activation. Journal of Biological Chemistry. 2004 Apr;279(16):16847–53. doi:10.1074/jbc.M309491200

201. Morikawa M, Derynck R, Miyazono K. TGF-β and the TGF-β Family: Context-Dependent Roles in Cell and Tissue Physiology. Cold Spring Harb Perspect Biol. 2016 May 2;8(5):a021873. doi:10.1101/cshperspect.a021873

202. Ong CH, Tham CL, Harith HH, Firdaus N, Israf DA. TGF-β-induced fibrosis: A review on the underlying mechanism and potential therapeutic strategies. Eur J Pharmacol. 2021 Nov;911:174510. doi:10.1016/j.ejphar.2021.174510

203. Eisinger K, Girke P, Buechler C, Krautbauer S. Adipose tissue depot specific expression and regulation of fibrosis-related genes and proteins in experimental obesity. Mammalian Genome. 2024 Mar 26;35(1):13–30. doi:10.1007/s00335-023-10022-3

204. Ruiz-Ojeda FJ, Méndez-Gutiérrez A, Aguilera CM, Plaza-Díaz J. Extracellular Matrix Remodeling of Adipose Tissue in Obesity and Metabolic Diseases. Int J Mol Sci. 2019 Oct 2;20(19):4888. doi:10.3390/ijms20194888

205. Lundgren CH, Brown SL, Nordt TK, Sobel BE, Fujii S. Elaboration of Type-1 Plasminogen Activator Inhibitor From Adipocytes. Circulation. 1996 Jan;93(1):106–10. doi:10.1161/01.CIR.93.1.106

206. Ghosh AK, Vaughan DE. PAI-1 in tissue fibrosis. J Cell Physiol. 2012 Feb 23;227(2):493–507. doi:10.1002/jcp.22783

207. Vaughan DE, Rai R, Khan SS, Eren M, Ghosh AK. Plasminogen Activator Inhibitor-1 Is a Marker and a Mediator of Senescence. Arterioscler Thromb Vasc Biol. 2017 Aug;37(8):1446–52. doi:10.1161/ATVBAHA.117.309451

208. Tominaga K, Suzuki HI. TGF-β Signaling in Cellular Senescence and Aging-Related Pathology. Int J Mol Sci. 2019 Oct 10;20(20):5002. doi:10.3390/ijms20205002

209. Buechler C, Krautbauer S, Eisinger K. Adipose tissue fibrosis. World J Diabetes. 2015;6(4):548. doi:10.4239/wjd.v6.i4.548

210. Bahn YJ, Wang Y, Dagur P, Scott N, Cero C, Long KT, et al. TGF-β antagonism synergizes with PPARγ agonism to reduce fibrosis and enhance beige adipogenesis. Mol Metab. 2024 Dec;90:102054. doi:10.1016/j.molmet.2024.102054

211. Freund A, Laberge RM, Demaria M, Campisi J. Lamin B1 loss is a senescence-associated biomarker. Mol Biol Cell. 2012 Jun;23(11):2066–75. doi:10.1091/mbc.e11-10-0884

212. Lv T, Wang C, Zhou J, Feng X, Zhang L, Fan Z. Mechanism and role of nuclear laminin B1 in cell senescence and malignant tumors. Cell Death Discov. 2024 Jun 1;10(1):269. doi:10.1038/s41420-024-02045-9

213. Dreesen O, Chojnowski A, Ong PF, Zhao TY, Common JE, Lunny D, et al. Lamin B1 fluctuations have differential effects on cellular proliferation and senescence. Journal of Cell Biology. 2013 Mar 4;200(5):605–17. doi:10.1083/jcb.201206121

214. de Oliveira RF, Salazar M, Matos L, Almeida H, Rodrigues AR, Gouveia AM. High copper levels induce premature senescence in 3T3-L1 preadipocytes. Biochimica et Biophysica Acta (BBA) - Molecular Cell Research. 2024 Jun;1871(5):119734. doi:10.1016/j.bbamcr.2024.119734

215. Lehrskov LL, Christensen RH. The role of interleukin-6 in glucose homeostasis and lipid metabolism. Semin Immunopathol. 2019 Jul 17;41(4):491–9. doi:10.1007/s00281-019-00747-2

216. Pedersen BK, Febbraio MA. Muscle as an Endocrine Organ: Focus on Muscle-Derived Interleukin-6. Physiol Rev. 2008 Oct;88(4):1379–406. doi:10.1152/physrev.90100.2007

217. Caslin HL, Bhanot M, Bolus WR, Hasty AH. Adipose tissue macrophages: Unique polarization and bioenergetics in obesity. Immunol Rev. 2020 May;295(1):101–13. doi:10.1111/imr.12853

218. Martinez FO, Gordon S, Locati M, Mantovani A. Transcriptional Profiling of the Human Monocyte-to-Macrophage Differentiation and Polarization: New

Molecules and Patterns of Gene Expression. The Journal of Immunology. 2006 Nov 15;177(10):7303–11. doi:10.4049/jimmunol.177.10.7303

219. Morris DL, Singer K, Lumeng CN. Adipose tissue macrophages: phenotypic plasticity and diversity in lean and obese states. Curr Opin Clin Nutr Metab Care. 2011 Jul;14(4):341–6. doi:10.1097/MCO.0b013e328347970b
220. Nance SA, Muir L, Lumeng C. Adipose tissue macrophages: Regulators of adipose tissue immunometabolism during obesity. Mol Metab. 2022 Dec;66:101642. doi:10.1016/j.molmet.2022.101642
221. Cancello R, Henegar C, Viguerie N, Taleb S, Poitou C, Rouault C, et al. Reduction of Macrophage Infiltration and Chemoattractant Gene Expression Changes in White Adipose Tissue of Morbidly Obese Subjects After Surgery-Induced Weight Loss. Diabetes. 2005 Aug 1;54(8):2277–86. doi:10.2337/diabetes.54.8.2277
222. Nawaz A, Aminuddin A, Kado T, Takikawa A, Yamamoto S, Tsuneyama K, et al. CD206+ M2-like macrophages regulate systemic glucose metabolism by inhibiting proliferation of adipocyte progenitors. Nat Commun. 2017 Aug 18;8(1):286. doi:10.1038/s41467-017-00231-1
223. Rhodes DH, Pini M, Castellanos KJ, Montero-Melendez T, Cooper D, Perretti M, et al. Adipose tissue-specific modulation of galectin expression in lean and obese mice: Evidence for regulatory function. Obesity. 2013 Feb 26;21(2):310–9. doi:10.1002/oby.20016
224. Kang H, Lee J. Adipose tissue macrophage heterogeneity in the single-cell genomics era. Mol Cells. 2024 Feb;47(2):100031. doi:10.1016/j.mocell.2024.100031
225. Wyatt AR, Yerbury JJ, Berghofer P, Greguric I, Katsifis A, Dobson CM, et al. Clusterin facilitates in vivo clearance of extracellular misfolded proteins. Cellular and Molecular Life Sciences. 2011 Dec 20;68(23):3919–31. doi:10.1007/s00018-011-0684-8
226. Satapathy S, Walker H, Brown J, Gambin Y, Wilson MR. The N-end rule pathway regulates ER stress-induced clusterin release to the cytosol where it directs misfolded proteins for degradation. Cell Rep. 2023 Sep;42(9):113059. doi:10.1016/j.celrep.2023.113059

227. Trougakos IP. The Molecular Chaperone Apolipoprotein J/Clusterin as a Sensor of Oxidative Stress: Implications in Therapeutic Approaches - A Mini-Review. Gerontology. 2013;59(6):514–23. doi:10.1159/000351207

228. Nicolai A, Li M, Kim DH, Peterson SJ, Vanella L, Positano V, et al. Heme Oxygenase-1 Induction Remodels Adipose Tissue and Improves Insulin Sensitivity in Obesity-Induced Diabetic Rats. Hypertension. 2009 Mar;53(3):508–15. doi:10.1161/HYPERTENSIONAHA.108.124701

229. Tu TH, Joe Y, Choi HS, Chung HT, Yu R. Induction of Heme Oxygenase-1 with Hemin Reduces Obesity-Induced Adipose Tissue Inflammation via Adipose Macrophage Phenotype Switching. Mediators Inflamm. 2014;2014:1–10. doi:10.1155/2014/290708

230. Drummond GS, Baum J, Greenberg M, Lewis D, Abraham NG. HO-1 overexpression and underexpression: Clinical implications. Arch Biochem Biophys. 2019 Sep;673:108073. doi:10.1016/j.abb.2019.108073

231. McClung JA, Levy L, Garcia V, Stec DE, Peterson SJ, Abraham NG. Heme-oxygenase and lipid mediators in obesity and associated cardiometabolic diseases: Therapeutic implications. Pharmacol Ther. 2022 Mar;231:107975. doi:10.1016/j.pharmthera.2021.107975

FACULDADE DE **MEDICINA**